

**THE UNIVERSITY OF CALGARY**

**Shear Strength of  
Reinforced Concrete Beams**

**by**

**William Kriski**

**A THESIS**

**SUBMITTED TO THE FACULTY OF GRADUATE STUDIES  
IN PARTIAL FULFILLMENT OF THE REQUIREMENTS FOR THE  
DEGREE OF MASTER OF SCIENCE**

**DEPARTMENT OF CIVIL ENGINEERING**

**CALGARY, ALBERTA**

**APRIL, 1996**

**© William Kriski 1996**

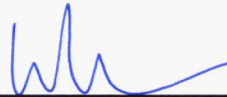
**THE UNIVERSITY OF CALGARY**  
**FACULTY OF GRADUATE STUDIES**

The undersigned certify that they have read, and recommend to the Faculty of Graduate Studies for acceptance, a thesis entitled "Shear Strength of Reinforced Concrete Beams" submitted by William Kriski in partial fulfillment of the requirements for the degree of Master of Science.



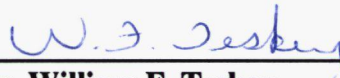
---

**Chairperson, Dr. R. E. Loov**  
**Department of Civil Engineering**



---

**Dr. W. H. Dilger**  
**Department of Civil Engineering**



---

**Dr. William F. Teskey**  
**Department of Geomatics Engineering**

Date: 1996/05/01

## ABSTRACT

The main objective of this thesis was to further develop Dr. Loov's model to predict the shear strength of beams using shear friction concepts. Twelve beams were tested and some existing test data was examined to aid in the development of the model. The major variables were  $a/d$  ratio, end anchorage and concrete strength.

Based on the tests, a shear friction model was developed. In this model the stirrups and the longitudinal reinforcement are assumed to provide a clamping force thereby increasing the shear stress that can be resisted. The predicted values from the shear friction model were compared to current code methods including CSA simplified and general methods, ACI methods and the CSA strut-and-tie method. The predictions using the shear friction model were found to be reasonable and encourage further research. Some code methods were found to be very conservative.

## **ACKNOWLEDGMENTS**

I would like to thank my supervisor Dr. R. E. Loov for his guidance, advice, experience and financial assistance which greatly assisted my completion of the thesis.

I would also like to thank a large number of the technical staff, namely Don Anson, Terry Quinn, Don McCullough, Dan Tilleman and Terry Nail for their help during building formwork, casting and testing.

Finally, thanks to the Natural Science and Engineering Research Council of Canada for their two year scholarship, and to the University of Calgary for the supplemental income.

## TABLE OF CONTENTS

APPROVAL PAGE .....	ii
ABSTRACT .....	iii
ACKNOWLEDGMENTS .....	iv
TABLE OF CONTENTS .....	v
LIST OF TABLES .....	viii
LIST OF FIGURES .....	x
NOTATION .....	xiv
1. INTRODUCTION .....	1
1.1 Problem Statement .....	1
1.2 Objectives .....	1
1.3 Outline of Thesis .....	2
2. LITERATURE REVIEW .....	3
2.1 Truss Analogy .....	3
2.2 CSA Methods .....	4
2.2.1 CSA Simplified Method .....	4
2.2.2 CSA General Method .....	5
2.3 ACI Methods .....	9
2.3.1 ACI Method for spans $l_r/d > 5$ .....	9
2.3.2 ACI Method for $2 \leq l_r/d \leq 5$ .....	11
2.4 Strut-and-Tie Model .....	12
2.5 Birkeland's Shear Friction Equation .....	13

2.6	Loov's Shear Friction Equation .....	13
2.7	A.H. Mattock's Tests .....	13
2.8	Shear Friction (CSA A23.3-94 Clause 11.6) .....	15
2.9	Tests of Dapped End Beams by Kumaraguru .....	18
<b>3.</b>	<b>PROPOSED SHEAR FRICTION EQUATIONS .....</b>	<b>25</b>
3.1	Loov's Equation .....	25
3.2	Development of Forces in Longitudinal Reinforcement .....	28
3.3	Development of Forces in Vertical Stirrups .....	29
3.4	Location of Normal Force on an Inclined Plane .....	30
3.5	Comparison of Shear Friction Model to Existing Test Data .....	30
3.5.1	Arthur Clark's Tests .....	31
3.5.2	Kani's Tests .....	34
3.5.3	Sarsam and Al-Musawi's Tests .....	37
<b>4.</b>	<b>EXPERIMENTAL PROGRAM .....</b>	<b>46</b>
4.1	Overview of Experimental Program .....	46
4.2	Objectives .....	46
4.3	Test Specimens .....	47
4.4	Test Setup and Procedure .....	50
4.5	Instrumentation .....	51
<b>5.</b>	<b>SHEAR FRICTION MODEL AND CODE COMPARISONS TO BEAM TESTS .</b>	<b>55</b>
5.1	Test Results .....	55
5.2	Shear Friction Model Predictions .....	64

5.3 Extended Shear Friction Model Predictions .....	69
5.4 CSA Predictions .....	74
5.4.1 CSA Simplified Method .....	74
5.4.2 CSA General Method .....	77
5.4.3 CSA Strut-and-Tie Methods .....	79
5.4.3.1 Strut-and-Tie Method using CSA code equations .....	79
5.4.3.2 Strut-and-Tie Method without Development Length Eqn	83
5.4.3.3 Strut-and-Tie Method without $f_{2max}$ Restriction .....	85
5.5 ACI Predictions .....	87
5.5.1 ACI Predictions using Equations 2.19 and 2.21 .....	87
5.5.2 ACI Predictions using Equations 2.20 and 2.21 .....	89
5.5.3 ACI Predictions using Equation 2.25 .....	90
5.5.4 ACI Predictions using Equations 2.26 and 2.29 .....	92
5.5.5 ACI Predictions using Equations 2.27 and 2.29 .....	94
6. CONCLUSIONS .....	124
7. RECOMMENDATIONS .....	126
REFERENCES .....	127

## LIST OF TABLES

### TABLE

3.1	Shear Friction Model of Clark's Tests .....	32
3.2	Shear Friction Model of Kani's Tests .....	35
3.3	Shear Friction Model of Sarsam and Al-Musawi's Tests .....	38
4.1	Test Beam Details .....	48
4.2	Concrete Mix Design (% by mass) .....	48
5.1	Details of Beam Failures .....	56
5.2	Crack Widths at Service Loads .....	58
5.3	Crack Widths at Stirrup Location .....	59
5.4	Force Development Comparison .....	60
5.5	Shear Friction Model Predictions using bond lengths from CSA A23.3-94 ....	65
5.6	Extended Shear Friction Model Predictions using strain measurements .....	71
5.7	CSA Simplified Method Predictions .....	75
5.8	CSA General Method Predictions .....	77
5.9	CSA Strut-and-Tie Predictions .....	81
5.10	CSA Strut-and-Tie Predictions without Development Equation .....	84
5.11	CSA Strut-and-Tie Predictions without $f_{2max}$ Restriction .....	86
5.12	ACI Predictions using Equations 2.19 and 2.21 .....	88
5.13	ACI Predictions using Equations 2.20 and 2.21 .....	89



5.14	ACI Predictions using Equation 2.25 .....	91
5.15	ACI Predictions using Equations 2.26 and 2.29 .....	93
5.16	ACI Predictions using Equations 2.27 and 2.29 .....	95

## LIST OF FIGURES

### FIGURE

2.1	Truss Analogy (Pillai and Kirk, 1988) . . . . .	19
2.2	Stirrups across inclined plane . . . . .	19
2.3	Table 11-1 of CSA A23.3 code (Canadian Standards Association, 1994) . . . . .	20
2.4	Optimum $\beta$ . . . . .	20
2.5	Strut-and-tie modelling of structure (Schlaich and Schaefer, 1991) . . . . .	21
2.6	Mattock's Tests . . . . .	21
2.7	Shear friction and allowable angles of reinforcement (Pillai and Kirk, 1988) . . .	22
2.8	Shear friction induced by separation of rough crack (Pillai and Kirk, 1988) . . .	22
2.9	Example applications of shear friction method (Pillai and Kirk, 1988) . . . . .	23
2.10	Kumaraguru's comparison of CSA method to test results (Kumaraguru, 1992) .	24
3.1	Loov's shear friction equation . . . . .	40
3.2	Forces on inclined plane . . . . .	40
3.3	Shear strength vs. tension force . . . . .	41
3.4	Possible effect of increased force in longitudinal reinforcement on shear strength . . . . .	42
3.5	Moment due to stirrups . . . . .	42
3.6	Rate of force development in longitudinal reinforcement . . . . .	42
3.7	Rate of force development in stirrups . . . . .	43

3.8	Free-body diagram of section of beam .....	43
3.9	Assumed normal stress distribution .....	44
3.10	Comparison of predictions using shear friction method to test results by Clark .	44
3.11	Comparison of predictions using shear friction method to test results by Kani ..	45
3.12	Comparison of prediction using shear friction method to test results by Sarsam and Al-Musawi .....	45
4.1	Reinforcement layout .....	53
4.2	Test setup .....	53
4.3	Gauge locations on longitudinal reinforcement .....	54
4.4	Gauge locations on stirrups .....	54
5.1	Beam 1 after failure, $a/d = 3.05$ .....	97
5.2	Beam 2 after failure, $a/d = 2.61$ .....	97
5.3	Beam 3 after failure, $a/d = 3.05$ .....	98
5.4	Beam 4 after failure, $a/d = 2.17$ .....	98
5.5	Beam 5 after failure, $a/d = 2.61$ .....	99
5.6	Beam 6 after failure, $a/d = 2.17$ .....	99
5.7	Beam 7 after failure, $a/d = 3.05$ .....	100
5.8	Beam 8 after failure, $a/d = 2.61$ .....	100
5.9	Beam 9 after failure, $a/d = 3.05$ .....	101
5.10	Beam 10 after failure, $a/d = 2.61$ .....	101
5.11	Beam 11 after failure, $a/d = 2.17$ .....	102

5.12	Beam 12 after failure, $a/d = 2.17$ .....	102
5.13	Failure load vs. $a/d$ ratio .....	103
5.14	Beam strength vs. $a/d$ ratio - shear friction .....	104
5.15	Horizontal crack after failure (end view) .....	105
5.16	Horizontal crack after failure (side view) .....	105
5.17	Stress-strain curve for stirrup .....	106
5.18	Strain in stirrup for beam 6 (outer stirrup) .....	107
5.19	Strain in stirrup for beam 6 (middle stirrup) .....	108
5.20	Strain in stirrup for beam 6 (inner stirrup) .....	109
5.21	Stress-strain curve for longitudinal reinforcement .....	110
5.22	Strains in longitudinal reinforcement for beam 6 (near support) .....	111
5.23	Strains in longitudinal reinforcement for beam 6 (at midspan) .....	112
5.24	Free-body diagram of section of beam .....	113
5.25	Beam strength vs. $a/d$ ratio - extended shear friction .....	114
5.26	Beam strength vs. $a/d$ ratio - CSA A23.3-94 simplified method .....	115
5.27	Beam strength vs. $a/d$ ratio - CSA A23.3-94 general method .....	116
5.28	Strut-and-tie model of test beam .....	117
5.29	Beam strength vs. $a/d$ ratio - strut-and-tie model using code equations .....	118
5.30	Beam strength vs. $a/d$ ratio - strut-and-tie model without development eqns. .	119
5.31	Beam strength vs. $a/d$ ratio - strut-and-tie model without $f_{2max}$ restriction ....	120
5.32	Beam strength vs. $a/d$ ratio - ACI method using Equation 2.25 .....	121
5.33	Beam strength vs. $a/d$ ratio - ACI method using Equation 2.26 and 2.29 .....	122

5.34 Beam strength vs.  $a/d$  ratio - ACI method using Equation 2.27 and 2.29 . . . . . 123

## NOTATION

a	shear span from centre of support plates to centre of load plate
a	maximum aggregate size in $\beta_2$ equation
c	cohesion stress used in CSA shear friction equation
avg	mean of sample population
A	area of inclined plane
$A_{cv}$	area of concrete section resisting shear transfer
$A_s$	area of reinforcement in tension zone
$A_v$	area of one stirrup
$A_{vf}$	area of shear friction reinforcement
$A_{vh}$	area of shear reinforcement parallel to longitudinal reinforcement
$A_{vmin}$	minimum area of shear reinforcement for one stirrup
$b_w$	width of beam web
c	vertical distance from the extreme compression fibre to the neutral axis
C.O.V.	coefficient of variation
d	distance from the extreme compression fibre to the centroid of the longitudinal tension reinforcement
$d_b$	diameter of a reinforcing bar
$d_v$	distance measured perpendicular to the neutral axis between the resultants of the tensile and compressive forces due to flexure
$E_s$	modulus of elasticity for longitudinal reinforcement
$f_y$	specified yield strength of the stirrups
$f_y$	specified yield strength of the longitudinal reinforcement or stirrups

$f_2$	stress in compressive concrete strut
$f_{2max}$	maximum allowable stress in concrete strut
$f'_c$	specified compressive concrete strength
$h$	overall height of member
$j$	lever arm factor
$k$	shear friction factor
$k_1$	bar location factor
$k_2$	coating factor
$k_3$	concrete density factor
$k_4$	bar size factor
$\ell_a$	length of reinforcement past outside face of support
$\ell_d$	development length
$\ell_n$	clear span length from inside face to inside face of the supports
$M_f$	factored moment at section
$M_{stirrup}$	moment due to stirrups crossing inclined plane about the intersection of the neutral axis and the inclined plane
$N$	unfactored permanent load perpendicular to shear plane, positive for tension
$n$	number of stirrups crossing inclined plane
$p$	distance from center of the support plate to the intersection of the longitudinal reinforcement and the inclined plane
$p_e$	bearing stress on support plate due to reaction force
ratio <sub>i</sub>	ratio of test failure load to predicted failure load
$R$	normal force on cracked horizontal plane

$R_i$	normal force on cracked inclined plane
$s$	spacing of stirrups
$\text{slope}_1$	rate of force development in longitudinal reinforcement applying to lengths of reinforcement past the outside face of the support
$\text{slope}_2$	rate of force development applying to lengths of reinforcement over the width of the bearing plates
$\text{slope}_3$	rate of force development applying to lengths of reinforcement between inside faces of the supports
$s_2$	spacing of reinforcement parallel to longitudinal reinforcement
$S$	shear force on cracked horizontal plane
$S_i$	shear force on cracked inclined plane
$T$	tension force in longitudinal reinforcement at a given location
$T_R$	sum of the components of forces normal to cracked inclined plane
$T_S$	sum of the components of forces parallel to cracked inclined plane
$T_v$	force in one stirrup
$T_{vt}$	total force in all stirrups crossing cracked inclined plane
$T_y$	yield force in longitudinal reinforcement
$u$	distance from point load to closest stirrup
$v_f$	factored shear stress acting on beam
$V_a$	vertical component of the interface shear
$V_c$	factored shear resistance attributed to the concrete
$V_{cg}$	factored shear resistance attributed to the concrete using CSA general method
$V_{cz}$	shear strength of uncracked concrete
$V_d$	dowel force in the longitudinal reinforcement



$V_{db}$	predicted shear force along span based on diagonal bending failure
$V_f$	factored shear force at section
$V_n$	nominal shear resistance of beam
$V_r$	factored shear resistance of beam
$V_{rg}$	factored shear resistance of beam using CSA A23.3-94 general method
$V_s$	factored shear resistance provided by the shear reinforcement
$V_{sf}$	predicted shear force based on shear friction failure
$V_{sg}$	factored shear resistance provided by the stirrups using CSA general method
$V_{s\max}$	maximum shear resistance allowed by CSA A23.3-94 Clause 11.3.4
$w$	width of shear plane for Mattock's tests
$w_c$	crack width
$w_1$	width of support plate used for test beams
$x$	distance from center of support plate to first stirrup in Kani's tests
$x_1$	distance of a stirrup from the center of support plate
$y_t$	vertical distance from top of beam to centroid of normal force on inclined plane
$\alpha_f$	angle between shear friction reinforcement and shear plane
$\alpha_1$	ratio of average stress of rectangular compressive stress block to the specified concrete strength
$\beta$	factor accounting for the shear resistance of cracked concrete
$\beta_e$	factor accounting for the increase in rate of force development in longitudinal reinforcement due to vertical pressure
$\beta_1$	ratio of depth of rectangular compressive stress block to depth of neutral axis
$\beta_1$	factor that depends on the average tensile strains in the cracked concrete using CSA general method

$\beta_2$	factor which prevents crack slipping failure using CSA general method
$\epsilon_s$	tensile strain in tensile tie reinforcement due to factored loads
$\epsilon_x$	longitudinal strain of flexural tension chord of member
$\epsilon_1$	principal tensile strain in cracked concrete due to factored loads
$\theta$	angle of inclination of diagonal compressive struts to the longitudinal axis of a beam using Table 11-1 of CSA A23.3-94
$\theta_{\min}$	angle of compressive strut where $f_2 > f_{2\max}$ or where $\epsilon_x$ becomes imaginary
$\theta_s$	smallest angle between compressive strut and intersecting tensile ties
$\lambda$	factor to account for low density concrete
$\mu$	coefficient of friction
$v$	shear stress on a plane according to Loov's equations
$v_n$	shear stress on a plane according to Birkeland's equations
$v_r$	shear resistance of a structural element given by CSA equations
$\rho$	longitudinal reinforcement ratio
$\rho_v$	transverse reinforcement ratio
$\rho_w$	longitudinal reinforcement ratio in ACI equations
$\sigma$	effective normal stress
$\tau$	shear stress
$\phi$	strength reduction factor
$\phi_c$	resistance factor for concrete
$\phi_s$	resistance factor for reinforcement

## 1. INTRODUCTION

### 1.1 Problem Statement

Current Canadian design methods for shear are based on a truss model in the form of a simplified and a general method. Although the truss model is an excellent conceptual tool, the actual mechanism of shear transfer is not directly accounted for. In the simplified method, the action of aggregate interlock and other mechanisms are taken into account by adding a concrete contribution term to the capacity of the truss. The general method allows a variable angle truss model to be used, but still adds a concrete contribution to the truss capacity. In the 1994 Canadian code, the shear strength provided by the concrete is often determined by limiting the "crack slip" across a shear crack. Also, the general method and strut-and-tie model use a concrete softening model which is felt to be questionable based on existing literature.

### 1.2 Objectives

The main objective in this thesis was to apply shear friction concepts, (formerly used in push-off tests) to beams. This was achieved by developing a model, comparing its predictions of shear strength to test data in existing literature, and by testing 12 beams and comparing the shear strength of these beams to the predicted values by the shear friction model.

Another objective was to compare the shear strengths predicted by current design methods such as the simplified and general method, the strut-and-tie model and ACI methods to the shear strengths produced in the twelve beam tests. Other objectives were

to observe the impact of different concrete strengths, anchorage lengths and  $a/d$  ratios on the shear strength of beams, and to determine the effectiveness of relatively small stirrups.

### **1.3 Outline of Thesis**

In chapter 2 of this thesis, the truss analogy, Canadian Standards Association (CSA) and American Concrete Institute (ACI) methods of shear design are described. In addition, the origin of Loov's shear friction equation is discussed along with details of a thesis which contained the application of shear friction concepts to dapped end beams. Another paper (Mattock, 1974) was examined which demonstrated the possibility of using shear friction reinforcement over a large range of angles.

In chapter 3, the development of the shear friction model is explained. The model is then used to predict the shear strength of a number of beams from a variety of past shear tests on beams.

In chapter 4, an overview of the testing procedure is given, including a description of the test specimens, set-up and instrumentation, and the objectives are outlined.

In chapter 5, a comparison of the shear friction model, CSA, and ACI shear design methods to the test results is given.

In chapter 6 and 7, conclusions and recommendations are presented.

## 2. LITERATURE REVIEW

### 2.1 Truss Analogy

The shear strength of a reinforced concrete beam is often determined with the aid of a truss analogy. In this pin-jointed truss, the concrete compression zone at the top of a reinforced concrete beam is represented by the top compression chord and the tension in the reinforcement is represented by the bottom tension chord. The web members in tension represent the stirrups and the web members in compression represent the concrete in compression between the inclined cracks. The diagonal compression chords are assumed to act at a 45° angle in the simplest truss analogy (Figure 2.1).

Therefore for a segment of a beam with vertical stirrups as shown in Figure 2.2 the total number of stirrups crossing the diagonal crack is assumed to be:

$$n = \frac{jd}{s} \quad (2.1)$$

where  $jd$  is the distance between the compressive and tensile resultants, and  $s$  is the spacing of stirrups. Assuming that the web reinforcement yields as the ultimate strength is reached, the total vertical component of the stirrup forces across the crack is:

$$\begin{aligned} V_s &= n A_v f_y \\ &= A_v f_y \frac{jd}{s} \end{aligned} \quad (2.2)$$

where  $A_v$  is equal to the cross-sectional area of one stirrup and  $f_y$  is equal to the yield strength of the stirrup. From force equilibrium,  $V_s$  also equals the shear strength of a beam subjected to a point load at its center. This is a very simple method of analysis, but it neglects the contribution of the uncracked concrete, dowel action and aggregate interlock to the shear resistance of a beam.

## 2.2 CSA Methods

### 2.2.1 CSA Simplified Method

The basic requirement for design is that:

$$V_r \geq V_f \quad (2.3)$$

where  $V_r$  is the factored shear resistance of a beam, and  $V_f$  is the factored shear force (Canadian Standards Association, 1994). Also,

$$V_r = V_c + V_s \quad (2.4)$$

where  $V_c$  is the shear carried by the concrete and  $V_s$  is the shear resistance provided by the web reinforcement. The shear strength of the uncracked concrete  $V_{cz}$ , the vertical component of the interface shear  $V_a$ , and the dowel force  $V_d$  in the longitudinal reinforcement are combined together into one term  $V_c$ , which is assumed to be constant during all stages of loading even though the individual terms have varying magnitudes.  $V_c$  is given as:

$$V_c = 0.2\lambda\phi_c\sqrt{f'_c}b_wd \quad (2.5)$$

where  $\lambda$  is a factor that accounts for the effects of low and semi-low density concrete and  $\phi_c$  is a material resistance factor equal to 0.6 for concrete ( $\phi_c = 0.65$  for precast concrete).

The shear resisted by vertical stirrups is equal to:

$$V_s = \frac{\phi_s A_v f_y d}{s} \quad (2.6)$$

where  $\phi_s$  is the material resistance factor for the stirrup reinforcement and is equal to 0.85.

$V_s$  is assumed to act over the effective depth,  $d$ , rather than  $jd$  as in the truss analogy.

Therefore, for a known factored shear force  $V_f$ , a beam can be designed by ensuring that  $V_c + V_s \geq V_f$ . The CSA code requires a minimum amount of shear reinforcement wherever  $V_f \geq V_c/2$  except for slabs and footings, concrete joist floors and certain classes of relatively wide and shallow beams. The minimum area of shear reinforcement is given as:

$$A_{v \min} = 0.06 \sqrt{f'_c} \frac{b_w s}{f_y} \quad (2.7)$$

In order to guard against brittle web crushing failure, shear compression failure and excessive crack widths, the CSA code gives an upper limit to the amount of shear reinforcement allowed, namely

$$V_{s \max} = 0.8 \lambda \phi_c \sqrt{f'_c} b_w d \quad (2.8)$$

The CSA code also limits the maximum spacing of vertical reinforcement to the smaller of 0.7d or 600 mm if  $v_f < 0.1 \phi_c f'_c$ , or 0.35d or 300 mm when  $v_f \geq 0.1 \phi_c f'_c$  (Clause 11.2.11).

### 2.2.2 CSA General Method

An outline of the general method can be found in existing literature (CPCA, 1995). However, some important points will be discussed and the design procedure will be outlined.

The general method for shear design (Canadian Standards Association, 1994) is based on the truss analogy and the modified compression field theory. It deals with the influence of diagonal tension cracking on the diagonal compressive strength, and the influence of shear on the design of longitudinal reinforcement in a more direct manner than

the simplified method.

The basic idea when designing a beam with the general method is to ensure that the diagonal compressive struts will not crush and that the stirrups have yielded at failure. This is accomplished implicitly through the use of  $\beta$  factors in the  $V_c$  term.

Members are proportioned so that

$$V_{\text{R}} \geq V_{\text{f}} \quad (2.9)$$

where  $V_{\text{R}}$  is the factored shear resistance of a beam, and  $V_{\text{f}}$  is the factored shear force.

Also for non-prestressed members:

$$V_{\text{R}} = V_{\text{cg}} + V_{\text{sg}} \quad (2.10)$$

where  $V_{\text{cg}}$  is the shear carried by the concrete and  $V_{\text{sg}}$  is the shear resistance provided by the web reinforcement. However,

$$V_{\text{R}} \leq 0.25 \phi_c f'_c b_w d_v \quad (2.11)$$

$V_{\text{cg}}$  is given as:

$$V_{\text{cg}} = 1.3 \lambda \phi_c \beta \sqrt{f'_c} b_w d_v \quad (2.12)$$

where  $\lambda$  is a factor that accounts for the effects of low and semi-low density concrete,  $\phi_c$  is a material resistance factor equal to 0.6 for concrete,  $\beta$  is a factor that depends on the average tensile strains in the cracked concrete and  $d_v$  is the distance perpendicular to the neutral axis between the resultants of the compressive and tensile forces ( $d_v \geq 0.9d$ ). The shear resisted by vertical stirrups is equal to:

$$V_{\text{sg}} = \frac{\phi_s A_v f_y d_v \cot \theta}{s} \quad (2.13)$$



The first step in design is to calculate the factored shear stress  $v_f = V_f / (b_w d_v)$  and then calculate  $v_f / (\phi_c f'_c)$ . The maximum longitudinal strain  $\epsilon_x$  for a non-prestressed member with no axial force is computed from:

$$\epsilon_x = \frac{0.5V_f \cot \theta + \frac{M_f}{d_v}}{E_s A_s} \quad (2.14)$$

based on an assumed value of  $\theta$ .

Using Table 11-1 in the CSA code (Figure 2.3) for sections with transverse reinforcement,  $\beta$  and  $\theta$  can be determined by trial and error using  $v_f / \phi_c f'_c$  and  $\epsilon_x$  at the most critical location. With these values  $V_{cg}$  is calculated and then  $V_{sg}$  is adjusted so that  $V_{cg} + V_{sg} \geq V_f$ . The minimum spacing of transverse shear reinforcement in the longitudinal direction shall not exceed:

$$600 \text{ mm or } 0.7d, \text{ when } v_f < 0.1\phi_c f'_c$$

$$300 \text{ mm or } 0.35d \text{ when } v_f \geq 0.1\phi_c f'_c$$

The  $\beta$  term is a factor that depends on the average tensile strains in the cracked concrete (CPCA, 1995).  $\beta_1$  is given as:

$$\beta_1 \leq \frac{0.33 \cot \theta}{1 + \sqrt{500 \epsilon_1}} \quad (2.15)$$

where  $\epsilon_1$  is the principal tensile strain in the cracked concrete due to factored loads.

However if the crack widths are too wide, the maximum shear is limited by crack slip.

Another equation which limits  $\beta$  to avoid these "crack slipping" failures is as follows (CPCA, 1995):

$$\beta_2 \leq \frac{0.18}{0.3 + 24 \frac{w_c}{a + 16}} \quad (2.16)$$

where  $a$  is the maximum aggregate size and  $w_c$  is the crack width. After analyzing Table 11-1 in the CSA code, it is apparent that the majority of  $\beta$  values in the table have been derived from  $\beta_2$ . This means that the failure of a beam in shear is predicted to be limited by the crack slipping (shear friction failure) and not from the failure of the truss.

For each box in Table 11-1, values of  $\beta$  and  $\theta$  are given. For a given box,  $\theta$  was chosen so that the stirrups would yield at failure (i.e.  $\theta < \theta_{\max}$ ) and so that the concrete would not crush and  $\epsilon_1$  remains real (i.e.  $\theta > \theta_{\min}$ ). In Figure 2.4,  $\beta$  values are plotted over a range of  $\theta$  values for the center box in Table 11-1. Using  $f'_c = 40$  MPa,  $\beta$  has been chosen using  $\beta_2$  which limits "crack slipping". At all angles between  $25^\circ$  and  $34^\circ$ , the stirrups would yield based on an  $f_y = 400$  MPa, and the concrete wouldn't crush since  $f_2 < f_{2\max}$  and  $\epsilon_1$  remains real.

For a simply supported beam subjected to a point load at its center, the most critical location for shear is at the midspan according to the general method. Since  $v_f$  is constant (ignoring self-weight), the highest moment, and therefore largest  $\epsilon_x$ , will occur at the midspan. For a given beam, it is possible to determine the predicted nominal shear strength by using a trial and error method along with Table 11-1. With a given  $f'_c$  and beam size,  $V_c$  can be calculated. For each box in Table 11-1 corresponding to  $v_f/\phi_c f'_c$  and an  $\epsilon_x$ , a value for  $V_f$  can be calculated knowing  $f'_c$ , and  $V_s$  can be determined by subtracting  $V_c$  from  $V_f$ . With  $V_s$  known, one can determine the required spacing,  $s$ , of the stirrups and can compare this value to the existing spacing of stirrups. One must also

match  $\epsilon_x$  with the value that would be obtained from the  $\epsilon_x$  equation. Once the spacing and  $\epsilon_x$  values are matched by altering the position in the chart, the calculated  $V_f$  term can be assumed to equal the shear resistance of the beam since  $V_f \leq V_{rg}$ .

## 2.3 ACI Methods

### 2.3.1 ACI Method for spans with $\ell_n/d > 5$

The basic requirement for design is that:

$$V_f \leq \phi V_n \quad (2.17)$$

where  $V_f$  is the factored shear force,  $V_n$  is the nominal ultimate shear capacity of a concrete beam, and  $\phi$  is a strength reduction factor equal to 0.85 for shear (American Concrete Institute, 1992) (note: ACI Ch.11 unchanged in 1994 revisions). Also,

$$V_n = V_c + V_s \quad (2.18)$$

where  $V_c$  is the shear carried by the concrete and  $V_s$  is the shear resistance provided by the web reinforcement based on the 45° truss analogy. Using SI units for the following equations, the ACI Code states that:

$$V_c = \sqrt{f'_c} b_w d / 6 \quad (2.19)$$

or as an alternative:

$$V_c = \left[ \sqrt{f'_c} + 120 \rho_w \frac{V_f d}{M_f} \right] b_w d \quad (2.20)$$

but not greater than:

$$0.3 \sqrt{f'_c} b_w d$$

Also,  $V_f/M_f$  shall not be taken greater than 1.0, where  $V_f$  and  $M_f$  are the factored shear and moment respectively acting at the section considered. The shear resisted by vertical stirrups is equal to:

$$V_s = \frac{A_v f_y d}{s} \quad (2.21)$$

The ACI code requires a minimum amount of shear reinforcement wherever  $V_u \geq \phi V_c/2$  except for slabs and footings, concrete joist floors and certain classes of relatively wide and shallow beams. The minimum area of shear reinforcement is given as:

$$A_{v \min} = \frac{b_w s}{3f_y} \quad (2.22)$$

In order to guard against brittle web crushing failure, shear compression failure and excessive crack widths, the ACI code gives an upper limit to the amount of shear reinforcement allowed, namely

$$V_{s \max} = 2 \sqrt{f'_c} b_w d/3 \quad (2.23)$$

To ensure that at least one stirrup will cross an assumed 45° inclined crack, the ACI code also limits the maximum spacing of vertical reinforcement to the smaller of  $d/2$  or 600 mm (Clause 11.5.4.1). Also when

$$V_s > \sqrt{f'_c} b_w d/3 \quad (2.24)$$

the maximum spacing of vertical reinforcement is reduced to  $d/4$  or 300 mm.

### 2.3.2 ACI Method for spans with $2 \leq \ell_n/d \leq 5$

For deep flexural members, the ACI code gives three options (American Concrete Institute, 1992). The shear strength can be calculated as:

$$V_n = \frac{1}{18}(10 + \ell_n/d)\sqrt{f'_c}b_wd \quad (2.25)$$

or  $V_n$  can be calculated by adding  $V_c$  and  $V_s$ .  $V_c$  is given as either:

$$V_c = \sqrt{f'_c} b_w d / 6 \quad (2.26)$$

or,

$$V_c = \left[ 3.5 - 2.5 \frac{M_f}{V_f d} \right] \left[ \sqrt{f'_c} + 120 \rho_w \frac{V_f d}{M_f} \right] b_w d / 7 \quad (2.27)$$

except that the first bracketed term in the second  $V_c$  equation shall not exceed 2.5 and

$$V_c \leq \sqrt{f'_c} b_w d / 2 \quad (2.28)$$

$M_f$  and  $V_f$  are calculated at the critical section as defined in Clause 11.8.5 to be at a distance  $0.5a$  for beams with concentrated loads, but not greater than  $d$ . The resistance of the shear reinforcement is given as:

$$V_s = \left[ \frac{A_v}{s} \left( \frac{1 + \ell_n/d}{12} \right) + \frac{A_{vh}}{s_2} \left( \frac{11 - \ell_n/d}{12} \right) \right] f_y d \quad (2.29)$$

where  $A_v$  is the area of shear reinforcement perpendicular to flexural tension reinforcement within a distance  $s$ , and  $A_{vh}$  is the area of shear reinforcement parallel to flexural reinforcement within a distance  $s_2$ . For deep flexural members  $A_v$  shall not be less than  $0.0015b_w s$  and  $s$  shall not exceed  $d/5$ , nor 450 mm (Clause 11.8.9).  $A_{vh}$  shall not be less than  $0.0025b_w s_2$ , and  $s_2$  shall not exceed  $d/3$  nor 450 mm (Clause 11.8.10).

## 2.4 Strut-and-Tie Model

Figure N11.1.2(b) in the 1994 CPCA Concrete Design Handbook shows that for a beam with an  $a/d$  ratio of less than about 2.5, the strut-and-tie model is most suitable for predicting the failure load. The beam is idealized to behave like a truss consisting of concrete compression struts and steel tension ties connected at nodal zones. These struts and ties actually represent stress fields acting over an area, modelled as forces acting in straight lines (see Figure 2.5). A description of the strut-and-tie procedure can be found in the existing literature (CPCA, 1995).

In the strut-and-tie model, the compressive strength of concrete in a strut is reduced if the strut is crossed by a tension tie. The maximum compressive stress allowed to act on the concrete is given as:

$$f_{2 \max} = \frac{f'_c}{0.8 + 170 \epsilon_1} \quad (2.30)$$

where  $\epsilon_1$  is the principal tensile strain in the cracked concrete and is equal to:

$$\epsilon_1 = 0.002 + \frac{0.004}{\cot^2 \theta_s} \quad (2.31)$$

assuming that the tension ties have yielded and that the maximum tensile strain in the direction of the tie,  $\epsilon_s$ , is equal to 0.002. Therefore as  $\theta_s$  decreases,  $f_{2 \max}$  decreases dramatically, greatly limiting the amount of load that a compressive strut is able to support.

## 2.5 Birkeland's Shear Friction Equation

In 1966, Birkeland presented a paper concerning shear transfer in reinforced concrete where he introduced the following equation for shear stress ( $v_n$ ) on a plane:

$$v_n = 33.5 \sqrt{\rho_v f_y} \quad (\text{psi}) \quad (2.32)$$

$$v_n = 2.78 \sqrt{\rho_v f_y} \quad (\text{MPa})$$

where  $\rho_v f_y$  was referred to as the clamping stress (Birkeland and Birkeland, 1966). The compressive strength of the concrete ( $f'_c$ ) was not considered to be a factor in determining shear strength.

## 2.6 Loov's Shear Friction Equation

In 1978, Loov presented a paper concerning the design of precast connections in which he gave the following relationship for shear stress ( $\tau$ ) and normal stress ( $\sigma$ ) on a crack:

$$\tau/f'_c = k \sqrt{\sigma/f'_c} \quad (2.33)$$

where  $k$  was assumed to equal 0.5 (Loov, 1978). This appears to have been the first time that  $f'_c$  was considered to be a factor in determining shear strength. He compared this equation to three suggested design equations and it appeared that his equation fit the experimental data from previous push-off tests better than the three design equations.

## 2.7 A.H. Mattock's Tests

Alan Mattock considered shear transfer in reinforced concrete across a shear plane (Mattock, 1974). Specifically, 23 pushoff specimens were tested, with either orthogonal

or parallel arrays of reinforcement at various angles to the shear plane. Some specimens were pre-cracked to model real-life situations such as shear transfer across cracks due to lateral restraint of shrinkage or temperature deformations.

Mattock tested a large range of angles of shear reinforcement to the shear plane for specimens with parallel reinforcement and an initially cracked shear plane. The graph in Figure 2.6 shows the test values for these specimens plotted as the shear stress ( $\tau$ ) divided by  $f'_c$  versus the clamping stress ( $\sigma$ ) divided by  $f'_c$  and the predicted values using Loov's equation. Mattock's equation for ultimate shear stress,  $v_u$  is given in imperial units as follows:

$$v_u = 400 \sin^2 \theta_1 + \frac{A_s f_s}{sw} (0.8 \sin^2 \theta_1 - 0.5 \sin 2\theta_1) \quad (2.34)$$

$$f_s = 0 \quad 0^\circ < \theta_1 < 51.3^\circ$$

$$f_s = -1.6 f_y \cos (\theta_1 + 38.7^\circ) \quad 51.3^\circ \leq \theta_1 < 90^\circ$$

$$f_s = f_y \quad 90^\circ \leq \theta_1 \leq 180^\circ$$

$f_s$  - stress in reinforcement (ksi)

$s$  - spacing of reinforcement (in.)

$w$  - width of shear plane (in.)

$\theta_1$  - angle of reinforcing bars to shear plane such that when  $0^\circ \leq \theta_1 < 51.3^\circ$ , the reinforcing bars tend to go into compression according to Mattock  
Also,  $\theta_1 = 180 - \alpha_r$  where  $\alpha_r$  is the angle between the shear friction reinforcement and shear plane such that when  $\alpha_r < 90^\circ$  the reinforcing bars tend to go into tension according to the CSA shear friction method.

$A_s$  - cross-sectional area of one reinforcing bar (in<sup>2</sup>)

A significant amount of shear strength occurs even when  $\theta_1$  is less than  $90^\circ$ .



Current codes (CSA, ACI) allow reinforcement in shear friction transfer to be considered effective only at angles  $90^\circ$  or greater so that the reinforcing bars will go into tension (Figure 2.7).

Mattock's tests appear to show that reinforcement placed at angles less than  $90^\circ$  will still go into tension (Mattock did not measure the reinforcement strains at the crack). This is based on the theory that two irregular surfaces moving transversely relative to each other have to separate slightly to allow the protruding aggregate particles to move past each other (see Figure 2.8). For angles less than about  $51^\circ$ , Mattock considered that there would be no stress in the steel but added a term to account for shear strength due to dowel action.

The angle between the critical shear crack and the longitudinal reinforcement in beams is typically between  $25^\circ$  and  $60^\circ$ . Over this range, the shear friction equation still matches the test results fairly well, although the shear friction equation assumes that the reinforcing bars are in tension. The shear friction predictions underestimate the shear strength in the  $90^\circ$  to  $150^\circ$  range of angles in Mattock's tests. This is most likely due to strain hardening, which results in a clamping stress and a force component parallel to the crack higher than that based on the yield stress of the steel.

### **2.8 Shear Friction (CSA A23.3-94 Clause 11.6)**

In the CSA code (Canadian Standards Association, 1994), Clause 11.1.3 states that shear friction concepts may be used to consider "interfaces between elements such as webs and flanges, between dissimilar materials and between concretes cast at different

times or at potential major cracks along which slip can occur." Examples of the above can be seen in Figure 2.9.

The shear resistance of a structural element is given by:

$$v_r = \lambda \phi_c (c + \mu \sigma) + \phi_s \rho_v f_y \cos \alpha_f \quad (2.35)$$

where:

$\alpha_f$  = angle between shear friction reinforcement and shear plane so that shear friction reinforcement where  $\alpha_f < 90^\circ$  will go into tension according to CSA A23.3-94

$\mu$  = coefficient of friction

$\rho_v$  = shear friction reinforcement ratio

$f_y$  = specified yield strength

$c$  = cohesion stress

$\sigma$  = normal stress on plane

$\phi_c$  = material resistance factor for concrete

$\phi_s$  = material resistance factor for reinforcement

Values of  $\mu$  and  $c$  are as follows (Clause 11.6.2):

$\mu = 1.4\lambda$ ,  $c = 1.0$  for concrete placed monolithically

$\mu = 1.0\lambda$ ,  $c = 0.5$  for concrete placed against hardened concrete with the surface clean and intentionally roughened to a full amplitude of at least 5 mm

$\mu = 0.5\lambda$ ,  $c = 0$  for concrete anchored to as-rolled structural steel by headed studs or by reinforcing bars

$\mu = 0.6\lambda$ ,  $c = 0.25$  for concrete placed against hardened concrete with the surface clean but not intentionally roughened

where  $\lambda$  is a factor to account for lower density concrete namely,

$\lambda = 1.0$  for normal density concrete

$\lambda = 0.85$  for semi-low density concrete

$\lambda = 0.75$  for low density concrete

The expression  $\lambda\phi_c(c+\mu\sigma)$  shall not be greater than  $0.25\phi_c f'_c$  nor  $7.0\phi_c$ . No account is made for concrete strength in these equations since the friction force available is considered to be a function of the normal force and the surface roughness.

An alternate to the above method has been included in the 1994 edition of the CSA code. This method is based on the work of Loov and Patnaik where the shear resistance was found to be a function of the concrete strength and the amount of reinforcement crossing the failure crack (Loov and Patnaik, 1994). The factored shear stress resistance is given as:

$$v_r = \lambda\phi_c k\sqrt{\sigma f'_c} + \phi_s \rho_v f_y \cos \alpha_f \quad (2.36)$$

where

$k = 0.5$  for concrete placed against hardened concrete

$k = 0.6$  for concrete placed monolithically

and the first term in the  $v_r$  equation cannot exceed  $0.25\phi_c f'_c$  nor  $7.0\phi_c$  MPa and  $\alpha_f$  is the angle between the shear friction reinforcement and the shear plane. The value of  $\sigma = \rho_v f_y \sin \alpha_f + N/A_g$  where  $\rho_v = A_{vf}/A_{cv}$ ,  $A_{vf}$  is the area of shear friction reinforcement,  $A_{cv}$  is the area of the concrete section resisting shear transfer and  $N$  is the unfactored permanent load perpendicular to the shear plane, positive for compression and negative for tension.

## 2.9 Tests of Dapped End Beams by Kumaraguru

Kumaraguru questioned the validity of equation 11-31 in CSA Standard A23.3-94 which is given as follows:

$$\epsilon_1 = \epsilon_s + \frac{(\epsilon_s + 0.002)}{\cot^2 \theta_s} \quad (2.37)$$

where  $\epsilon_1$  is the principal tensile strain,  $\epsilon_s$  is the strain in the longitudinal reinforcement and  $\theta_s$  is the smallest angle between the reinforcement and the compression strut

(Kumaraguru, 1992). This equation leads to a reduction in the allowable compressive stress due to the action of reinforcement in tension across the strut. Kumaraguru tested 6 dapped end beams with different dapped end lengths and showed that the variation in nib capacity does not match that predicted using the Canadian code (Figure 2.10).

Kumaraguru also found that a shear friction model accurately predicted the strength of the dapped end beams using a  $k = 0.55$  in Loov's equation (see section 3).

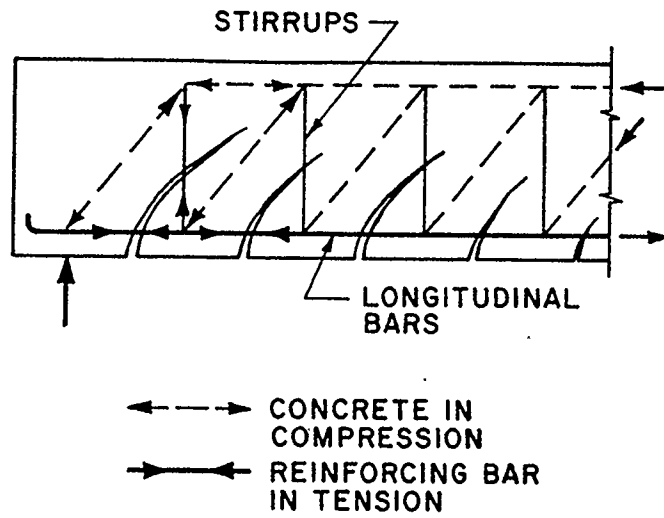


Figure 2.1: Truss Analogy (Pillai and Kirk, 1988)

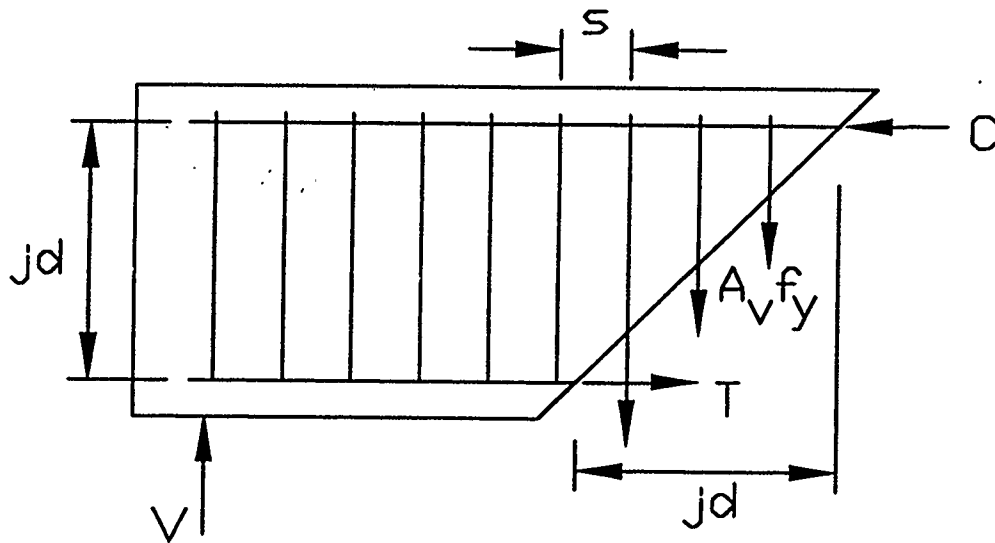


Figure 2.2: Stirrups across inclined plane

$\frac{v_f}{\lambda \phi_c f'_c}$		Longitudinal strain, $\epsilon_x$						
		$\leq$	$\leq$	$\leq$	$\leq$	$\leq$	$\leq$	$\leq$
		0.0000	0.00025	0.0005	0.00075	0.0010	0.0015	0.0020
$\leq 0.050$	$\beta$	0.405	0.290	0.208	0.197	0.185	0.162	0.143
	$\theta$	27.0°	28.5°	29.0°	33.0°	36.0°	41.0°	43.0°
$\leq 0.075$	$\beta$	0.405	0.250	0.205	0.194	0.179	0.158	0.137
	$\theta$	27.0°	27.5°	30.0°	33.5°	36.0°	40.0°	42.0°
$\leq 0.100$	$\beta$	0.271	0.211	0.200	0.189	0.174	0.143	0.120
	$\theta$	23.5°	26.5°	30.5°	34.0°	36.0°	38.0°	39.0°
$\leq 0.125$	$\beta$	0.216	0.208	0.197	0.181	0.167	0.133	0.112
	$\theta$	23.5°	28.0°	31.5°	34.0°	36.0°	37.0°	38.0°
$\leq 0.150$	$\beta$	0.212	0.203	0.189	0.171	0.160	0.125	0.103
	$\theta$	25.0°	29.0°	32.0°	34.0°	36.0°	36.5°	37.0°
$\leq 0.200$	$\beta$	0.203	0.194	0.174	0.151	0.131	0.100	0.083
	$\theta$	27.5°	31.0°	33.0°	34.0°	34.5°	35.0°	36.0°
$\leq 0.250$	$\beta$	0.191	0.167	0.136	0.126	0.116	0.108	0.104
	$\theta$	30.0°	32.0°	33.0°	34.0°	35.5°	38.5°	41.5°

Figure 2.3: Table 11-1 of CSA code (Canadian Standards Association, 1994)

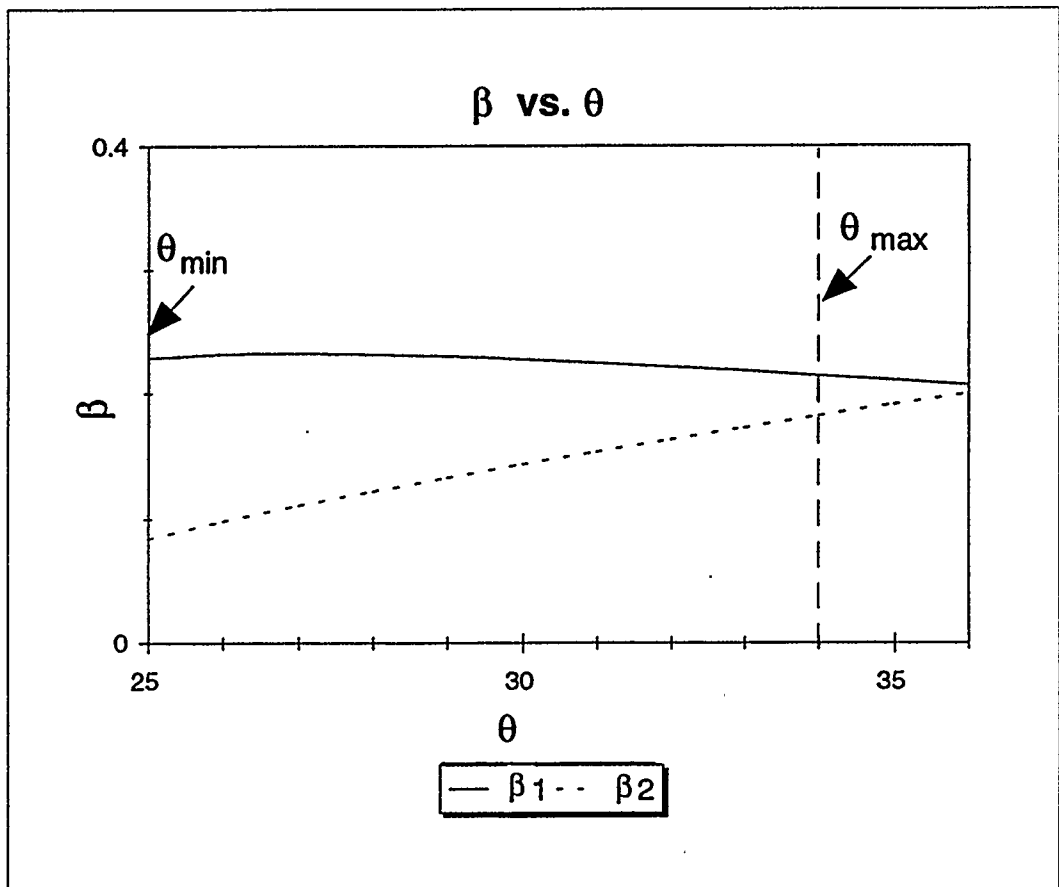


Figure 2.4: Optimum  $\beta$

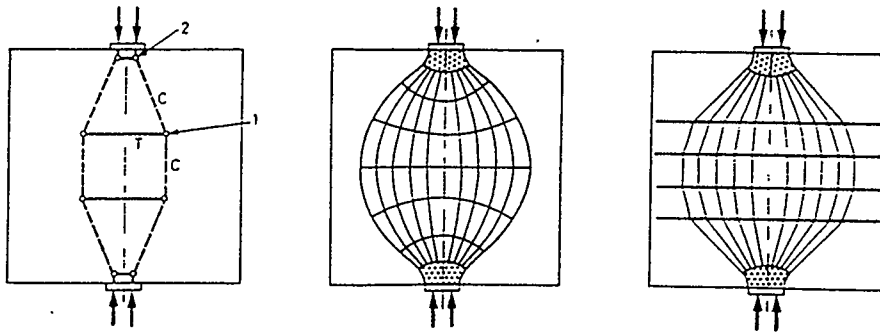


Figure 2.5: Strut-and-tie modelling of structure (Schlaich and Schaefer, 1991)

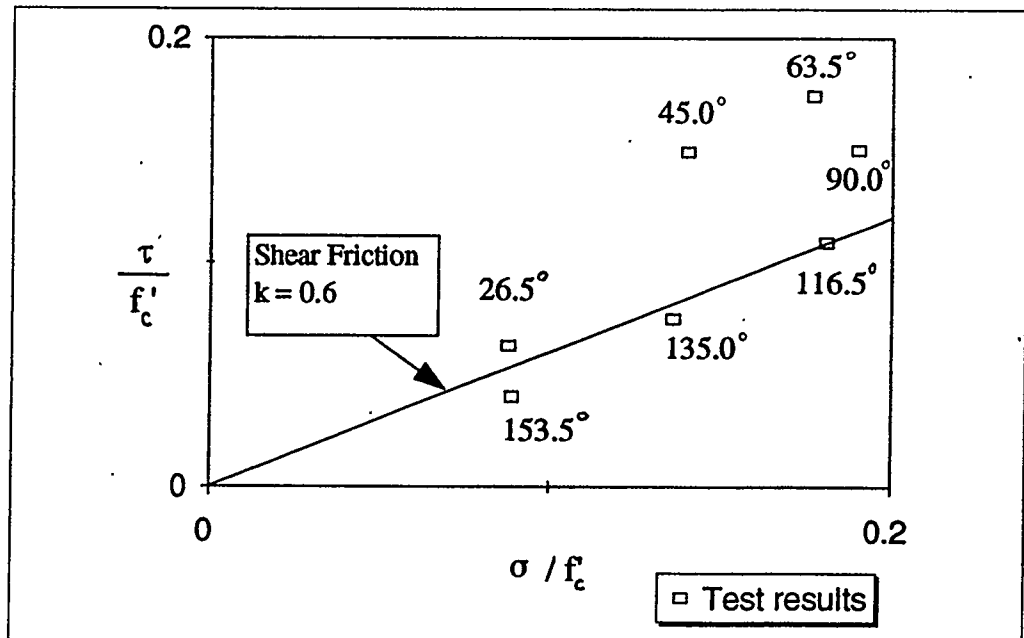


Figure 2.6 Mattock's tests

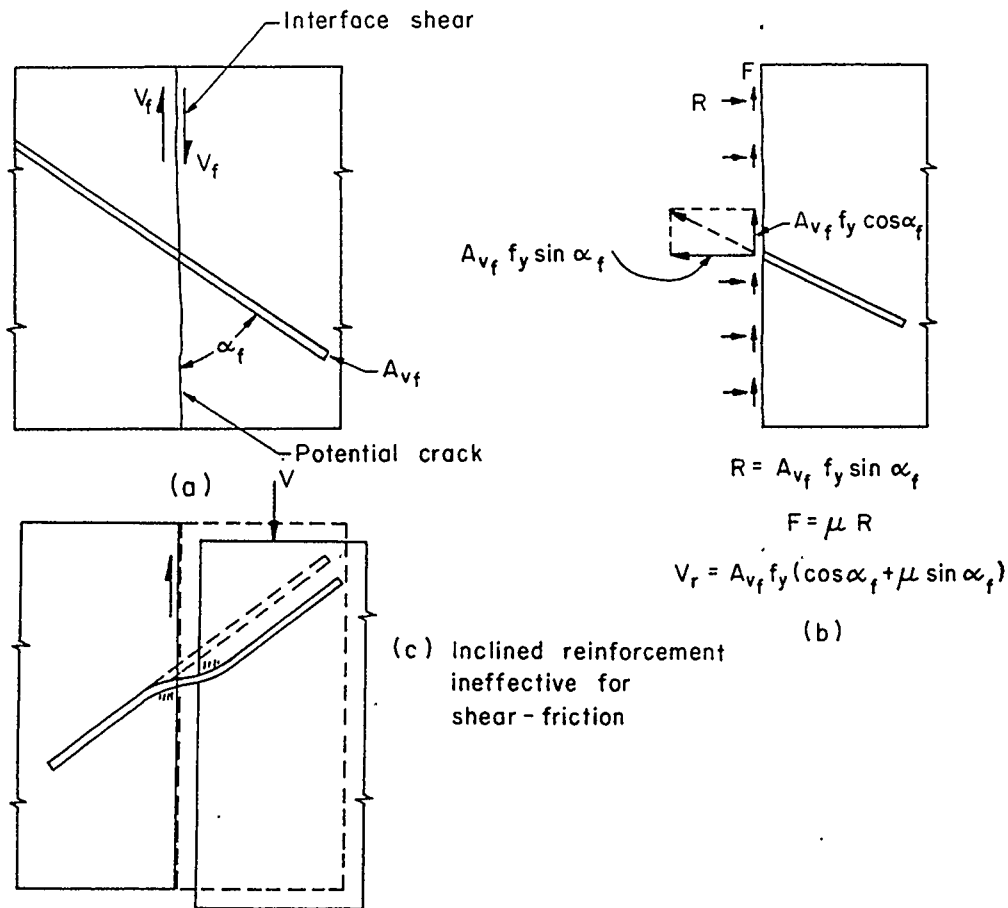


Figure 2.7: Shear friction and allowable angles of reinforcement (Pillai and Kirk, 1988)

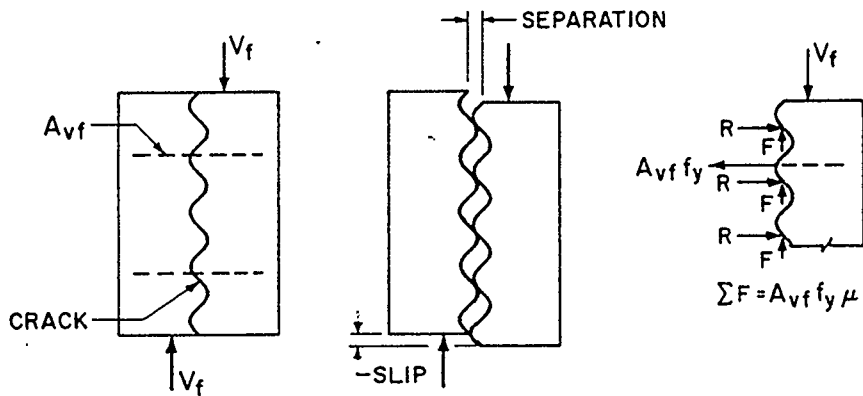
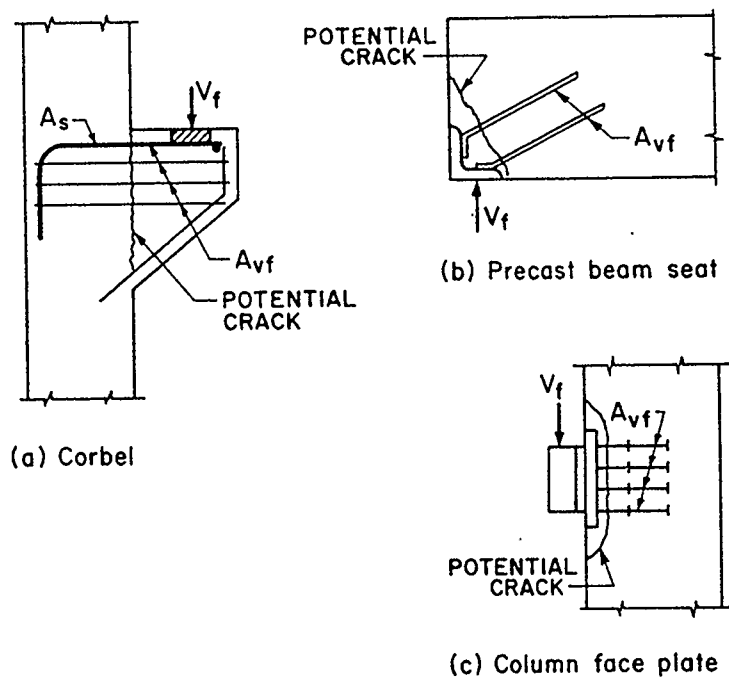
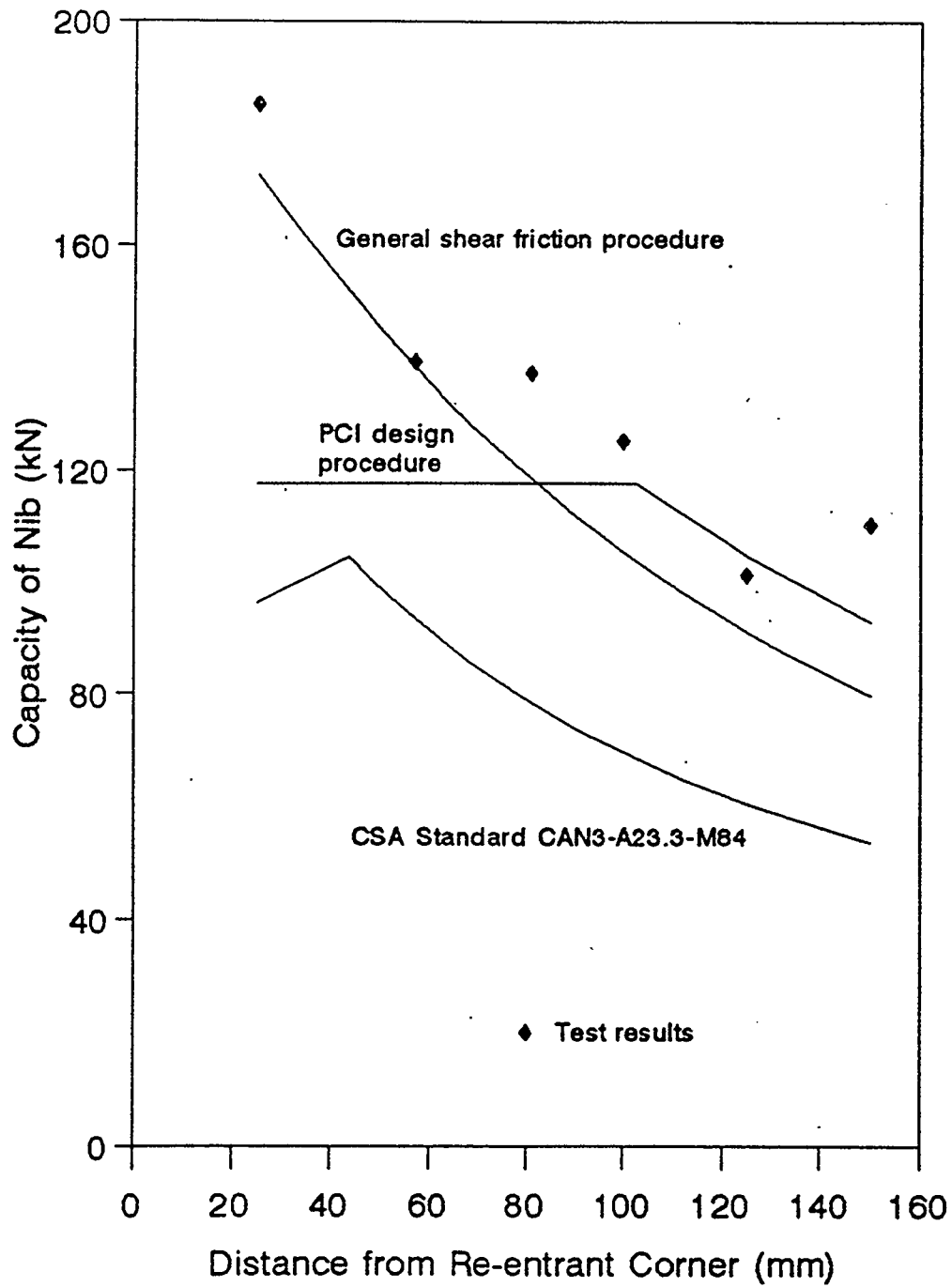


Figure 2.8: Shear friction induced by separation of rough crack (Pillai and Kirk, 1988)





**Figure 2.9: Example applications of shear friction method (Pillai and Kirk, 1988)**



**Figure 2.10: Kumaraguru's comparison of CSA method to test results (Kumaraguru, 1992)**

### 3. PROPOSED SHEAR FRICTION EQUATIONS

#### 3.1 Loov's Equation

Loov's equation for shear stress can be written as:

$$v = k\sqrt{\rho_v f_y f'_c} \quad (3.1)$$

where  $k$  is a constant and was estimated at 0.6 (Figure 3.1). The term  $\rho_v f_y$  is referred to as the clamping stress assuming the reinforcement yields. In this thesis, Loov's shear friction equation has been adapted for use in predicting the shear strength of beams. The clamping stress is provided by longitudinal reinforcement as well as by vertical stirrups but neither are necessarily assumed to have yielded. The force in each bar is based on the force that could be developed at the crack based on bond development lengths. Loov's equation can be written as:

$$v = k\sqrt{\sigma f'_c} \quad (3.2)$$

where  $v$  is the shear stress on the shear plane at failure and  $\sigma$  is the normal stress on the shear plane at failure. For an inclined plane with  $v = S_i/A$  and  $\sigma = R_i/A$  the above equation becomes:

$$\frac{S_i}{A} = k\sqrt{\frac{R_i}{A} f'_c} \quad (3.3)$$

where  $S_i$  is the shear force acting on an inclined plane of area  $A$  and  $R_i$  is the normal force acting on the inclined plane (Figure 3.2). For a beam subjected to loads to the right of the crack and solving for  $R_i$  and  $S_i$  using force equilibrium we obtain:

$$R_i = T \sin \theta - V_{cr} \cos \theta + T_{cr} \cos \theta \quad (3.4)$$

$$S_i = T \cos \theta + V_{cr} \sin \theta - T_{cr} \sin \theta$$

where  $T$  = tension force in longitudinal reinforcement at the inclined crack

$\theta$  = angle between longitudinal reinforcement and the inclined crack

$T_v$  = sum of vertical stirrup forces crossing inclined crack

Solving for  $V_{sf}$ , the shear strength of a beam based on shear failure on an inclined plane, and simplifying we can obtain:

$$V_{sf} = b_1 \left[ \sqrt{1 - c_1/b_1^2} - 1 \right] \quad (3.5)$$

where

$$b_1 = \frac{T_s \sin \theta + 0.5k^2 f'_c A \cos \theta}{\sin^2 \theta}$$

$$c_1 = \frac{T_s^2 - k^2 f'_c A T_R}{\sin^2 \theta}$$

with

$$T_s = T \cos \theta - T_v \sin \theta$$

$$T_R = T \sin \theta + T_v \cos \theta$$

All possible failure planes between the inside edge of the support plate and the inside edge of the load plate to a maximum angle of  $90^\circ$  are examined. The maximum shear strength on each plane is calculated and then the lowest shear strength when comparing all the possible failure planes is taken as the governing shear strength. Because  $T \sin \theta$  increases the clamping force while  $T \cos \theta$  increases the applied shear, it is possible that the maximum shear strength ( $V_{sf}$ ) of a beam may occur when the longitudinal reinforcement has not yielded (Figure 3.3). For a beam with  $k = 0.6$ ,  $T_v = 122.4 \text{ kN}$ ,  $A = 0.2 \text{ m}^2$ ,

$\rho = 0.021$ ,  $f_y = 500$  MPa,  $f'_c = 30$  MPa, and  $\theta = 29^\circ$ . This phenomenon is highly dependent on the minimum possible  $\theta$  and the longitudinal steel ratio and is more likely to occur for high clamping stresses, where the shear strength of the inclined plane ( $v$ ) remains relatively constant with increases in normal stress. In Figure 3.4, two examples are given of equilibrium on an inclined plane with two different tension forces ( $T$ ) in the longitudinal steel using the same values as above. For the first case  $T = 765$  kN giving a shear strength  $V = 246$  kN, and for the second case  $T = 1300$  kN giving a shear strength of 149 kN. Therefore the critical failure plane may occur when the longitudinal reinforcement where the plane intersects the longitudinal reinforcement has not yielded.

Another type of failure which can be called a diagonal bending failure can also occur in a beam. This failure is similar to bending failure but it is hypothesized to occur on an inclined plane. As an approximation, the  $\alpha_1$  and  $\beta_1$  factors that are normally applied on a vertical section for determining ultimate moment capacity are applied to an inclined section as well. The depth of the compression block,  $c$ , is therefore:

$$c = \frac{T}{\alpha_1 f'_c b_w \beta_1} \quad (3.6)$$

where  $T$  is the force in the longitudinal reinforcement at the inclined crack. The moment due to the stirrups about the intersection of the crack and the neutral axis is:

$$M_{\text{stirrup}} = \Sigma \left[ T_v \left( p + \frac{d - c}{\tan \theta} - x_i \right) \right] \quad (3.7)$$

and is shown in Figure 3.5, where  $p$  is the distance from the centre of the support to the start of the inclined crack at the level of the reinforcement,  $(d-c)/(\tan \theta)$  is the horizontal

projection of the inclined crack between the reinforcement and the neutral axis,  $x_i$  is the distance from each stirrup to the center of the support plate and  $T_v$  is the force in each stirrup crossing the crack. Taking moments about the neutral axis and rearranging the equation for  $V_{db}$ , which is the shear force at the support when diagonal bending failure occurs, gives:

$$V_{db} = \frac{T \left( d - \beta_1 \frac{c}{2} \right) + M_{stirrup}}{\left( \frac{d - c}{\tan \theta} + p \right)} \quad (3.8)$$

### 3.2 Development of Forces in Longitudinal Reinforcement

Wang stated that the force in the longitudinal reinforcement develops at a faster rate when it is subjected to a vertical pressure at bearing plate locations (Wang, 1993). It is assumed therefore that the force development in the longitudinal reinforcement develops at three different rates for beams without full anchorage at the supports. The first slope (slope1) is obtained by dividing the yield force by the development length (Clause 12.2.2 CSA A23.3-94) and applies to that portion of reinforcement overhanging the support plates assuming no stirrups are present. The second slope (slope 2) is obtained by dividing the first slope by a factor  $\beta_e$  which is dependent on the external pressure from the reactions at the support bearing plates. The external pressure is assumed to act only over the width of the bearing plate,  $w_1$ .  $\beta_e$  is given as:

$$\beta_e = \frac{1 + \frac{13 p_e}{f'_c}}{1 + \frac{17 p_e}{f'_c}} \quad (3.9)$$

where  $p_e = V_{sf}/(b_w w_1)$  and  $\text{slope2} = \text{slope1}/\beta_e$  where  $b_w$  is the width of the beam. The third slope (slope3) is obtained by dividing the yield force by the development length (CSA A23.3-94 Clause 12.2.2) and applies to that portion of reinforcement between the inside faces of the support and load plates assuming the CSA code requirements for stirrup size and spacing are satisfied (Figure 3.6). The code equations for development length are conservative when applied to test results because the capacity reduction factor is not defined but included implicitly.

For a given shear crack, the maximum force in the reinforcement at the crack depends on the force that can develop from the end of the bar to the intersection of the shear crack and the bar. Therefore a longer anchorage length can increase the clamping force across an inclined crack and can be expected to increase the shear capacity.

### **3.3 Development of Forces in Vertical Stirrups**

Due to the hook anchorage and the added length in addition to the hook, it is assumed that the full yield force in #15 stirrups and smaller develops over the distance from the top of the hook to the point of tangency between the hook and the vertical stirrup leg. This assumption is based on CSA A23.3-94 Clause 12.13.2. The force development in the stirrup is assumed to be symmetrical about the mid-height of the stirrup as shown in Figure 3.7.

For a given shear plane each stirrup will cross the crack at a different point along its length. Using the above assumptions, the force in each stirrup can be estimated and resolved into components perpendicular and parallel to the inclined shear plane.

### 3.4 Location of Normal Force on an Inclined Plane

A free body diagram of a beam to the left of a possible inclined crack and above a possible horizontal crack showing the forces on the section is given in Figure 3.8.

Moments can be taken about point Q to find the location of  $R_i$ , the normal force on the inclined plane. The vertical distance that  $R_i$  acts from the top of the beam is given as follows:

$$y_i = d - \left( \frac{R \cdot p + \sum T_v(x_i - p)}{R_i} \right) \sin \theta \quad (3.10)$$

where  $p$  is the distance from the center of the support plate to point Q,  $x_i$  is the distance from each stirrup to the centre of the support,  $R_i$  is the normal force on the inclined plane and  $R$  is the normal force on the horizontal plane. The resultant normal force on the inclined plane should be located at the centroid of the assumed stress distribution function (Figure 3.9). This may be assumed to be a trapezoidal distribution or a triangular distribution depending on the location of  $R_i$ .

### 3.5 Comparison of Shear Friction Model to Existing Test Data

Experimental data from existing tests was examined to determine the validity of applying the shear friction model to beams. The ratio of P-test/P-SF represents the ratio of the beam strength in the test to the beam strength predicted by the shear friction model. The coefficient of variation (C.O.V.) was calculated using the following equation:

$$\text{C.O.V.} = \sqrt{\frac{\sum \left( \frac{\text{ratio}_i}{\text{avg}} - 1 \right)^2}{n - 1}} \quad (3.11)$$



where  $ratio_i$  is the ratio of P-test/P-SF for each beam,  $avg$  is the sample mean of the ratios of P-test/P-SF for the beams, and  $n$  is equal to the number of test beams. The given equation uses Bessel's correction which accounts for the fact that a sample out of a population of possible test beams was analyzed.

### 3.5.1 Arthur Clark's Tests

In 1951 Arthur Clark presented a paper in the Journal of the American Concrete Institute discussing his tests of beams which failed in shear (Clark, 1951). These beams had different longitudinal and transverse reinforcement ratios, four span lengths and various concrete strengths. For all the beams  $b_w$  was equal to 203 mm and  $h$  was equal to 457 mm. Based on the information given in his paper, full anchorage of the longitudinal reinforcement was assumed and  $f_y$ , the yield stress of the reinforcement, was given as 46.5 ksi (321 MPa). Clark used 3/8" ( $d_b = 9.53$  mm) stirrups with  $f_{vy}$ , the yield stress of the stirrups, equal to 48.0 ksi (331 MPa) without support bars to anchor the hooks. For this thesis it was assumed that each stirrup would develop 1/2 of its yield force by the start of the straight portion of the stirrup leg. This assumption was made since it was felt that the lack of stirrup anchorage would somewhat reduce the rate of force development around the hook. The bearing plates were 3.5" (88.9 mm) wide and 1" (25.4 mm) thick. The concrete cover below the longitudinal reinforcement was assumed to be 19.1 mm. This data was entered into the shear friction model with  $k = 0.6$  and the results are shown in Table 3.1. In this table,  $a$  is equal to the shear span length,  $s$  is equal to the spacing of stirrups and  $\rho$  is equal to the longitudinal steel ratio.

Table 3.1 Shear Friction Model of Clark's Tests							
Beam	a (mm)	$f'_c$ (MPa)	s (mm)	$\rho$	V-test (kN)	V-SF (kN)	$\frac{\text{V-test}}{\text{V-SF}}$
A1-1	914	24.6	183	0.0310	222.5	240.7	0.92
A1-2	914	23.6	183	0.0310	209.1	235.4	0.89
A1-3	914	23.4	183	0.0310	222.5	234.2	0.95
A1-4	914	24.8	183	0.0310	244.7	241.2	1.01
B1-1	762	23.4	191	0.0310	278.8	278.1	1.00
B1-2	762	24.7	191	0.0310	256.6	286.9	0.89
B1-3	762	23.7	191	0.0310	284.8	280.3	1.02
B1-4	762	23.3	191	0.0310	268.1	277.8	0.97
B1-5	762	24.6	191	0.0310	241.5	286.5	0.84
B2-1	762	23.2	95	0.0310	301.1	337.2	0.89
B2-2	762	26.3	95	0.0310	322.2	359.5	0.90
B2-3	762	24.9	95	0.0310	334.9	349.3	0.96
C1-1	610	25.6	203	0.0207	277.7	273.1	1.02
C1-2	610	26.3	203	0.0207	311.1	278.3	1.12
C1-3	610	24.0	203	0.0207	245.9	259.8	0.95
C1-4	610	29.0	203	0.0207	285.9	296.0	0.97
C3-1	610	14.1	203	0.0207	223.7	179.3	1.25
C3-2	610	13.8	203	0.0207	200.3	177.0	1.13
C3-3	610	13.9	203	0.0207	188.1	178.2	1.06
						Avg. =	0.99
						C.O.V. =	0.10

The average V-test/V-SF was 0.99 with a C.O.V. of 0.10. Thus for a variety of stirrup spacings, compressive strengths, longitudinal steel ratios and a/d ratios, the shear

friction model predicted the shear strengths of these 19 beams amazingly well (Figure 3.10). A slightly lower  $k$  value or smaller  $A$  would need to be used for design to eliminate the unconservative predictions.

Clark's beam tests showed that the shear strength increased with decreasing  $a/d$  ratio, smaller spacing of stirrups and increased concrete compressive strength. The shear friction model followed the same general trends. When the  $a/d$  ratio was reduced from beam set A1 to beam set B1 while the longitudinal steel ratio, concrete strength, stirrup size and spacing were kept constant, the average shear strength increased as predicted by the shear friction model. The shear friction along an inclined crack increases for beams with smaller  $a/d$  ratios because the slope of the crack cannot be as flat as the slope in longer beams. The longitudinal reinforcement is more perpendicular to the crack and can provide more clamping force than a beam with a higher  $a/d$  ratio. When the spacing of stirrups was reduced from beam set B1 to beam set B2 while keeping other variables constant, the average shear strength increased. This agrees with the shear friction model because a smaller stirrup spacing increases the number of stirrups across an inclined plane, thereby increasing the shear stress that can be resisted along the crack. The transition from beam set C1 to C3 shows that the reduction of a beam's concrete strength reduces its shear strength. This agrees with the shear friction model based on the assumption that the shear stress varies with the square root of  $f'_c$ .

### 3.5.2 Kani's Tests

Two sets of data were studied from Kani's extensive series of tests (Kani et al, 1979). The tests of beams 713 to 717 involved varying the spacing and position of 4 stirrups along the shear span and the tests of beams 543 to 545 investigated the effects of placing one stirrup at a constant distance from the support while varying the  $a/d$  ratio. Full anchorage capability of the longitudinal reinforcement in each beam was assumed due to the use of anchor plates at the ends of each beam. The results of the shear friction model using  $k = 0.6$  are compared to test results in Table 3.2 and Figure 3.11. The value  $x/d$  is the distance from the first stirrup to the center of the support divided by the effective depth ( $d$ ). The value  $s/d$  is the spacing of the stirrups divided by  $d$  and  $u/d$  is the distance from the last stirrup to the closest load point divided by  $d$ . For all beams  $b_w$  was equal to approximately 152 mm and  $d$  was equal to 274 mm. The dimensions of the support and loading plates have not been provided. Both have been assumed to be 4 inches (102 mm) wide. The bottom and top concrete cover was assumed to be 19.1 mm.

For beams 713 to 717,  $a/d = 5.0$ ,  $f_y = 400$  MPa,  $f_{vy} = 421$  MPa,  $f'_c = 26.5$  MPa, and  $\rho = 0.027$  with slight variations in these values for each beam. Kani used four closed #3 stirrups ( $d_b = 9.53$  mm) with hooks around the tension reinforcement but no support bars to provide anchorage at the top. It was felt that this anchorage was more effective than the anchorage of the stirrups in Clark's tests, but not as effective as stirrups anchored around support bars. Therefore it was assumed that  $2/3$  of the stirrup's yield force could be developed at the start of the straight portion of the stirrup leg. For beams 543 to 545,  $f_{vy} = 365$  MPa,  $f_y = 355$  MPa,  $f'_c = 28.7$  MPa,  $\rho = 0.027$  and one #3 stirrup

( $d_b = 9.53$  mm) was used. There were slight variations in these values for each beam. The  $a/d$  ratio varied from 1.98 for beam 543 to 2.72 for beam 545.

Beam	$a/d$	$x/d$	$s/d$	$u/d$	V-test (kN)	V-SF (kN)	Failure Type	V-test/V-SF
713	4.92	2.95	0.49	0.50	57	45	Shear	1.27
714	4.98	2.49	0.62	0.63	54	58	Shear	0.93
715	4.98	1.99	0.75	0.74	62	72	Shear	0.86
716	4.85	1.48	0.87	0.86	66	72	Bending	0.92
717	4.85	0.98	0.99	1.00	67	72	Bending	0.93
543	1.98	1.24	-	0.74	150	125	Shear	1.20
543A	2.23	1.24	-	0.99	145	126	Bending	0.92
544	2.47	1.23	-	1.24	117	129	Shear	0.88
545	2.72	1.24	-	1.48	102	129	Shear	0.79
							Avg. =	0.97
							C.O.V. =	0.16

The average V-test/V-SF was 0.97 with a C.O.V. of 0.16. A slightly lower  $k$  value or smaller  $A$  would need to be used for design to eliminate the unconservative predictions.

Beams 713 to 717 showed a general but small increase in shear strength as the first stirrup was moved closer to the support, the spacing of stirrups increased and the last stirrup was moved away from the load. The spacing would have little effect on the strength since the same number of stirrups was used in each case. However the movement

of the last stirrup away from the load, indicated by the increasing  $u/d$  ratio, could be expected to result in a steeper and stronger failure plane since the weakest plane occurred when the last stirrup was avoided. The stirrups in Kani's tests were 3/8 inches (9.53 mm) in diameter so they had a significant impact on the slope of the failure plane. As the  $u/d$  ratio increased, the predicted beam strength based on shear failure became larger than the predicted beam strength due to moment failure. The shear friction model agreed with the test results, with the prediction of moment failure being the reason for the constant predicted shear strength (based on moment failure) of 71.6 kN for beams 715 to 717.

For beams 543 to 545, Kani used 1 stirrup at a constant distance from the support and varied the  $a/d$  ratio. According to the shear friction model, this would have little impact on the shear strength of the beam, because the weakest shear plane occurred at the same angle for these beams (i.e. avoiding the stirrup). Small changes in predicted shear strengths were due to slight changes in  $f_y$  and  $f'_c$ . The shear strength based on diagonal bending failure would be affected due to the change in moment arms, but the diagonal bending moment was not critical in these tests. There also was a slight change in concrete and steel yield strengths in beams 543 to 545. It is interesting to note in Kani's test results for these beams that one of the beams experienced a moment failure, but that subsequent beams with longer  $a/d$  ratios did not experience moment failure. A possible explanation for the reduction in beam strength with increasing  $a/d$  ratio but constant stirrup location, is that beams other than beam 543A may have experienced moment failure. He labelled the failure mode of these beams as a slow diagonal failure, and the beams' failure loads were stated as a percentage of moment capacity ranging from 85.7% to 92.5%. These values

suggested that the beams were at or very near moment failure. Another possible explanation for the reduction in beam strength with increasing  $a/d$  ratio and constant stirrup location is that the stirrup had less impact than expected on the failure plane angle. If the stirrup had no impact on the location of the failure plane, the increasing  $a/d$  ratio would allow the failure plane angle to be as flat as possible and would weaken the shear strength of the beam.

### 3.5.3 Sarsam and Al-Musawi's Tests

Test data from the ACI Journal in November 1992 was also examined (Sarsam and Al-Musawi, 1992). Sarsam and Al-Musawi investigated the effect of high-strength concrete on the shear strength of beams. Full anchorage of the longitudinal and transverse reinforcement was assumed based on the given information. It was assumed that the stirrup would develop its full yield capacity over the distance from the top of the stirrup to the start of the straight portion of the stirrup leg. The results of the 14 beam tests and the predicted values from the shear friction model using  $k = 0.6$  are shown in Table 3.3.

For all the beams  $b_w = 180$  mm,  $h = 270$  mm and  $d = 233$  mm. The stirrups measured 4 mm in diameter and had an  $f_{vy} = 820$  MPa. Various longitudinal bars were used with diameters of 16 mm ( $f_y = 525$  MPa), 20 mm ( $f_y = 495$  MPa) and 25 mm ( $f_y = 543$  MPa) to give the required longitudinal steel ratios ( $\rho$ ). The bearing plates were 100 mm wide, 25 mm thick and 180 mm long. The bottom, top and side concrete cover was equal to 25 mm.

Table 3.3 Shear Friction Model of Sarsam and Al-Musawi's Tests							
Beam	a/d	s (mm)	$f'_c$ (MPa)	$\rho$	V-test (kN)	V-SF (kN)	V-test/V-SF
AL2-N	4.0	150	40.4	0.0223	115	99	1.16
AL2-H	4.0	150	75.3	0.0223	123	108	1.14
AS2-N	2.5	150	39.0	0.0223	189	148	1.28
AS2-H	2.5	150	75.5	0.0226	201	176	1.14
AS3-N	2.5	100	40.2	0.0223	199	160	1.24
AS3-H	2.5	100	71.8	0.0223	199	175	1.14
BL2-H	4.0	150	75.7	0.0282	138	141	0.98
BS2-H	2.5	150	73.9	0.0282	224	229	0.98
BS3-H	2.5	100	73.4	0.0282	228	229	1.00
BS4-H	2.5	75	80.1	0.0282	207	229	0.90
CL2-H	4.0	150	70.1	0.0351	147	168	0.88
CS2-H	2.5	150	70.2	0.0351	247	233	1.06
CS3-H	2.5	100	74.2	0.0351	247	250	0.99
CS4-H	2.5	75	75.7	0.0351	221	277	0.80
						Avg. =	1.05
						C.O.V. =	0.13

The average V-test/V-SF was 1.05 with a C.O.V. of 0.13. The shear friction model again gave good results (Figure 3.12). The predicted strengths were based on either a shear failure or a diagonal bending failure on a vertical section at midspan. The strengths of beams BS4-H and CS4-H with a stirrup spacing of 75 mm were lower than companion beams with stirrup spacings of 100 mm and 150 mm. This is opposite to what is expected, therefore the predicted values are slightly unconservative for these cases. One...



possibility is that the 75 mm spacing of stirrups was too congested and affected the crack pattern thereby weakening the beam. From the limited number of normal strength concrete beams tested, it did seem however that similar beams generally showed a slight increase in shear strength with an increase in concrete strength and decreasing  $a/d$  ratio.

It is possible some of these beams failed in moment because the test capacities for beams AL2-N, AL2-H, AS2-N, AS2-H, AS3-N and AS3-H exceeded the theoretical moment capacities. These 6 beams had the lowest longitudinal steel ratio of all the test beams and used very small stirrups which were 4 mm in diameter. Beams AL2-N and AL2-H had an  $a/d$  ratio of 4 increasing the likelihood of moment failure. Beams AS3-N and AS3-H had a shorter  $a/d$  ratio of 2.5, but had a smaller spacing of stirrups. The possibility of moment failure would explain the small increases in shear strength with increasing  $f'_c$ .

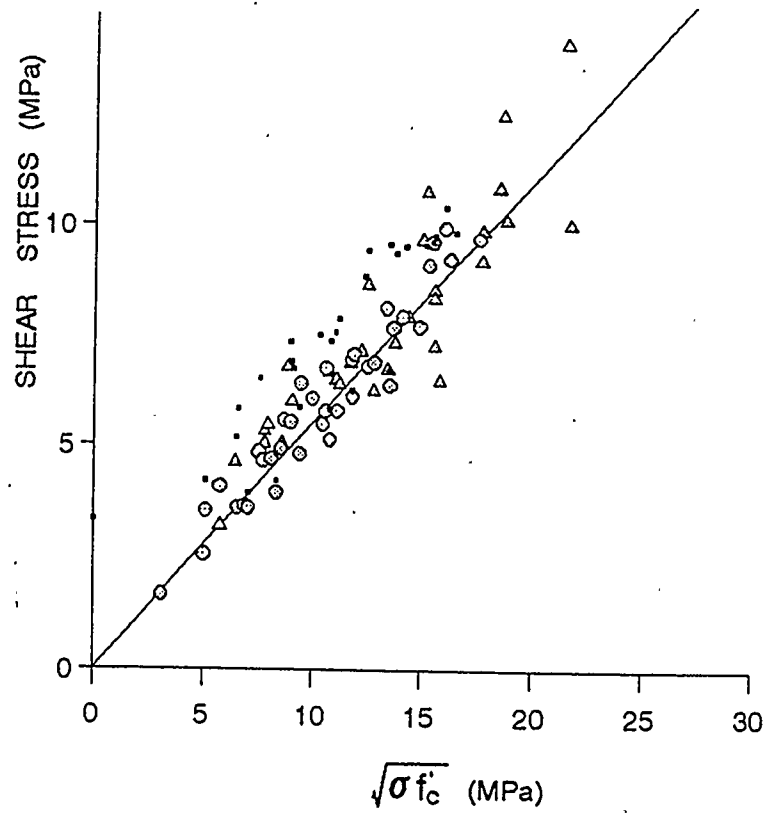


Figure 3.1: Loov's shear friction equation

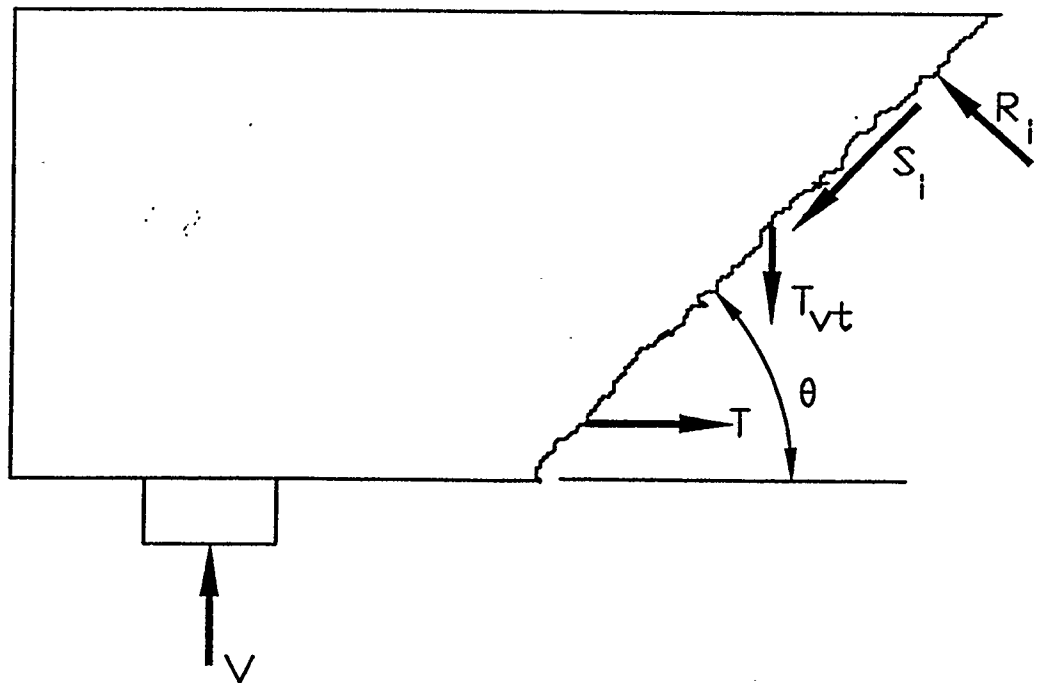
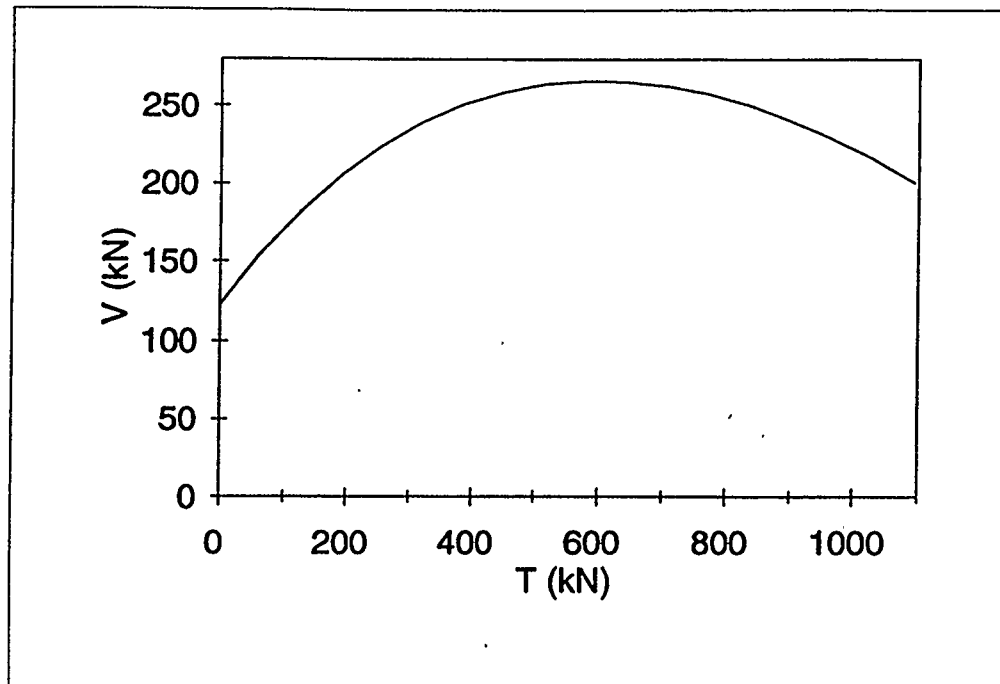
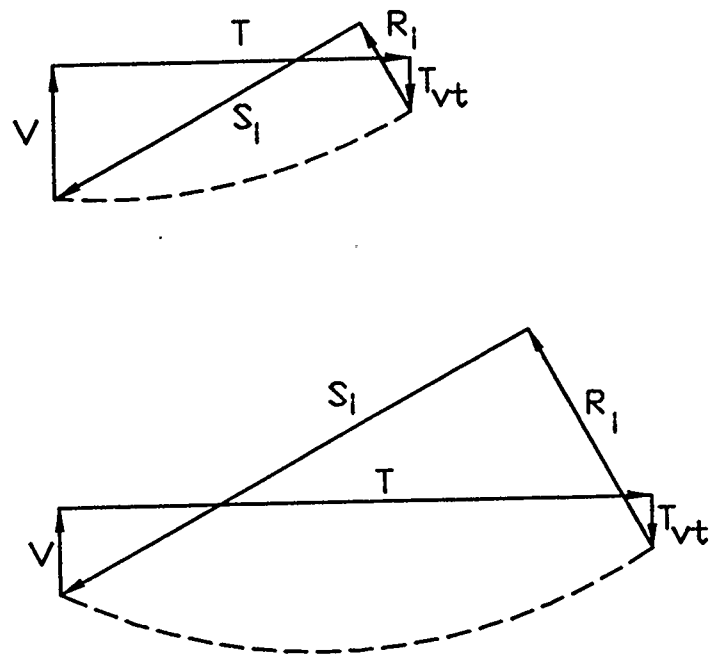


Figure 3.2: Forces on inclined plane



**Figure 3.3: Shear strength vs. tension force**



**Figure 3.4: Possible effect of increased force in longitudinal reinforcement on shear strength**

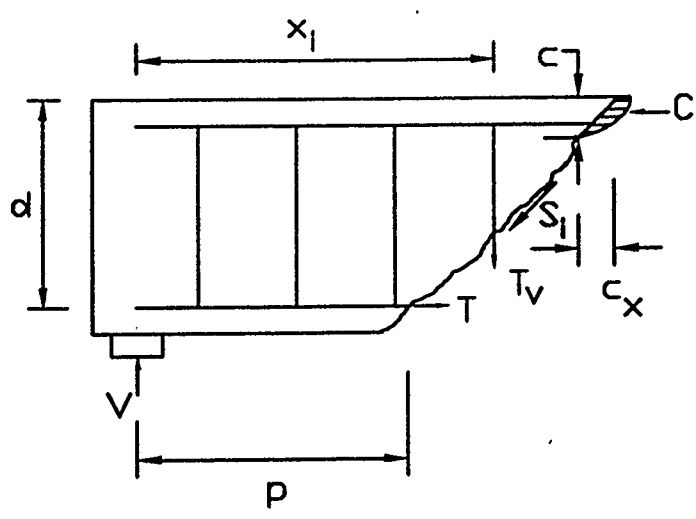


Figure 3.5: Moment due to stirrups

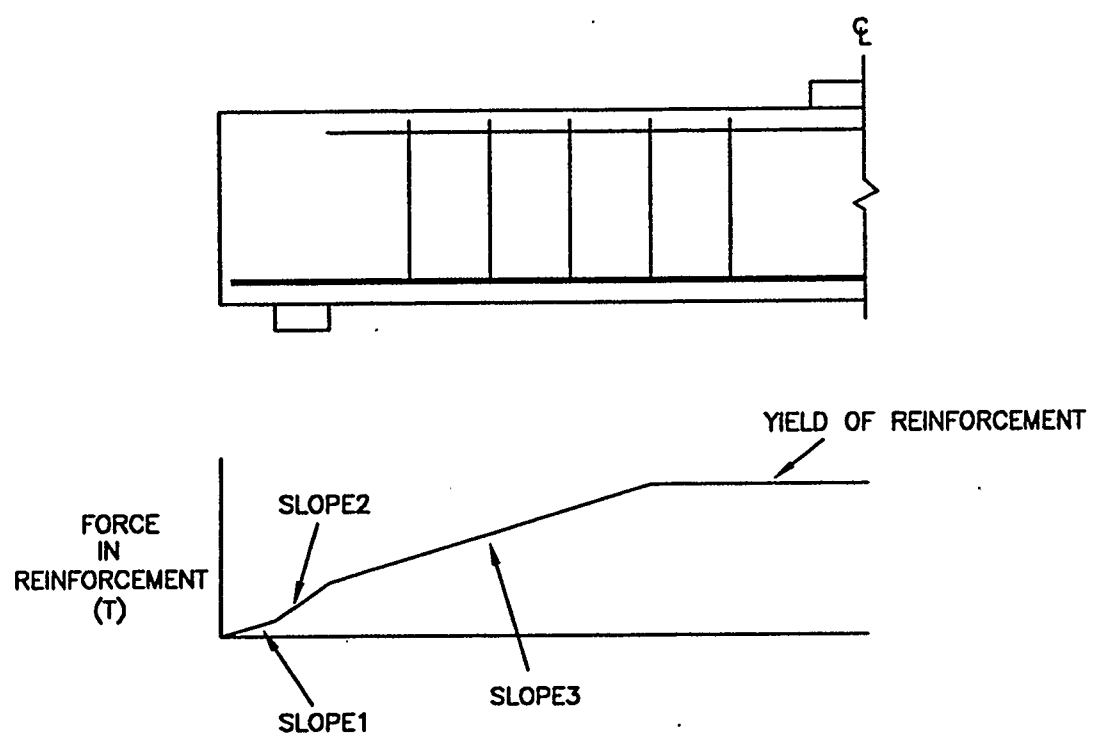


Figure 3.6: Rate of force development in longitudinal reinforcement

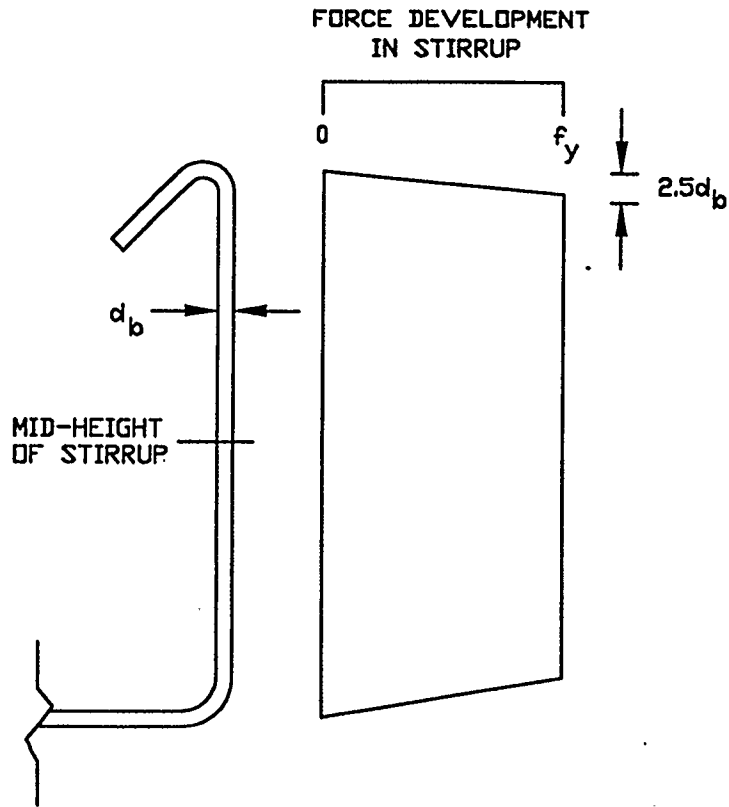


Figure 3.7: Rate of force development in stirrups

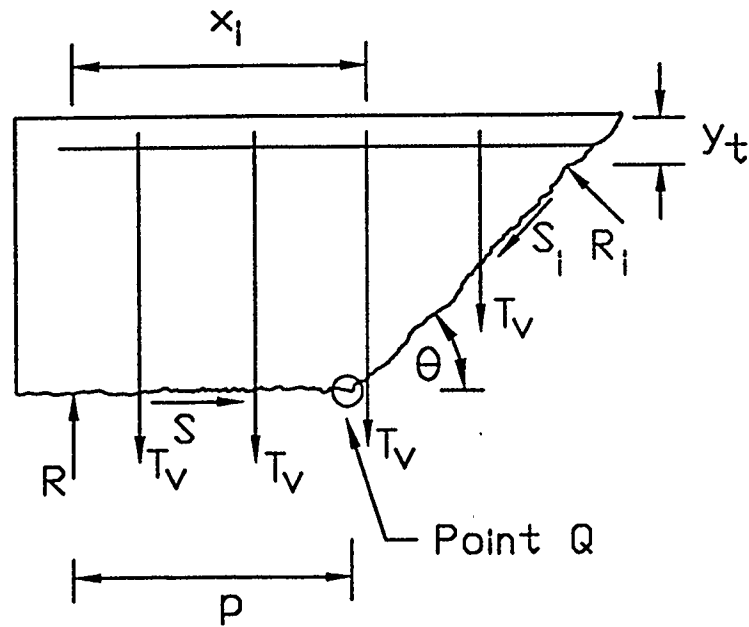


Figure 3.8: Free-body diagram of section of beam

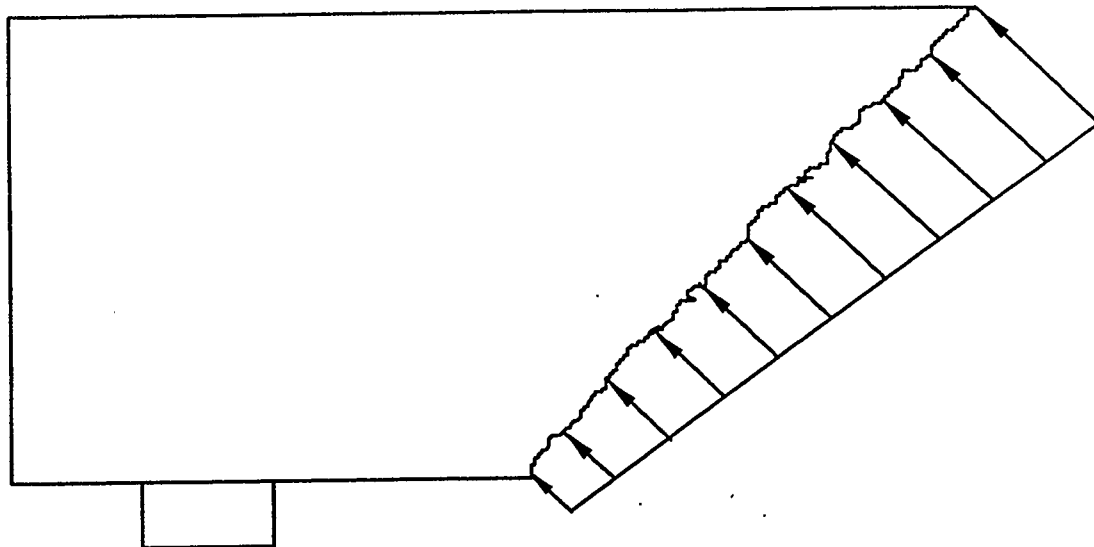


Figure 3.9: Assumed normal stress distribution

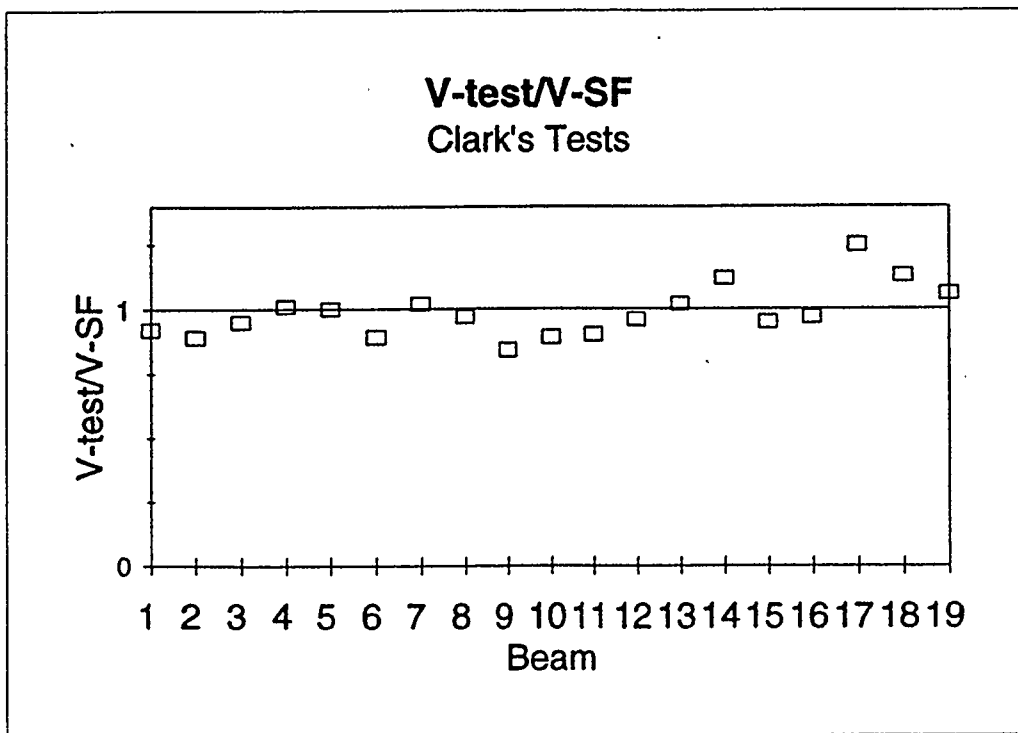
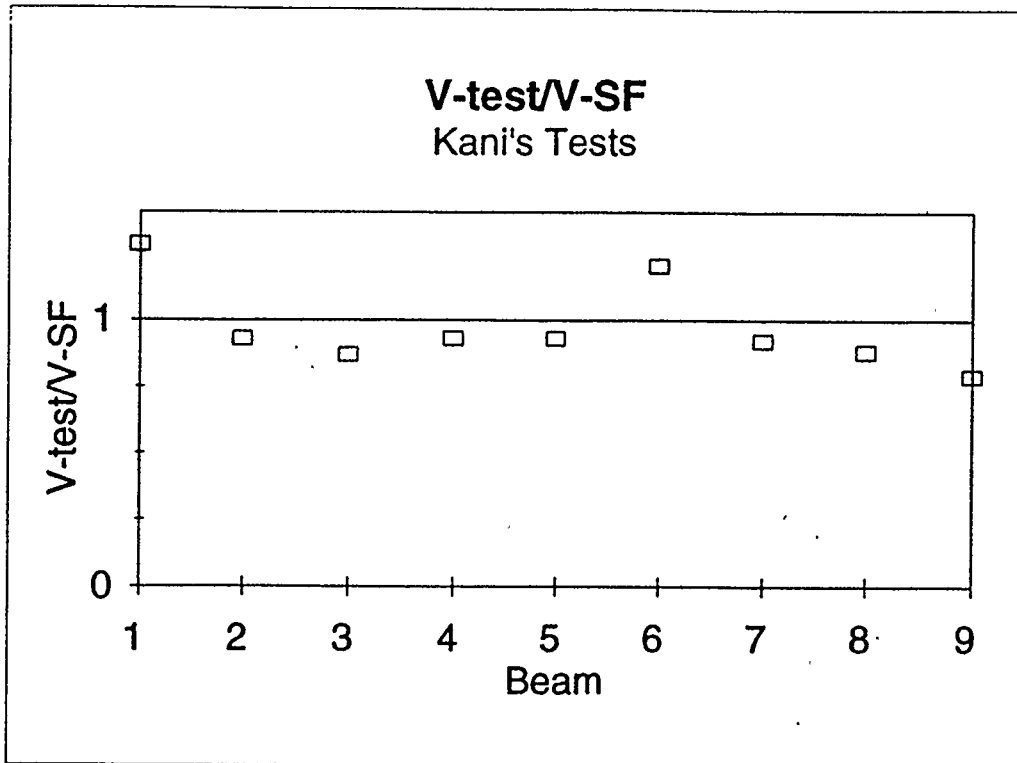
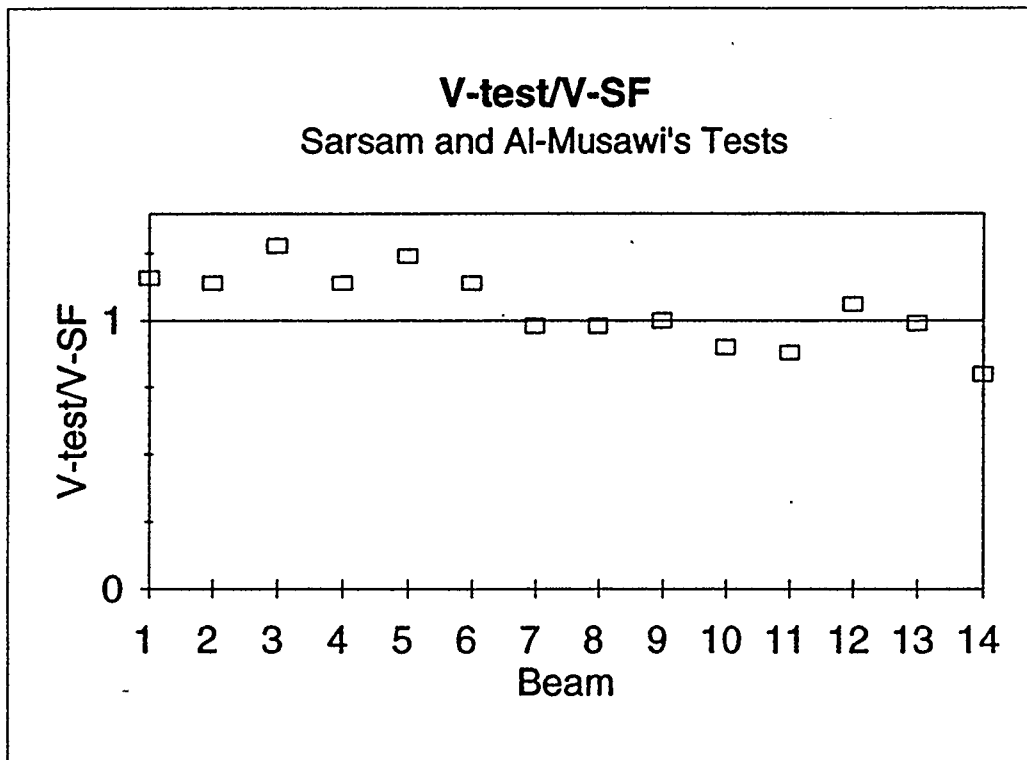


Figure 3.10 Comparison of predictions using shear friction method to test results by Clark



**Figure 3.11: Comparison of predictions using shear friction method to test results by Kani**



**Figure 3.12: Comparison of predictions using shear friction method to test results by Sarsam and Al-Musawi**

## 4. EXPERIMENTAL PROGRAM

### 4.1 Overview of Experimental Program

Twelve rectangular reinforced concrete beams were tested to investigate the validity of the proposed shear friction equations for intermediate length beams. The beams had varying  $a/d$  ratios, concrete strengths and end anchorage lengths for the longitudinal reinforcement. All beams had the same cross-section, spacing and size of vertical stirrups, and longitudinal reinforcement ratios. A single load at midspan was used to test the beams.

### 4.2 Objectives

The main objective of the beam testing was to determine the validity of a shear friction model for determining the shear strength of beams. In the past, shear friction was mainly examined during pushoff or pulloff tests in which the reinforcement was perpendicular to the crack or at angles which would cause the reinforcement to go into tension upon the sliding movement of the specimen on opposite sides of the crack. As was shown previously, reinforcement at angles greater than  $90^\circ$  also seems effective (see section 2.5). Therefore the longitudinal reinforcement in concrete beams can be expected to play an important role in increasing the friction that can be resisted by a crack. Other objectives include:

1. To investigate the effects of different end anchorages (length of reinforcement past support) on the beam behaviour and shear strength.
2. To investigate the effects of different  $a/d$  ratios on the beam behaviour and



shear strength.

3. To investigate the effects of concrete strength on the beam behaviour and shear strength.
4. To predict the shear strength of the 12 beams using the CSA, ACI and proposed shear friction methods and compare the predictions.
5. To investigate the effectiveness of small stirrups ( $d_b = 5.68$  mm), the  $135^\circ$  hook anchorage, and 150 mm spacing in providing shear strength.

### 4.3 Test Specimens

Twelve reinforced concrete beams were tested. For all 12 beams  $b_w = 360$  mm,  $h = 400$  mm and  $d = 345$  mm. Three different  $a/d$  ratios (3.05, 2.61 and 2.17) were used and each beam had a different overhang referring to the length of reinforcement past the outside edge of the support plate. Six beams were of normal strength concrete (about 30 MPa) and six were of high strength concrete (about 77 MPa) as seen in Table 4.1. The concrete compressive strength for each beam was obtained by testing 3 cylinders and averaging their strengths. The overhang shown in Table 4.1 is the length of reinforcement past the outer face of each support.

The concrete composition consisting of water, Type 10 Portland cement, concrete sand, coarse aggregate (14 mm maximum size), silica fume and Rheobuild 1000 superplasticizer for the normal and high strength concrete mixes used in the tests are shown in Table 4.2.

Beam	$f'_c$ (MPa)	Beam length (m)	a/d	overhang (mm)
1	28.9	2.80	3.05	300
2	30.2	2.40	2.61	250
3	28.9	2.26	3.05	30
4	28.9	2.16	2.17	280
5	30.1	1.98	2.61	40
6	33.6	1.78	2.17	90
7	74.3	2.56	3.05	180
8	77.8	2.36	2.61	230
9	77	2.22	3.05	10
10	76.3	1.94	2.61	20
11	81.5	1.88	2.17	140
12	77.7	1.64	2.17	20

Material	Normal Strength Concrete	High Strength Concrete
Water	7.84%	6.16%
Cement	11.92%	17.23%
Concrete Sand	31.64%	31.38%
Coarse Aggregate	48.56%	43.31%
Silica Fume	0.00%	1.93%
Superplasticizer	208 ml	3.74l

The reinforcing steel for every beam consisted of 5 Grade 400 No. 25 bars ( $f_y = 433$  MPa) providing an area of  $2500 \text{ mm}^2$ . A bar spacing of approximately 64 mm provided a clear distance of over 1.4 times the bar diameter between the No. 25 bars as required by the CSA code. The stirrups measured 5.68 mm in diameter and had a yield stress of almost 600 MPa. The area of each stirrup (2 legs) is  $50.7 \text{ mm}^2$  which satisfies the minimum requirement given by the CSA code is given as:

$$A_{v \text{ min}} = 0.06 \sqrt{f'_c} \frac{b_w s}{f_y} \quad (4.1)$$

where  $A_{v \text{ min}}$  equals approximately  $30 \text{ mm}^2$  for the beams with normal strength concrete and approximately  $48 \text{ mm}^2$  for the beams with high strength concrete. The spacing of 150 mm also satisfies clause 11.2.11 which states that  $s \leq 600 \text{ mm}$  or  $0.7d$  for the shear stresses that occurred during each beam test. For the stirrups, at least 60 mm of straight bond length was provided beyond the  $135^\circ$  hook as required. Two #10 bars were used to provide support and anchorage for each leg of the stirrup and were extended to each support (Figure 4.1):

For each of the three different  $a/d$  ratios, two beams were tested with normal strength concrete and two beams were tested with high strength concrete. For each  $a/d$  ratio, two different end anchorages were used. One beam had a short overhang length which provided enough development force capability to resist the tension induced by shear (CSA Clause 11.4.9.1) and the other had a longer overhang to prevent a diagonal bending failure as described in Section 3.1.

The beams were covered with burlap and cured until being tested, and the

cylinders were placed in a fog room at 100% humidity. The beams were tested at approximately 14-17 days from the time of casting and the appropriate concrete cylinders were tested on the day of the beam test.

#### **4.4 Test Setup and Procedure**

Each concrete beam was supported by and plastered to two hardened steel plates (which then sat on rollers allowing for horizontal movement during testing. The plates were 100 mm wide, 38 mm thick and 420 mm long. Another steel plate was plastered to the top surface of the beam at the midspan. The plates were used to prevent concentrated compressive stresses which could crush the concrete at the load points. Each beam was tested in an Amsler testing machine (type 200 DB 76) shown in Figure 4.2. An oil pump driven by an electric motor is built into the pendulum dynamometer and pumps oil into a piston thus driving the loading ram upwards. The ram lifts a stiffened steel beam which supports each test beam and produces a load at midspan and reactions at the supports when the concrete beam is in contact with the cross-head.

The load was applied in stages so that cracks could be marked, crack widths measured and photographs taken. Crack measurements were taken up to 50-60% of the predicted failure load (ie. up to typical service loads). During testing, it was observed that from a certain load level and upwards the crack pattern remained relatively unchanged. Therefore once the major cracks stopped propagating the beam was taken to failure without further stoppages unless a change in crack pattern occurred.

#### **4.5 Instrumentation**

For all tests the loads that were applied were measured by a pendulum dynamometer located within the testing machine and recorded with the Labtech Notebook data acquisition program. The analog signal from the gauges was converted to a digital signal using the Measurement Systems Datascan 7000 data acquisition unit. Calibration factors for the load and displacement transducers, as well as gauge factors for the strain gauges were input into the Labtech Notebook file for each test.

Two displacement transducers were placed at the centerline of the beam underneath each bottom edge of the beam to measure vertical displacements during the tests. A graph of load versus displacement was plotted during the test to give some visual assistance in determining the onset of failure.

Strains in the reinforcing steel were measured using electrical resistance gauges. These strains were recorded with the Labtech Notebook program as well. Before the strain gauges were attached, the reinforcing bars and stirrups were ground smooth at the desired location and then the gauges were glued to the bars. A length of wire was connected to each gauge that would eventually be connected to the data acquisition system. They were covered with wax and wrapped in electrical tape to prevent water from damaging the gauges upon casting. The gauges were attached on 3 of the 5 bars near the end of the bar and at the centre (Figure 4.3). These gauges were attached at the neutral axis of the bar to prevent erroneous results due to the bending of the bar. The gauges at the centre measured strains at the location of maximum moment and the end gauges measured the strains in the reinforcement at or near the critical crack location.

Strain gauges in the stirrups were attached at the level of the stirrup near where the critical crack was expected to occur. This was on a straight line from the inside edge of support to the closest edge of the loading plate (Figure 4.4). Gauges were attached on both legs as a backup in case one gauge was non-functional.

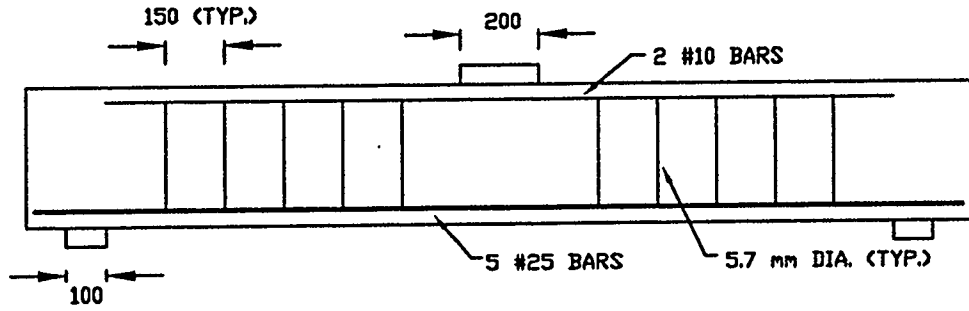


**Figure 4.1: Reinforcement layout**

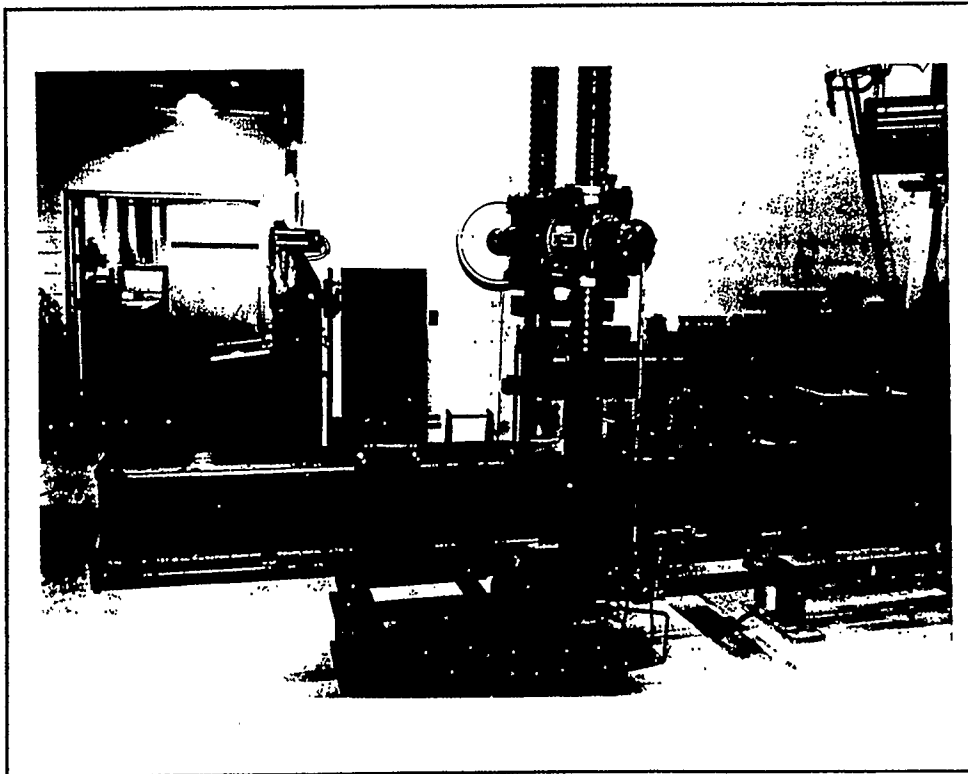


**Figure 4.2: Test setup**

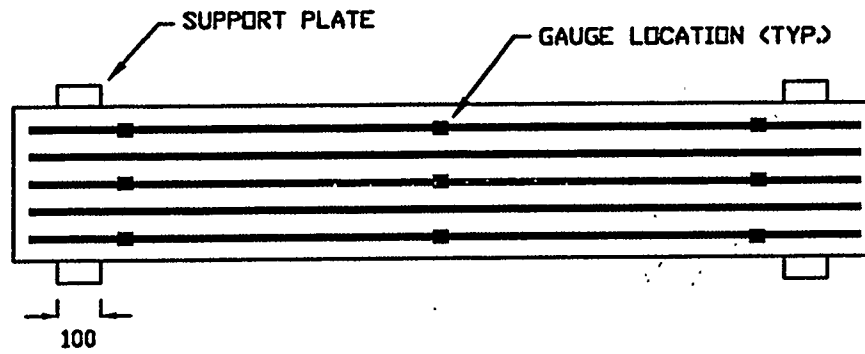


**Figure 4.3: Gauge locations on longitudinal reinforcement**

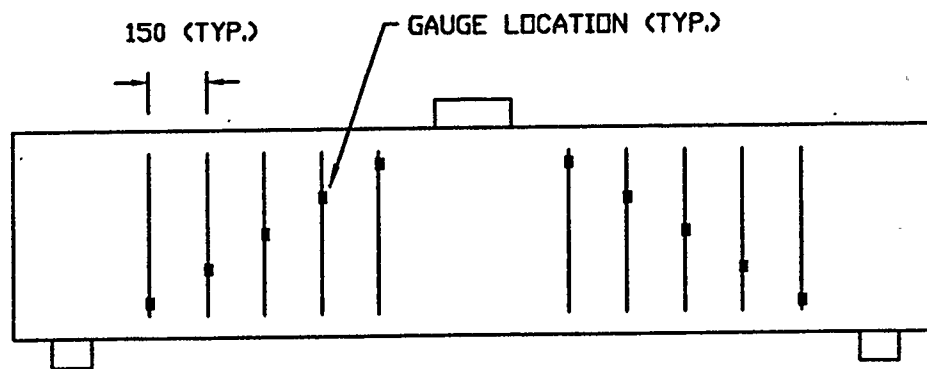


**Figure 4.4: Gauge locations on stirrups**



## 5. SHEAR FRICTION MODEL AND CODE COMPARISONS TO BEAM TESTS

### 5.1 Test Results

All beams failed due to a loss of shear capacity across a crack. This occurred on either an inclined plane or a horizontal plane as described in section 5.3. The measured inclined crack angle, the tensile force in the longitudinal reinforcement at the crack, the length of horizontal crack plane and the failure load are given in Table 5.1. The forces in the reinforcement were approximated by interpolating between two strains at locations on the reinforcement where the forces were known based on the strain gauge readings. Therefore there is considerable uncertainty in these tensile forces. The angles were measured between the longitudinal reinforcement and a straight line from the point where the main inclined crack appeared to intersect the reinforcement to the edge of the load plate. Many of the main inclined cracks were not straight, therefore there is some uncertainty in these values. There was also some uncertainty in the measured horizontal crack lengths due to the difficulty in determining the exact start of the inclined crack at the level of the longitudinal reinforcement.

<b>Table 5.1 Details of Beam Failures</b>					
<b>Beam</b>	<b>a/d</b>	<b>Crack angle (°)</b>	<b>Tensile force in reinforcement (kN)</b>	<b>Length of hor. crack plane (mm)</b>	<b>Failure load (kN)</b>
1	3.05	29.9	740	700	498
2	2.61	28.6	1037	550	767
3	3.05	26.2	639	330	449
4	2.17	37.5	1050	530	889
5	2.61	28.1	604	240	586
6	2.17	37.5	633	340	662
7	3.05	27.9	1003	530	609
8	2.61	31.2	1043	510	782
9	3.05	29.9	657	410	484
10	2.61	33.3	1000	345	781
11	2.17	42.6	1083	465	1024
12	2.17	53.0	1083	460	1189

Upon initial loading, a vertical flexural crack typically appeared near the midspan of the beam. Further flexural cracks developed further from midspan as the load was increased. The flexural cracks nearest the support then began to flatten and head towards the load plate. As the main flexure-shear crack neared the load plate a horizontal crack started to propagate from the outermost flexural crack at the level of the longitudinal reinforcement. At this point the cracks usually stabilized until failure when the main inclined crack opened up and extended from the edge of the load plate to a point at the level of the longitudinal reinforcement. The horizontal crack usually propagated along the reinforcement to the end of the beam at failure. Photos of each beam after failure can be

seen in Figure 5.1-5.6 and 5.7-5.12 for the normal and high strength concrete specimens respectively.

Table 5.2 shows the approximate crack widths for the 12 test beams at 60% of the predicted failure load using the CSA simplified method. This method gave the highest predicted loads of all the methods except for the ACI method using equation 2.25 which only applied to 8 of the 12 beams. These crack widths were obtained by interpolating between known crack widths at known load levels. This load level represents the typical service load that a beam might be subjected to during its lifetime. The maximum crack width under service loads given indirectly by CSA A23.3-94 Clause 10.6.1 is approximately 0.4 mm assuming interior exposure (CPCA, 1995).

Beam	Crack width at 60% of predicted failure by CSA simplified method (mm)
1	0.059
2	0.079
3	0.093
4	0.082
5	0.084
6	0.069
7	0.16
8	0.16
9	0.21
10	0.16
11	0.21
12	0.18

At 60% of the predicted failure load, all the crack widths satisfied Canadian code requirements. By observation, it appears that the crack width limitations would also be satisfied using the predicted loads based on all other methods except for the ACI method using equation 2.25. Based on the crack widths measured in the tests, it appears that the spacing and size of stirrups used in these test beams is adequate to prevent excessive cracking at service loads. This is reassuring since the maximum spacing and the minimum area of shear reinforcement as required by the CSA code were satisfied.

Table 5.3 shows the approximate crack widths at strain values in the stirrups that relate to yield strains for stirrups with  $f_y = 400$  MPa and  $f_y = 500$  MPa. The crack widths

are approximate because they were interpolated between known crack widths at known load levels. Also, the cracks did not always intersect the stirrup at the gauge location, so the actual crack widths at these strain levels may be smaller than recorded because the strains at the crack were most likely higher than that read by the gauges.

Beam	Crack width at $\epsilon_t = 0.0020$ (mm)	Crack width at $\epsilon_t = 0.0025$ (mm)
1	0.5 - 0.9	0.5 - 0.9
2	0.4 - 0.5	0.5 - 0.6
3	0.7 - 0.8	0.7 - 0.8
4	> 0.9	> 0.9
5	0.5 - 0.7	0.7 - 1.6
6	0.2 - 0.5	0.2 - 0.5
7	> 0.2	> 0.2
8	0.5 - 0.6	0.5 - 0.6
9	> 0.2	> 0.2
10	0.4 - 0.5	0.4 - 0.5
11	> 0.3	> 0.3
12	0.5 - 0.6	0.5 - 0.6

It appeared that most crack widths were less than 1 mm when Grade 400 and Grade 500 stirrups would have yielded, and in some cases the crack widths were less than 0.5 mm. This indicates that for wider cracks at failure when slippage of the cracked surfaces occurs, yielding of the stirrups seems certain to have taken place.

Table 5.4 shows the estimated force developed in each longitudinal bar at the given location from the end of the bar based on the average strains recorded by the gauges, as

well as the force at this location based on Clause 12.2.3 of the CSA code, assuming no stirrups are present along the developed length and  $f'_c$  is not limited to less than 64 MPa.

$F_y$  represents the force in the reinforcement assuming yielding has occurred.

Beam	Gauge location (mm)	Force based on gauge (kN)	Force based on CSA equation (kN)
1	400	95	71
2	350	190	64
3	130	116	23
4	380	217 ( $F_y$ )	66
5	50	88	9
6	300	83	58
7	400	211	114
8	400	180	117
9	200	101	58
10	200	169	58
11	300	217 ( $F_y$ )	90
12	200	217 ( $F_y$ )	58

In all 12 beams the forces in the reinforcement appeared to be much higher than that predicted by the CSA equation. The longitudinal reinforcement for beam 5 developed approximately 40% of its full capacity over a 50 mm length. The longitudinal reinforcement for beams 4, 11 and 12 reached over 90% of its full capacity over a 200 to 400 mm length. These observations suggest that the CSA code equation for development length (Clause 12.2.3) is too conservative for beams supported like these test beams.

Figure 5.13 shows a graph of failure load versus  $a/d$  ratio. The general trends

showed an increase in shear strength with increasing concrete strength, increasing overhang, and decreasing  $a/d$  ratio. The general increase in shear strength with increasing concrete strength in the beam tests agrees with Loov's shear friction equation which gives shear strength varying with the square root of  $f'_c$ . An increased anchorage length also increased the shear strength in most beams, but is affected by the location of the critical shear crack which determines the length available for force development. This was expected since a longer anchorage length meant that a higher normal force was available on the inclined plane, resulting in a higher shear friction force across the crack. The beams showed a general increase in strength with decreasing  $a/d$  ratio which also was expected. A smaller  $a/d$  ratio usually meant that a steeper crack angle occurred in beams which resulted in a higher friction force across the crack, since the main reinforcement is closer to being perpendicular to the inclined crack. In Figure N11.1.2.(b) of the CPCA Concrete Design Handbook, it can be seen that there is also a general increase in strength in beams tested previously over the range of  $a/d$  ratios from 3.05 to 2.17 (CPCA, 1995).

Some peculiarities were observed during the testing. For beam 1, the horizontal crack along the level of the longitudinal reinforcement did not extend to the end of the reinforcement, but ended at the inside of the support.

Beam 2 experienced 2 vertical cracks near failure extending from the top of the beam to about mid-depth of the beam above the supports. At failure, many short diagonal cracks parallel to the main inclined crack appeared near the load. Some of these diagonal cracks extended underneath the load plate.

The main inclined crack for beam 3 flattened as it approached the load, but at

failure a steeper crack occurred extending between the corner of the load plate and the flattened crack.

Beam 4 experienced 2 short vertical cracks extending from the top of the beam at the location of the supports similar to beam 2. The main diagonal crack was very steep near the load plate and was flatter nearer the support. Some spalling of the concrete in the compression zone near the load plate occurred at failure.

At failure, beam 5 did not appear to have cracked through the entire section. It seems to have failed along a horizontal plane at the end of the beam at the level of the longitudinal reinforcement. This was impossible to observe during the testing due to the speed of crack propagation at failure. Beam 5 had a short overhang which may have reduced its anchorage capability and increased the likelihood of a horizontal shear failure. Due to the location of the inclined crack, the horizontal crack plane was very short increasing the shear stress across this plane. Another flexure-shear crack extended under the load plate as the beam approached failure.

Some spalling of the concrete in the compression zone near the load plate occurred at failure for beam 6. An inclined crack flattened and extended under the load plate as the beam approached failure..

For beam 7, one flexure-crack flattened and extended under the load plate as the beam approached failure.

The main inclined crack for beam 8 flattened as it approached the load, but at failure a steeper crack occurred extending between the corner of the load plate and the flattened crack where it crossed the closest stirrup. The horizontal crack was fairly



irregular. It appeared that all but one stirrup leg broke in the shear span before failure occurred.

At failure, beam 9 did not appear to have cracked through the entire section. It failed along a horizontal plane at the end of the beam in the same way as beam 5. Beam 9 had a short overhang which may have reduced its anchorage capability and increased the likelihood of a horizontal shear failure.

Beam 10 had a particularly irregular cracking pattern at failure. A portion of the inclined crack was vertical giving the crack a rough surface. This crack may have strengthened the inclined plane in shear, dramatically decreasing the beam's ability to slip along this plane. A fair amount of spalling occurred at failure. Beam 10, which had an anchorage length that was 210 mm shorter than the anchorage length of beam 8, had the same strength as beam 8.

The main inclined crack for beam 11 flattened as it approached the load plate, but a steeper crack formed at failure extending between the inclined crack and the corner of the load plate. It appeared that all 3 stirrups in the shear span broke before failure occurred.

As beam 12 approached failure, the flexural cracks began to propagate again and approached the top of the beam. With a shorter overhang, beam 12 was stronger than beam 11 (the same beam with a longer overhang). This appeared to be due to a much steeper crack that occurred in beam 12, which means a higher normal force could develop along the sloping crack since the longitudinal reinforcement was more perpendicular to the inclined plane. The steeper crack also meant that a longer length of longitudinal

reinforcement was bonded to the concrete resulting in a higher developed force and a higher friction force across the crack. In effect, the added anchorage length in beam 11 as compared to beam 12 would have had little effect on the development force since the length of reinforcement beyond the main inclined crack was about the same.

## 5.2 Shear Friction Model Predictions

Table 5.5 shows the predictions using the shear friction model. The  $l_a$  term refers to the overhang length, which is the length of reinforcement past the outside face of the support. The predictions were based either on failure of the inclined plane, diagonal bending failure, or on moment failure. For the shear failure on an inclined plane and diagonal bending failure calculations, development length equations from the CSA code (even though these contain implicit material resistance factors) were used to calculate the force in the longitudinal reinforcement, and the weakest plane governed the failure prediction. Values of shear strength are fairly sensitive to changes in the failure plane angles, especially when they are governed by minimum angles (between edges of load plates).

The average  $P\text{-test}/P\text{-SF}$  was 1.24 and the C.O.V. was 0.29, where  $P$  represents the failure load. A comparison of test loads to predicted loads is shown in Figure 5.14 where the beam strength refers to the load ( $P$ ) at midspan at failure. The beam strength predictions for beams 1, 7, 8 and 9 are unconservative. It was hypothesized that these beams failed due to a shear failure on a horizontal plane at a lower load than the load based on failure of the inclined plane as predicted by the shear friction model.

Beam	a/d	$f'_c$ (MPa)	$l_a$ (mm)	P-test (kN)	P-SF (kN)	P-test/P-SF
1	3.05	28.9	300	498	536	0.93
2	2.61	30.2	250	767	546	1.40
3	3.05	28.9	30	449	406	1.11
4	2.17	28.9	280	889	570	1.56
5	2.61	30.1	40	586	414	1.42
6	2.17	33.6	90	662	532	1.24
7	3.05	74.3	180	609	688	0.89
8	2.61	77.8	230	782	810	0.97
9	3.05	77.0	10	484	526	0.92
10	2.61	76.3	20	781	554	1.41
11	2.17	81.5	140	1024	900	1.14
12	2.17	77.7	20	1189	624	1.91
					Average =	1.24
					C.O.V. =	0.29

The prediction for beam 12 was very conservative. The actual inclined crack for beam 12 was very steep and it appeared that the shear strength on this plane was very high, meaning that failure may have occurred on the horizontal plane. Other possible reasons for conservative results are that the forces in the longitudinal reinforcement were based on development equations in the CSA code which seem to be very conservative for these beams, and because the inclined cracks were usually somewhat steeper in the test beams than those used for the predictions. A higher longitudinal force induces a higher

shear force across a potential failure plane, and a steeper crack is stronger than a flatter crack because the longitudinal steel, which has a much larger cross-sectional area than the stirrups, would be more perpendicular to the crack, inducing a higher friction force. The predictions for beams 7 and 8 were based on moment failure because the predicted shear strengths were higher than the predicted shear force along the shear span at moment failure. This seemed to occur using the shear friction model because these 2 beams had long overhangs and had higher concrete strengths which increased their predicted shear strengths.

#### Example calculation

For beam 2, the following equations for forces parallel and perpendicular to the crack were used:

$$T_R = T \sin \theta + T_v \cos \theta$$

$$T_S = T \cos \theta - T_v \sin \theta$$

where  $T = 604$  kN and  $T_v = 95$  kN based on development equations and considering that the failure plane was found to occur when  $\theta = 28.9^\circ$ . These equations gave  $T_S = 483$  kN and  $T_R = 375$  kN. The area of the inclined plane is given as:

$$A = \frac{bd}{\sin \theta} \quad (5.1)$$

and with  $b = 360$  mm and  $d = 345$  mm,  $A = 257 \times 10^3$  mm<sup>2</sup>.

Using  $f'_c = 30.2$  MPa, and  $k = 0.6$  in the following equations:

$$b_1 = \frac{T_S \sin \theta + 0.5k^2 f'_c A \cos \theta}{\sin^2 \theta}$$

$$c_1 = \frac{T_s^2 - k^2 f'_o A T_R}{\sin^2 \theta}$$

gives  $b_1 = 6.251 \cdot 10^3$  kN and  $c_1 = -3.489 \cdot 10^6$  kN<sup>2</sup>. Substituting these values into the equation for  $V_{sf}$ , namely:

$$V_{sf} = b_1 \left[ \sqrt{1 - c_1/b_1^2} - 1 \right]$$

gives a  $V_{sf} = 273$  kN based on the inclined plane.

To calculate the shear strength based on the diagonal bending failure criteria, moments are taken about the intersection of the inclined crack and the neutral axis of the beam. The weakest plane was found to occur where  $\theta = 23.2^\circ$  (different from  $\theta$  for shear friction failure). Using the following equations for  $\alpha_1$  and  $\beta_1$ :

$$\alpha_1 = 0.85 - 0.0015 f'_o \quad (5.2)$$

$$\beta_1 = 0.97 - 0.0025 f'_o$$

$\alpha_1 = 0.805$  and  $\beta_1 = 0.895$ . The depth of the compression zone is equal to:

$$c = \frac{T}{\alpha_1 f'_o b_w \beta_1}$$

and with  $T = 604$  kN,  $b = 360$  mm and  $f'_o = 30.2$  MPa,  $c = 77$  mm. The moment due to the stirrups about the intersection of the crack and the neutral axis is:

$$M_{stirrup} = \Sigma \left[ T_v \left( p + \frac{d - c}{\tan \theta} - x_i \right) \right]$$

where  $p$  is the distance from the centre of the support to the start of the inclined crack at the level of the reinforcement and was equal to 175 mm,  $(d-c)/(\tan \theta)$  is the horizontal

projection of the inclined crack between the longitudinal reinforcement and the neutral axis and was equal to 625 mm,  $x_i$  is the distance from each stirrup to the centre of the support plate and  $T_v$  is the force in each stirrup based on where the crack intersects each stirrup.  $M_{stirrup} = 30 \text{ kN}\cdot\text{m}$  (using  $x_i = 200, 350, 500$  and  $650 \text{ mm}$  for the four stirrups respectively and  $T_v = 7.1 \text{ kN}, 30.6 \text{ kN}, 30.6 \text{ kN}$  and  $18.7 \text{ kN}$  respectively). To solve for  $V_{db}$ , moments about the intersection of the crack and the neutral axis are taken giving:

$$V_{db} = \frac{T \left( d - \beta_1 \frac{c}{2} \right) + M_{stirrup}}{\left( \frac{d - c}{\tan \theta} + p \right)}$$

This equation gives  $V_{db} = 329 \text{ kN}$  for beam 2 based on a diagonal bending failure. The internal moment was calculated at a vertical section located halfway between the centre of the load plate and the edge of the load plate. The load corresponding to the moment capacity of the beam was therefore approximated using the following equation:

$$P_m = \frac{2 \cdot T_y \left( d - \beta_1 \frac{c}{2} \right)}{a - \frac{w_2}{4}} \quad (5.3)$$

and was equal to 722 kN, using  $T_y = 1083 \text{ kN}$  (based on  $A_s f_y$  where  $A_s = 2500 \text{ mm}^2$  and  $f_y = 433 \text{ MPa}$ ),  $d = 345 \text{ mm}$ ,  $a = 900 \text{ mm}$ ,  $c = 138 \text{ mm}$ . Based on these calculations the critical shear strength is equal to 273 kN based on shear failure on an inclined plane and gives a predicted failure load of 546 kN.

### 5.3 Extended Shear Friction Model Predictions

An extended model was created due to the particular failure mode of some of the twelve test beams. For many of the beams the major inclined shear crack was steeper than expected (i.e. not the flattest possible) and a relatively long horizontal crack appeared at failure at the level of the reinforcement (Figure 5.15 and Figure 5.16). It was not certain which of the 2 main cracks (horizontal or inclined) initiated failure in the tests due to the speed of the crack propagation at failure, but it was hypothesized that failure would occur on the weaker of the two planes as predicted by the shear friction model. The horizontal shear occurring at the level of the reinforcement may have become critical before failure on an inclined plane occurred. This is somewhat different from typical bond failures since the bottom half of the reinforcing bars were still firmly embedded in the concrete and did not pull out of the concrete. Using the strain data, forces in the longitudinal reinforcement and stirrups were estimated. Using equilibrium and Loov's equation, values of shear ( $V$ ) that would result in shear failure (using  $k = 0.6$ ) were calculated for each beam, assuming either shear or diagonal bending failure on an inclined plane, or shear failure on a horizontal plane. The lowest value for  $V$  was considered to be the failure shear for that beam. For values of  $R_i$  (normal force) on the inclined plane, checks were made to ensure that moment equilibrium was achieved and that  $R_i$  acted within the beams' depth and according to the stress distribution approximations as discussed in section 3.4.

The shear acting on the horizontal plane was assumed to be equal to the force in the longitudinal steel at the furthest point along the horizontal crack from the support. Based on equilibrium the normal force  $R$  on the horizontal crack was assumed to be equal

to the shear force (V), assuming that a vertical crack is located between the support and the closest stirrup and that no shear is transferred across this crack. It was also assumed that no shear is taken by the concrete located below the reinforcement since it is felt that this concrete is very flexible. Therefore  $V = R$ , where R is given as:

$$R = \frac{S^2}{k^2 f'_c A} \quad (5.4)$$

which is a rearrangement of Loov's equation.

The results are shown in Table 5.6. The predictions were based either on failure of the inclined plane, failure on a horizontal plane, diagonal bending failure, or on moment failure. For the shear failure on an inclined plane, shear failure on a horizontal plane and diagonal bending failure calculations, strain measurements from the tests were used to estimate forces in the stirrups and longitudinal reinforcement across the inclined and horizontal cracks. The lengths of the horizontal crack and the angle of the main inclined crack were measured and used in these calculations.



Beam	a/d	$f'_c$ (MPa)	$l_a$ (mm)	P-test (kN)	P-SF (kN)	P-test/P-SF
1	3.05	28.9	300	498	497.1	1.00
2	2.61	30.2	250	767	612.0	1.25
3	3.05	28.9	30	449	383.0	1.17
4	2.17	28.9	280	889	617.3	1.44
5	2.61	30.1	40	586	590.5	0.99
6	2.17	33.6	90	662	643.3	1.03
7	3.05	74.3	180	609	530.4	1.15
8	2.61	77.8	230	782	534.1	1.46
9	3.0	77.0	10	484	458.8	1.05
10	2.61	76.3	20	781	758.2	1.03
11	2.17	81.5	140	1024	568.4	1.8
12	2.17	77.7	20	1189	892.5	1.33
					Average =	1.22
					C.O.V. =	0.26

The extended shear friction model gave an average P-test/P-SF of 1.22 and a C.O.V. of 0.26. Predicted values for P-SF were based on actual forces in the stirrups and longitudinal reinforcement, and actual failure plane angles, and were calculated based on the weaker of either the inclined or horizontal shear failure plane. Even though there was only a slight change in P-test/P-SF and the C.O.V. using the extended model, all but one of the predictions are conservative and the only unconservative prediction is within 1% of the test value. The predictions for beams 8 and 11 worsened with the extended model

because a lower shear strength was predicted due to failure on a horizontal plane.

### Example calculation

The yield force of a stirrup based on the stress-strain curve shown in Figure 5.17 is 30.6 kN using a 0.2% offset. For beam 6, it appeared that the 3 stirrups on the side of the beam that failed had fully yielded but did not break prior to reaching peak load (Figures 5.18 - 5.20). Although some of the strain gauges did not indicate yielding of all of the stirrups, the strains were close to yield and the gauges were not located exactly at the crack where the highest strain was assumed to be. It was therefore assumed that all 3 stirrups had yielded giving a  $T_w$  of 91.8 kN.

The yield force in the 5 longitudinal bars was calculated as 1083 kN based on the stress-strain curve shown in Figure 5.21. A tension force in the longitudinal reinforcement ( $T$ ) at the crack equal to 633 kN based on the average strain in 3 of the 5 longitudinal bars (Figures 5.22 - 5.23) was estimated by interpolating between the strains near the support and the strains at the midspan to estimate the strains at the crack. Due to the distance between the gauges and the crack location, there was considerable uncertainty in the strains estimated. Using  $\theta = 37.5^\circ$  for the angle of the inclined failure plane,  $V_{sf}$  was equal to 353.8 kN.  $V_{db}$  was equal to 390.7 kN.

For failure on the horizontal plane, Loov's equation was rearranged as follows:

$$R = \frac{S^2}{k^2 f'_c A}$$

and assuming that  $k = 0.55$  since it was felt that the coefficient of friction would be less between a concrete and steel interface than between two concrete surfaces. Using

$A = 1.224 \cdot 10^6 \text{ mm}^2$  based on a horizontal crack length equal to 340 mm and  $b = 360 \text{ mm}$ ,  $f'_c = 33.6 \text{ MPa}$  and  $S = 633 \text{ kN}$ ,  $R = 322 \text{ kN}$ . Assuming a flexible area of concrete below the reinforcement as discussed in Section 5.3,  $V = R$ . Therefore  $V = 321.7 \text{ kN}$ . Taking the lowest of the three values of shear strength based on inclined shear failure, horizontal shear failure and diagonal bending failure, the predicted shear strength of the beam would be 321.7 kN resulting in a predicted load capacity of  $2 \cdot V$  or 643.3 kN. The load at midspan at the theoretical moment capacity was found to be 966.3 kN. A check was made to ensure that the resultant  $R_i$  on the inclined plane acted within the beam's depth as discussed in Section 3.4. The shear force on the inclined plane  $S_i$  based on a horizontal shear failure was calculated from:

$$S_i = \Sigma(T_v \sin \theta) - R \sin \theta - S \cos \theta \quad (5.5)$$

and the normal force on the inclined plane  $R_i$  was calculated from

$$R_i = \frac{S - S_i \cos \theta}{\sin \theta} \quad (5.6)$$

Taking moments about Point Q in Figure 5.24,  $R_i$  acts at a vertical distance  $y_i$  from the top of the beam where  $y_i$  is calculated as:

$$y_i = d - \left( \frac{R \cdot p + \Sigma T_v (x_i - p)}{R_i} \right) \sin \theta$$

where  $p$  is the distance from the centre of the support to the start of the inclined crack at the level of the longitudinal reinforcement and  $x_i$  is the distance from each stirrup to the centre of the support. In the case of beam 6,  $y_i = 78 \text{ mm}$ . The other 11 beam strengths were predicted in a similar manner.

The predictions of shear strength for the 12 test beams as shown previously in Table 5.4 given by the shear friction model were reasonable. This model's equations take into account the  $a/d$  ratio, anchorage length and  $f'_c$  and therefore reflect the changes in shear strength due to alterations in these variables. In Figure 5.25, plots of beam strength vs.  $a/d$  ratio for both the test and predicted values are shown. The predictions by the shear friction model were influenced by the forces, angles and length of horizontal cracks measured during the test which tended to affect the expected trends using the shear friction equations. For example, for the high strength concrete beams with longer overhangs, the predicted shear strengths remained almost constant as the  $a/d$  ratio decreased. This was due to the fact that the shear friction model predicted horizontal shear failure which was not directly dependent on the  $a/d$  ratio, but rather the shear force on the plane and the length of the plane. This matched the trend between beams 8 and 10. The shear friction model also matched the trend between beams 11 and 12, where the shear strength increased with a shorter overhang length.

## **5.4 CSA Predictions**

### **5.4.1 CSA Simplified Method**

The predictions given by the simplified method gave reasonable results and are shown below in Table 5.7. Material resistance factors were set to 1.0 in the calculations. The predictions given by the CSA simplified method are generally conservative with an average  $P$ -test/ $P$ -Simplified of 1.48 and a C.O.V. of 0.28. However, the prediction for beam 9 was unconservative. This was due to the fact that the predicted shear strengths

for the six high strength beams were essentially the same. A reduction in the shear capacity of beam 9 as compared to beam 7 due to a decrease in anchorage length was not reflected using this method and appeared to be the reason for the unconservative prediction.

<b>Table 5.7 CSA Simplified Method Predictions</b>				
Beam	a/d	P-test (kN)	P-simplified (kN)	P-test/P-Simplified
1	3.05	498	408	1.22
2	2.61	767	414	1.85
3	3.05	449	408	1.1
4	2.17	889	408	2.18
5	2.61	586	414	1.42
6	2.17	662	429	1.54
7	3.05	609	569	1.07
8	2.61	782	579	1.35
9	3.05	484	577	0.84
10	2.61	781	575	1.36
11	2.17	1024	589	1.74
12	2.17	1189	578	2.06
			Average =	1.48
			C.O.V. =	0.28

#### Example Calculation

For beam 1, with an  $f'_c$  of 28.9 MPa,  $b_w = 360$  mm,  $d = 345$  mm,  $s = 150$  mm,  $f_y = 600$  MPa,  $A_v = 50.7$  mm<sup>2</sup>,  $\phi_c = 1.0$ ,  $\phi_s = 1.0$ ,  $\lambda = 1.0$  and using the following equations for  $V_c$  and  $V_s$ :

$$V_c = 0.2\lambda\phi_c \sqrt{f'_c} b_w d$$

$$V_s = \frac{\phi_s A_v f_y d}{s}$$

$V_c = 133.5$  kN and  $V_s = 70.4$  kN giving a total P-Simplified ( $2 \cdot V$ ) of 408 kN versus a P-test of 498 kN. The other 11 beam strengths were calculated in a similar manner. The theoretical moment capacities for the beams were calculated in the same manner as for the shear friction method and were not critical in these calculations.

No account is made for the  $a/d$  ratio or overhang length in these shear equations (Figure 5.26). The compressive strength is accounted for, but there are essentially 2 predicted values (roughly 410 kN and 580 kN) of shear strength based on the 2 average values of  $f'_c$  for the 12 beams. Therefore any increases in shear strength due to increased overhangs or decreasing  $a/d$  ratio are not reflected in the simplified method.

Since the predicted shear values are low and there is no moment at the ends of the beams, the required anchorage lengths as stated by the CSA code are satisfied in all 12 beams tests, even though some beams had overhangs as little as 10 mm past the support plate. The best predictions occurred for the longest span (except for beam 9) suggesting the need for a better model for the smaller  $a/d$  ratios.

### 5.4.2 CSA General Method

Comparisons of the general method to the test results were made and the results are shown below in Table 5.8. Material resistance factors were set to 1.0 in the calculations.

<b>Table 5.8 CSA General Method Predictions</b>				
Beam	a/d	P-test (kN)	P-General (kN)	P-test/P-General
1	3.05	498	393	1.27
2	2.61	767	411	1.87
3	3.05	449	393	1.14
4	2.17	889	423	2.10
5	2.61	586	411	1.43
6	2.17	662	439	1.51
7	3.05	609	505	1.21
8	2.61	782	530	1.48
9	3.05	484	510	0.95
10	2.61	781	527	1.48
11	2.17	1024	558	1.84
12	2.17	1189	550	2.16
			Average =	1.54
			St.Dev. =	0.25

The CSA general method's predictions are fairly conservative with an average P-test/P-General of 1.54 and a C.O.V. of 0.25.

#### Example Calculation

For beam 6 with an  $f'_c$  of 33.6 MPa, the shear strength was determined using a trial

and error method as discussed in Section 2.2.2. As the final guess  $v_f/\phi_c f'_c = 0.0585$ ,  $\epsilon_x = 0.00133$ ,  $\theta = 39.1^\circ$  and  $\beta = 0.168$ .

Using:

$$V_f = \frac{V_f}{\phi_c f'_c} \phi_c f'_c b_w d_v$$

with  $b_w = 360$  mm,  $d_v = 311$  mm,  $V_f = 219.7$  kN. Using:

$$V_{cg} = 1.3 \phi_c \beta \sqrt{f'_c} b_w d_v$$

with  $\beta = 0.168$ ,  $V_{cg} = 141.7$  kN. With:

$$V_{sg} = V_f - V_{cg} \quad (5.7)$$

$V_{sg} = 78.0$  kN. From  $V_{sg}$  the spacing of stirrups,  $s$ , can be calculated from:

$$s = \frac{A_v f_y d_v}{\tan \theta \cdot V_{sg}} \quad (5.8)$$

using an  $A_v = 50.7$  mm<sup>2</sup>,  $f_y = 600$  MPa,  $s = 150$  mm. This matches the spacing in the test beam. The assumed value of  $\epsilon_x$  must be matched with the  $\epsilon_x$  from the following equation:

$$\epsilon_x = \frac{0.5 V_f \cot \theta + M_f/d_v}{E_s A_s}$$

with  $E_s = 200000$  MPa,  $A_s = 2500$  mm<sup>2</sup> and  $M_f = V_f a$  where  $a$  is the shear span length and is equal to 750 mm.  $\epsilon_x = 0.00133$  which checks with the original guess. Therefore the predicted shear strength of beam 6 is 219.7 kN. The other 11 beams were calculated in a similar manner. The theoretical moment capacities were calculated in the same manner as with the shear friction method and were not critical in these calculations.

A very slight increase in shear strength is predicted for decreasing  $a/d$  ratios, but



no account for the overhang length is made in the shear equations. There are essentially 2 predicted values of shear strength based on the 2 average values of  $f'_c$  for the 12 beams of different lengths and different end anchorages (Figure 5.27). The best predictions occurred for the longest spans, but worsened as the span was shortened. Also, there was one slightly unconservative prediction for beam 9 with a P-test/P-General of 0.97. This was minimally unconservative but indicated, as did the Simplified Method, that since the predicted values were essentially constant, the reduction in shear capacity with increasing  $a/d$  ratio was not reflected and led to an unconservative estimate for beam 9.

### **5.4.3 CSA Strut-and-Tie Methods**

#### **5.4.3.1 CSA Strut-and-Tie Method using CSA code equations**

The CSA strut-and-tie method was used to predict the failure loads of the test beams, and the model along with the forces  $F_1$  to  $F_6$  are shown in Figure 5.28. When applying the strut-and-tie method, different assumptions were made, giving three sets of predicted values. For the CSA strut-and-tie method using CSA code equations, the force developed in the longitudinal reinforcement was based on the CSA code equation,  $f_{2max}$  was based on code equations, and the stirrups were assumed to be capable of reaching yield. The second strut-and-tie method assumed that there was no restriction on the amount of force that the reinforcement could develop and that  $f_{2max}$  was based on code equations. The third strut-and-tie method assumed that  $f_{2max}$  was equal to  $0.6 \cdot f'_c$  as opposed to the code equations and that there was no restriction on the amount of force that the reinforcement could develop. In all cases, the height of the vertical tension tie

representing the stirrups was varied to determine the maximum strength of the beam for this model. By varying the height of the vertical tension tie, the angle between the longitudinal reinforcement and the tension tie was altered which affected the forces in the struts and ties as well as the limiting values of  $f_{2max}$ . The bottom node was located at the intersection of the support and the level of the reinforcement. The top node was located at the intersection of the point load and the centroid of the compression block. The point load at the centre of the beam was split into two loads acting at 1/4 and 3/4 points of the load plate in order to analyze half of the beam. Material resistance factors ( $\phi_c, \phi_s$ ) were set to 1.0 in the calculations.

The predictions given by this method are very conservative with an average P-test/P-Strut-and-Tie<sub>1</sub> of 2.64 and a C.O.V. of 0.38 as shown in Table 5.9. The predicted strength was limited by the maximum forces that could be developed in the horizontal and vertical tension ties. The force in the horizontal tension ties were limited by the development length equation and the force in the vertical tension tie representing the stirrups was limited by the maximum force that the stirrups could carry assuming that each stirrup yields.

Table 5.9 CSA Strut-and-Tie Predictions using CSA Code Equations				
Beam	a/d	P-test (kN)	P-Strut-and-Tie <sub>1</sub> (kN)	P-test/P-Strut and Tie <sub>1</sub>
1	3.05	498	368	1.35
2	2.61	767	356	2.15
3	3.05	449	128	3.51
4	2.17	889	388	2.29
5	2.61	586	164	3.57
6	2.17	662	260	2.55
7	3.05	609	412	1.48
8	2.61	782	496	1.58
9	3.05	484	176	2.75
10	2.61	781	228	3.43
11	2.17	1024	428	2.39
12	2.17	1189	256	4.64
			Average =	2.64
			C.O.V. =	0.38

### Example calculation

It is assumed that along the anchorage length overhanging the support bond is not affected by the stirrups, since none are present along this length. Therefore the following equation is assumed to apply:

$$l_d = 0.6k_1k_2k_3k_4 \frac{f_y d_b}{\sqrt{f'_c}} \quad (5.9)$$

where  $k_1$  is the bar location factor,  $k_2$  is the coating factor,  $k_3$  is the concrete density factor,  $k_4$  is the bar size factor. For beam 1, with  $k_1 = k_2 = k_3 = k_4 = 1.0$  based on Clause

12.2.3,  $f_y = 433$  MPa,  $d_b = 25.2$  mm, and  $f'_c = 28.9$  MPa,  $l_d = 1220$  mm. The length of reinforcement to the inside face of the support is:

$$\ell = l_a + w_1 \quad (5.10)$$

which is equal to 400 mm, where  $oh$  is the overhang length and is equal to 300 mm,  $w_1$  is the support plate width and equals 100 mm. Therefore the maximum allowable tension in the reinforcement at the inside face of the support is:

$$T = \frac{\ell}{l_d} T_y \quad (5.11)$$

where  $T_y = 1083$  kN based on an  $f_y = 433$  and an  $A_s = 2500$  mm<sup>2</sup>. This equation gives  $T = 355$  kN. The depth of the compression block is based on the following equation:

$$a = \frac{F_c}{0.85 b_w f'_c} \quad (5.12)$$

where  $F_c$  is the force in the tension tie near the midspan. The critical forces using this model were  $F_2$ , which was the force in the tension tie near the support and was limited by the anchorage force that could be developed and  $F_4$ , which was the force in the vertical tension tie and was limited by the maximum force that could be developed in the vertical tension tie based on the number of stirrups. For beam 1 there were 5 stirrups giving a maximum force of approximately 153 kN based on yielding of the stirrups. The force in the compressive strut ( $F_1$ ) nearest the support was not critical in these cases due to the restrictive development equation. For beam 1, the maximum beam strength occurred when  $\theta_1 = 30.0^\circ$ . This gave  $F_4 = 147$  kN and  $F_2 = 355$  kN which satisfied the limits of 153 kN and 355 kN respectively. The other 11 beams were calculated in a similar manner.

In Figure 5.29, it can be seen that the predictions given by this strut-and-tie model showed a slight increase in strength for decreasing  $a/d$  ratios. The predictions for the high strength concrete beams were only slightly higher in general than the normal strength concrete beams due to a faster rate of force development in the longitudinal reinforcement. The predictions for beams with short overhangs were very conservative because these beams were largely affected by the restrictive CSA development equation.

#### **5.4.3.2 CSA Strut-and-Tie Method without Development Length Equation**

If the development length equation for the longitudinal reinforcement was ignored and full anchorage capability were assumed, the predicted values improved substantially. The following table gives the predictions using this strut-and-tie model.

<b>Table 5.10 CSA Strut-and-Tie Method Predictions without Development Length Equation</b>				
Beam	a/d	P-test (kN)	P-Strut-and-Tie <sub>2</sub> (kN)	P-test/P-Strut-and-Tie <sub>2</sub>
1	3.05	498	420	1.19
2	2.61	767	468	1.64
3	3.05	449	420	1.07
4	2.17	889	516	1.72
5	2.61	586	468	1.25
6	2.17	662	584	1.13
7	3.05	609	716	0.85
8	2.61	782	808	0.97
9	3.05	484	672	0.72
10	2.61	781	804	0.97
11	2.17	1024	1000	1.02
12	2.17	1189	996	1.19
			Average =	1.14
			C.O.V. =	0.26

This improved results from an average P-test/P-Strut-and-Tie<sub>2</sub> of 2.64 to 1.14 and a C.O.V. from 0.38 to 0.26. For beams 1 to 10, the critical factors were the force in the vertical tension tie and the force in the compressive strut ( $F_1$ ). The maximum predicted strengths for these beams occurred when both  $F_1$  and  $F_4$  were at their limit. For beams 11 and 12 the predicted beam strength was limited by the maximum force in  $F_6$ , based on the yield force in the longitudinal reinforcement.

From Figure 5.30, it can be seen that the increase in strength with decreasing a/d

ratios was very well reflected in strut-and-tie method 2 after the restrictive development equation was removed. The general increase in strength with increasing  $f'_c$  was also reflected using this model. As a consequence of removing the development equation restriction, the effect of a change in anchorage length was not reflected in this model.

#### **5.4.3.3 CSA Strut-and-Tie Method without Develop Length Equation and $f_{2max}$ Restriction**

By removing the  $f_{2max}$  restriction and the development length equation and adding a limiting compressive stress of  $0.6 \cdot f'_c$  for compressive struts, the following results were obtained.

<b>Table 5.11 CSA Strut-and-Tie Method Predictions without Development Equation and <math>f_{2max}</math> Restriction</b>				
Beam	a/d	P-test (kN)	P-Strut-and-Tie <sub>3</sub> (kN)	P-test/P-Strut-and-Tie <sub>3</sub>
1	3.05	498	592	0.84
2	2.61	767	660	1.16
3	3.05	449	592	0.76
4	2.17	889	728	1.22
5	2061	586	660	0.89
6	2.17	662	828	0.8
7	3.05	609	696	0.88
8	2.61	782	820	0.95
9	3.05	484	696	0.7
10	2.61	781	820	0.95
11	2.17	1024	1000	1.02
12	2.17	1189	996	1.19
			Average =	0.95
			C.O.V. =	0.18

This gives many unconservative results but the average P-test/P-Strut-and-Tie<sub>3</sub> was 0.95 and the C.O.V. was 0.18. From Figure 5.31, it can be seen that the results are very good and match the trend of shear strength variation as it increases with decreasing a/d ratios. The compressive strength was also reflected in this model as it predicted higher shear strengths for beams with higher concrete compressive strengths.

Using the strut-and-tie model, one can account for the a/d ratios, anchorage lengths and concrete strengths. However the development equation and  $f_{2max}$  equation are



very restrictive and reduce the effectiveness of the model significantly.

## **5.5 ACI Predictions**

### **5.5.1 ACI Predictions using Equations 2.19 and 2.21**

This method refers to the calculation of shear strength based on the addition of the simplest  $V_c$  and  $V_s$  terms for the beams with an  $a/d$  ratio of 3.05 where  $\ell_v/d > 5$ . The other 8 beams required special provisions since they were considered to be deep flexural members by the ACI code. The results of this method's predictions are shown in Table 5.12.

Table 5.12 ACI Predictions using Equation 2.19 and 2.21				
Beam	a/d	P-test (kN)	P-Method 1 (kN)	P-test/P-Method 1
1	3.05	498	362.6	1.37
3	3.05	449	362.6	1.24
7	3.05	609	483.4	1.26
9	3.05	484	483.4	1.00
			Average =	1.22
			C.O.V. =	0.13

Method 1 gave good results with an average P-test/P-Method 1 of 1.22 with a C.O.V. of 0.13.

#### Example calculation

For beam 1,  $V_c$  was calculated using:

$$V_c = \sqrt{f'_c} b_w d / 6$$

and was equal to 110.9 kN based on an  $f'_c = 28.9$  MPa,  $b_w = 360$  mm, and  $d = 345$  mm.

$V_s$  was calculated using:

$$V_s = \frac{A_v f_y d}{s}$$

and was equal to 70.4 kN based on  $A_v = 50.7$  mm<sup>2</sup>,  $f_y = 600$  MPa,  $s = 150$  mm. Using:

$$V_n = V_c + V_s$$

$V_n = 181.3$  kN. The other 3 beams were calculated in a similar manner. The theoretical moment capacities were not critical in these calculations.

This method did not take into account the a/d ratio or overhang length. However,

only one  $a/d$  ratio was analyzed using this model. There are essentially 2 predicted values of shear strength based on the normal and high strength concrete strengths. The  $V_s$  term is identical for each beam since the spacing and size of the stirrups are constant for all 12 test beams. In general, increases in beam strength are observed due to decreases in  $a/d$  ratio which do not appear to be reflected in this model. However, this model seemed appropriate for longer span beams.

### 5.5.2 ACI Predictions using ACI Equations 2.20 and 2.21

This method is used when  $\ell_n > 5$  and is an alternative to method 1 involving a more complicated  $V_c$  term. The results are shown below in Table 5.13. The other 8 beams were considered to have deep shear spans and were analyzed differently.

Beam	$a/d$	P-test (kN)	P-Method 2 (kN)	P-test/P-Method 2
1	3.05	498	301.6	1.65
3	3.05	449	301.6	1.49
7	3.05	609	422.4	1.44
9	3.05	484	422.4	1.15
			Average =	1.43
			C.O.V. =	0.15

This method gave conservative results with an average P-test/P-Method 2 of 1.43 with a C.O.V. of 0.15. The  $V_c$  term was more complicated and has been found to be suspect (American Concrete Institute, 1992), but seemed to give reasonable although

somewhat conservative results.

### Example calculation

For beam 1,  $V_c$  was calculated using:

$$V_c = \left( \sqrt{f'_c} + 120 \rho_w \frac{V_f d}{M_f} \right) b_w d / 7$$

and was equal to 148.4 kN based on an  $f'_c = 28.9$  MPa,  $\rho_w = 0.020$ ,  $b_w = 360$  mm,  $d = 345$  mm and  $V_f d / M_f$  equal to 1 at the critical section.  $V_s$  was equal to 70.4 kN based on  $A_v = 50.7$  mm<sup>2</sup>,  $f_y = 600$  MPa,  $s = 150$  mm. Therefore  $V_n = 218.8$  kN. The other 3 beams were calculated in a similar manner. The theoretical moment capacities were not critical in these calculations.

This method did not take into account the  $a/d$  ratio or overhang length. However, this model was applied to only one  $a/d$  ratio. Although the  $a/d$  ratio is included indirectly in the  $M_f / (V_f d)$  term in the  $V_c$  equation, this term is limited to a value of one for these test beams (Clause 12.8.5). There are essentially 2 predicted values of shear strength based on the normal and high strength concrete strengths. The  $V_s$  term is identical for each beam since the stirrup size and spacing are constant.

### **5.5.3 ACI Predictions using Equation 2.25**

This method applies when  $2 \leq \ell_n \leq 5$  and involved using the simple  $V_n$  equation which accounts for the beam span. The results of this model's predictions are shown in Table 5.14 for beams with  $a/d$  ratios of 2.61 and 2.17.

Table 5.14 ACI Predictions using Equation 2.25				
Beam	a/d	P-test (kN)	P-Method 3 (kN)	P-test/P-Method3
2	2.61	767	759.7	1.01
4	2.17	889	905.3	0.98
5	2.61	586	791.0	0.74
6	2.17	662	966.3	0.69
8	2.61	782	814.4	0.96
10	2.61	781	816.1	0.96
11	2.17	1024	989.1	1.04
12	2.17	1189	985.9	1.21
			Average =	0.95
			C.O.V. =	0.17

### Example calculation

The shear strengths of the beams were calculated using the following equation for

$V_n$ :

$$V_n = \frac{1}{18} \left( 10 + \frac{\ell_n}{d} \right) \sqrt{f'_c} b_w d$$

For beam 2,  $V_n = 564$  kN using an  $\ell_n = 1700$  mm,  $b_w = 360$  mm,  $d = 345$  mm, and  $f'_c = 30.2$  MPa. The other beams were calculated in a similar manner. However, all the predicted values were based on moment failure due to the high predictions by Method 3 based on the  $V_n$  equation.

This method gave unconservative predictions with an average P-test/P-Method 3 of 0.95 and a C.O.V. of 0.17. By observing the equation for  $V_n$ , it can be seen that the

predicted shear strength decreases with a decreasing beam span (Figure 5.32) which was not the case in the beam tests, nor in general as seen in Table N11.1.2.(b) of the CPCA Concrete Design Handbook. The predicted beam strength based on shear failure was less for beams 11 and 12 than for beams 8 and 10 which is not correct. It should be noted that these beams did not satisfy the ACI code minimum reinforcement requirements. The predicted values would have most likely been even more conservative with the required amount of reinforcement.

#### **5.5.4 ACI Predictions using Equations 2.26 and 2.29**

This method is an alternate to the previous method and applies when  $2 \leq \ell_n \leq 5$ . It was applied to beams with a/d ratios of 2.61 and 2.17. The results of this method's prediction are shown below in Table 5.15.

Beam	P-test (kN)	P-Method 4 (kN)	P-test/P-Method 4
2	767	296.2	2.59
4	889	281.2	3.16
5	586	296.0	1.98
6	662	298.4	2.22
8	782	412.2	1.90
10	781	412.1	1.90
11	1024	402.0	2.55
12	1189	402.0	2.96
		Average =	2.41
		C.O.V. =	0.20

This method gave very conservative results with an average P-test/P-Method 4 of 2.41 with a C.O.V. of 0.2.

The beam strengths were calculated by adding  $V_c$  and  $V_s$ . The following equation for  $V_c$  was used:

$$V_c = \sqrt{f'_c} b_w d / 6$$

#### Example calculation

For beam 2 this gives a  $V_c = 113.3$  kN using an  $f'_c$  of 30.2 MPa,  $b_w = 360$  mm and  $d = 345$  mm.  $V_s$  was calculated from:

$$V_s = \left[ \frac{A_v}{s} \left( \frac{1 + \ell_n/d}{12} \right) + \frac{A_{vh}}{s_2} \left( \frac{11 - \ell_n/d}{12} \right) \right] f_y d$$

giving  $V_s = 34.8$  kN for  $\ell_n = 1700$  mm,  $d = 345$ ,  $s = 150$  mm and  $f_y = 600$  MPa. This resulted in a  $V$  of 148.1 kN. The other 7 beams were calculated in a similar manner. The theoretical moment capacities were not critical in these calculations.

This  $V_c$  equation did not take the  $a/d$  ratio into account (Figure 5.33). The  $V_s$  equation has a term to account for the clear span  $\ell_n$ , but  $V_s$  decreases with a decrease in beam span which is the opposite of what was expected. Neither equation accounted for anchorage length in calculating shear strength but an increase in strength was predicted for increasing  $f'_c$ .

It should be noted that these beams did not satisfy the ACI code minimum reinforcement requirements. The predicted values would have most likely been even more conservative with the required amount of reinforcement.

#### **5.5.5. ACI Predictions using Equations 2.27 and 2.29**

This method applies when  $2 \leq \ell_n \leq 5$  and is an alternative to the 2 previous methods. It involved using a more complicated  $V_c$  term and a  $V_s$  term in calculating the shear strength. This method was applied to beams with  $a/d$  ratios of 2.61 and 2.17 and the results are given in Table 5.16.



Beam	P-test (kN)	P-Method 5 (kN)	P-test/P-Method 5
2	767	371.2	2.07
4	889	356.2	2.50
5	586	370.8	1.58
6	662	372.8	1.78
8	782	481.2	1.63
10	781	481.2	1.62
11	1024	471.0	2.17
12	1189	471.0	2.52
		Average =	1.98
		C.O.V. =	0.20

This method gave conservative results with an average P-test/P-Method 5 of 1.98 with a C.O.V. of 0.20.

#### Example calculation

The  $V_c$  as mentioned previously has been found to be suspect and is given as:

$$V_c = \left( 3.5 - 2.5 \frac{M_f}{V_f d} \right) \left( \sqrt{f'_c} + 120 \rho_w \frac{V_f d}{M_f} \right) b_w d / 7$$

For beam 2,  $V_c = 150.8$  kN with  $f'_c = 28.6$  MPa,  $\rho_w = 0.020$  and  $M_f/V_f d$  limited to one.

$V_s$  was calculated from:

$$V_s = \left[ \frac{A_v}{s} \left( \frac{1 + \ell_n/d}{12} \right) + \frac{A_{vh}}{s_2} \left( \frac{11 - \ell_n/d}{12} \right) \right] f_y d$$

and gave a  $V_s$  of 34.8 kN using  $A_v = 50.7 \text{ mm}^2$ ,  $s = 150 \text{ mm}$ ,  $\ell_n = 1700 \text{ mm}$ ,  $A_{vh} = 0$ ,  $f_y = 600 \text{ MPa}$  and  $d = 345 \text{ mm}$ . Therefore  $V_n = 185.6 \text{ kN}$ . For a beam subjected to a point load, the  $V_c$  term does not take the  $a/d$  ratio into account since  $M_f/V_f d$  is limited to one. The  $V_s$  term accounts for  $\ell_n$  but tends to predict the opposite to what happened in the tests. For a decreasing  $\ell_n$  term, the ACI code predicts a decreasing  $V_s$  term which is not as expected. The model does account for  $f'_c$  in its  $V_c$  equation, but does not account for anchorage length as shown in Figure 5.34. The theoretical moment capacities were not critical in these calculations.

It should be noted that the tests beams do not satisfy the ACI code requirements. This would have resulted in even more conservative predictions had they been reinforced as required.

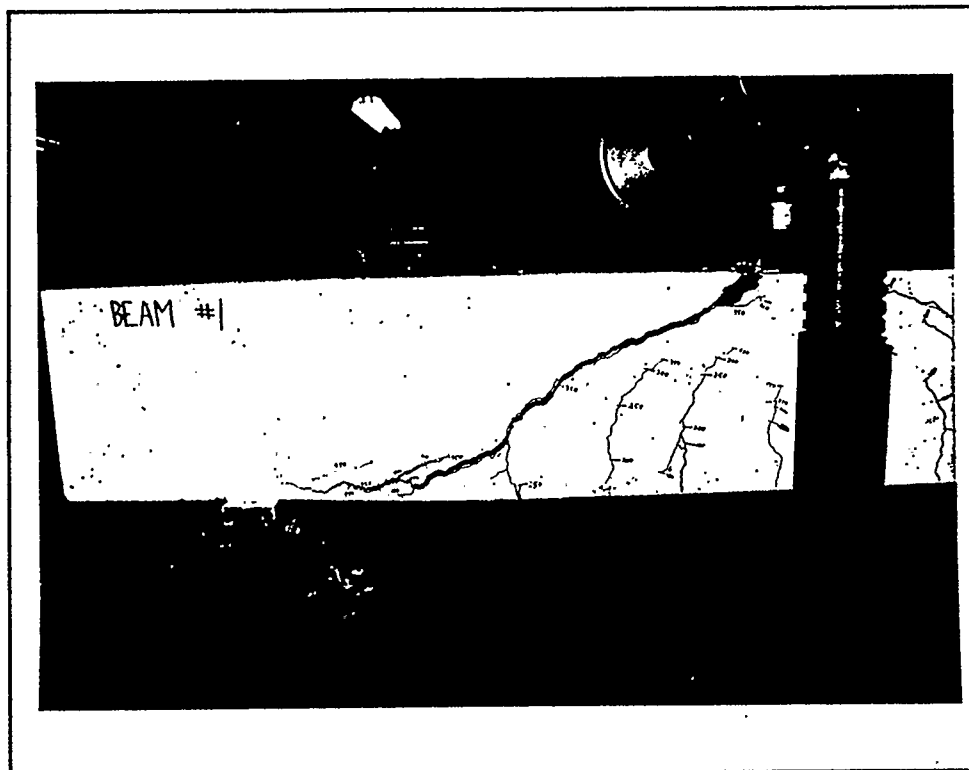


Figure 5.1: Beam 1 after failure,  $a/d = 3.05$

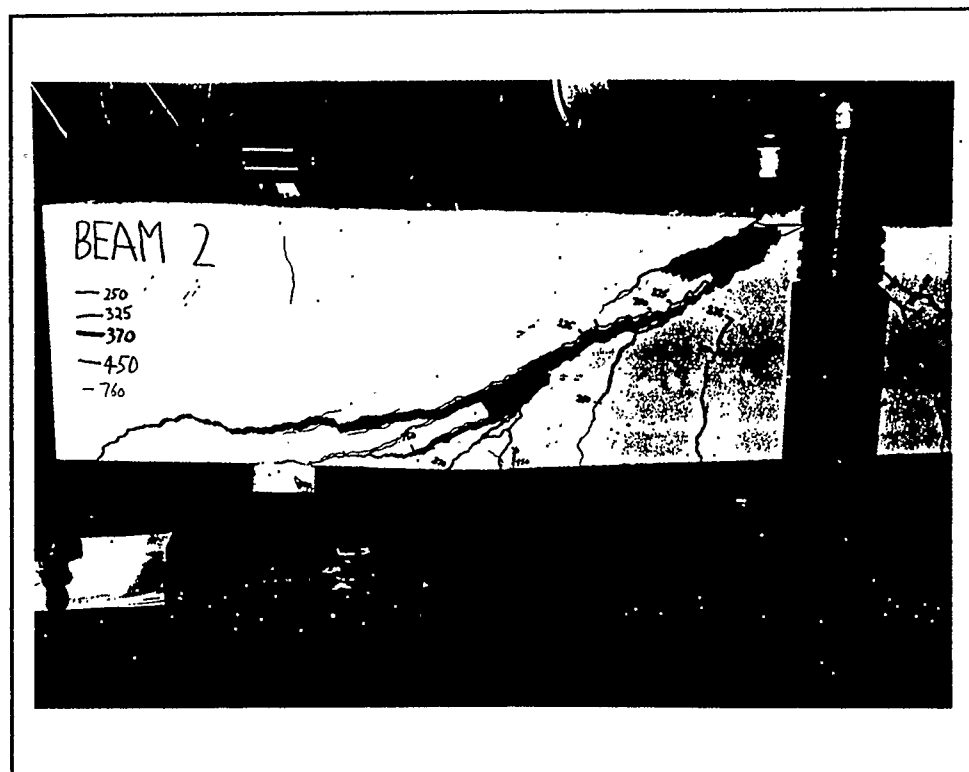


Figure 5.2: Beam 2 after failure,  $a/d = 2.61$

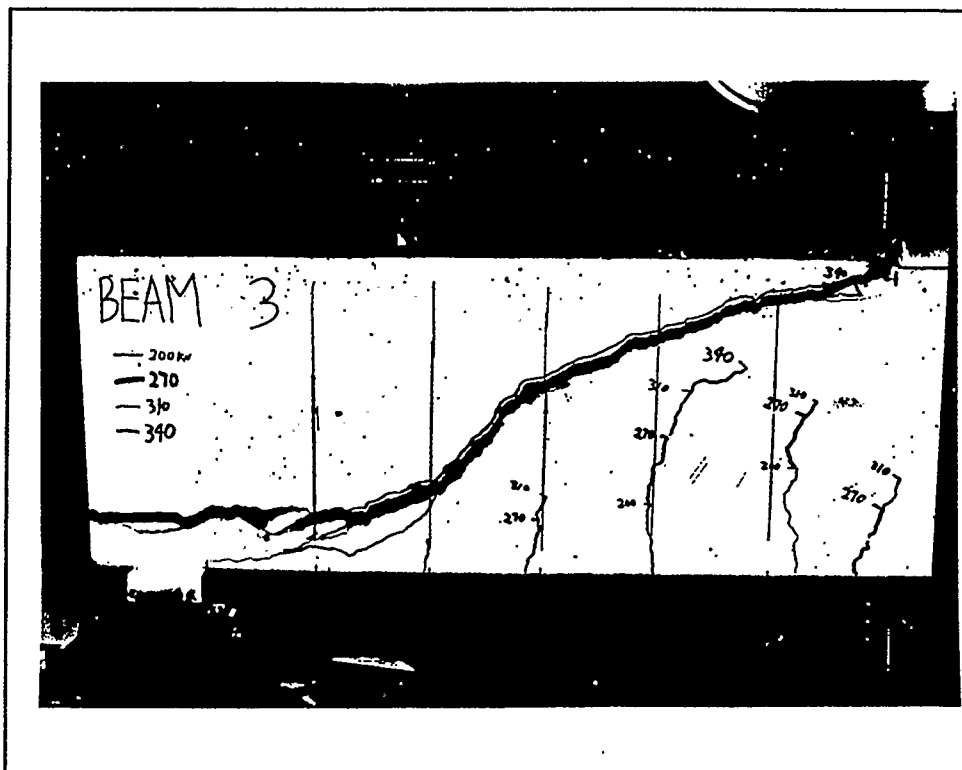


Figure 5.3: Beam 3 after failure,  $a/d = 3.05$

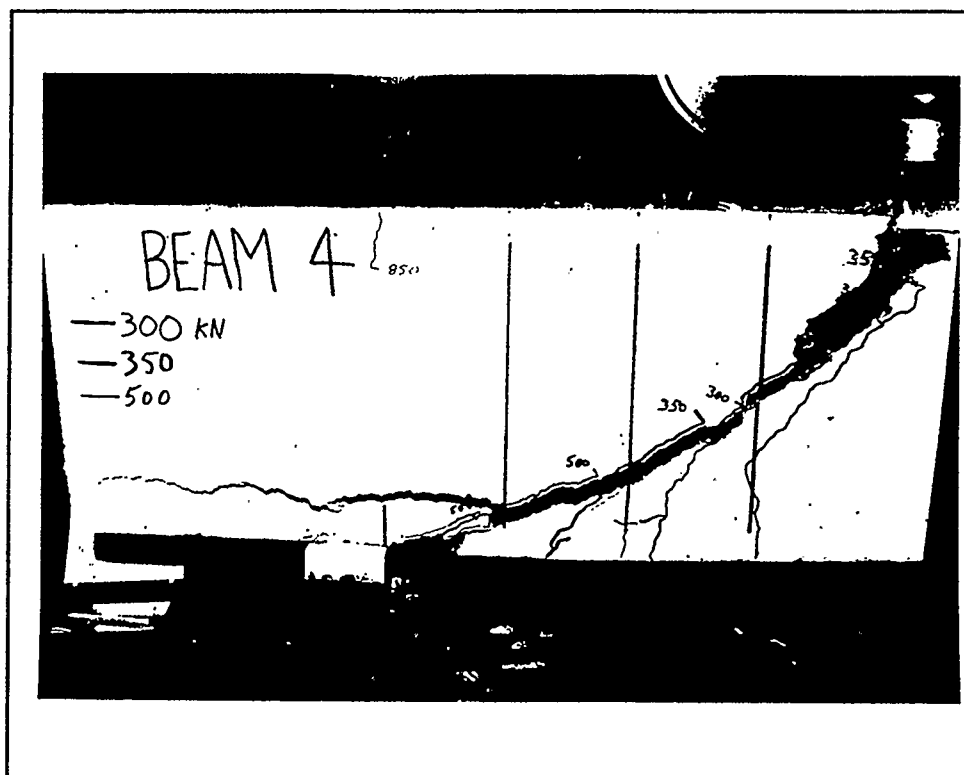


Figure 5.4: Beam 4 after failure,  $a/d = 2.17$

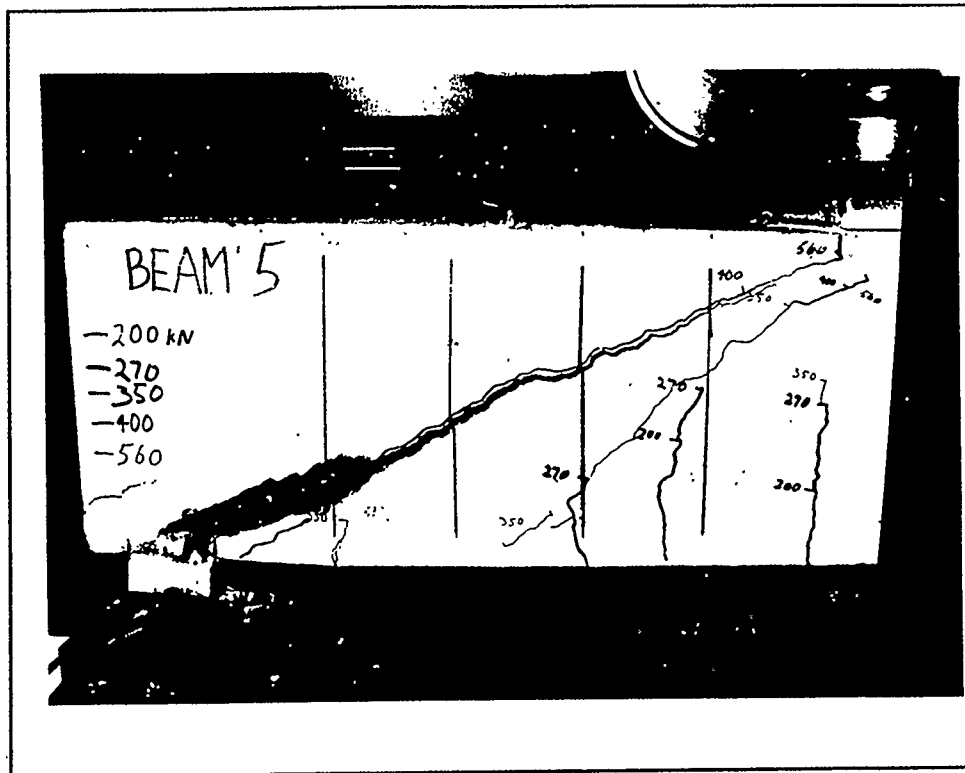


Figure 5.5: Beam 5 after failure,  $a/d = 2.61$

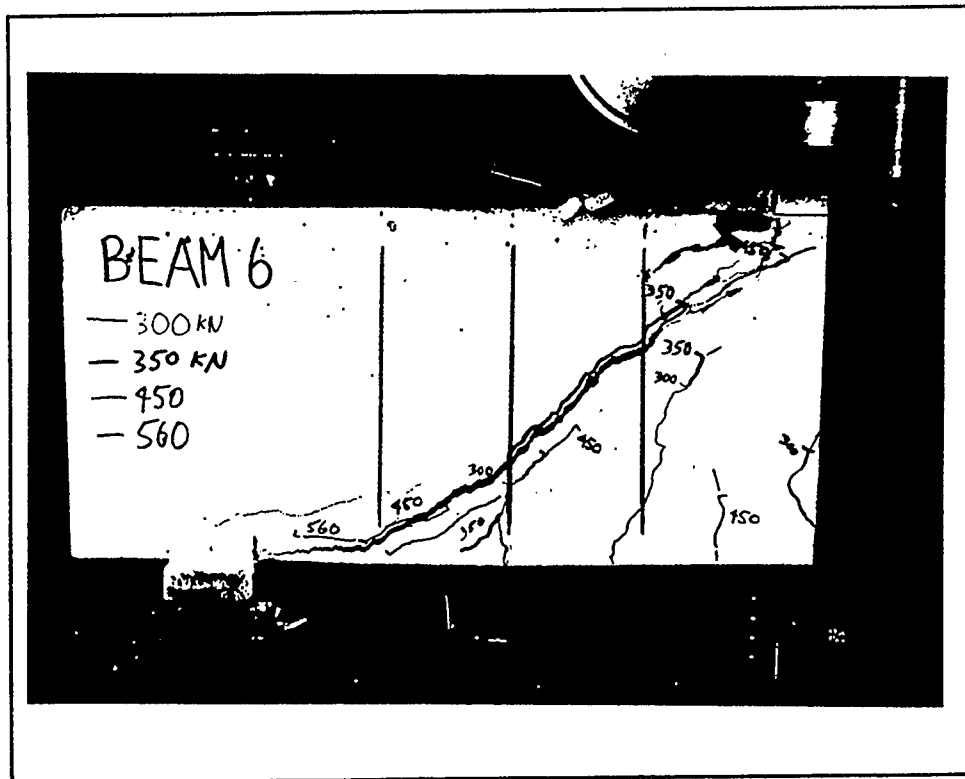


Figure 5.6: Beam 6 after failure,  $a/d = 2.17$

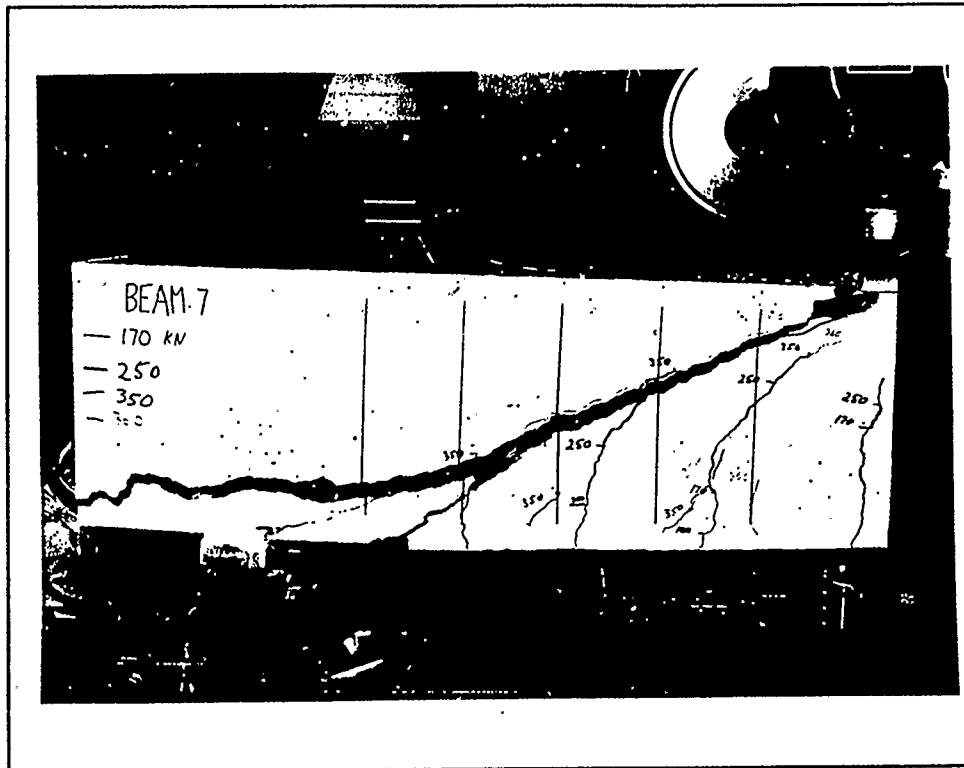


Figure 5.7: Beam 7 after failure,  $a/d = 3.05$

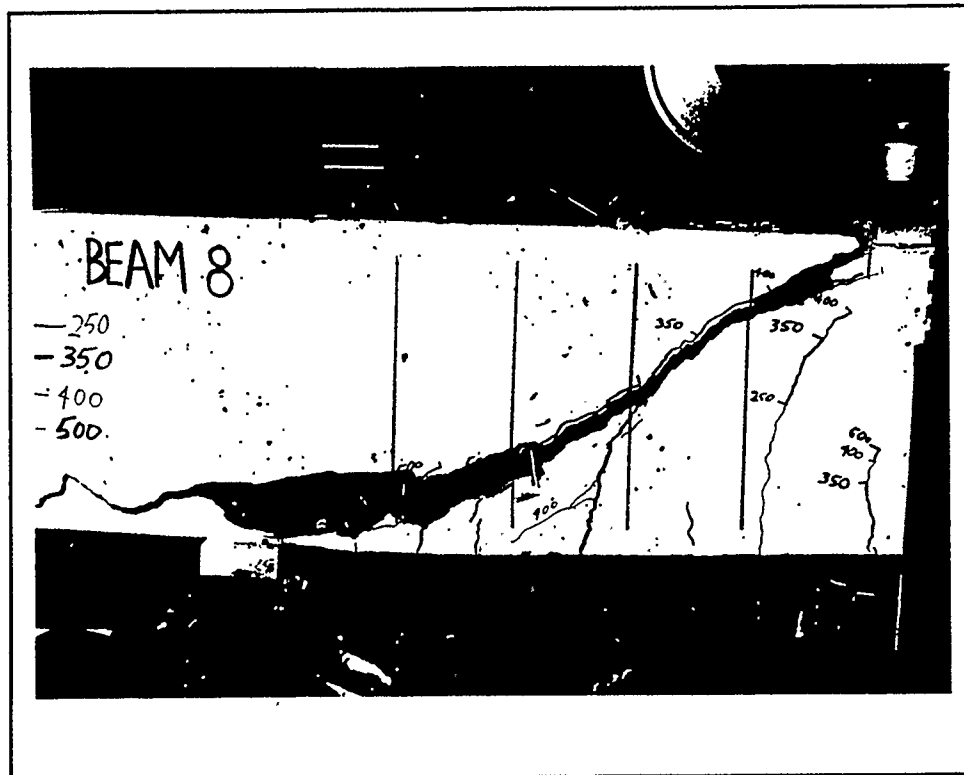


Figure 5.8: Beam 8 after failure,  $a/d = 2.61$

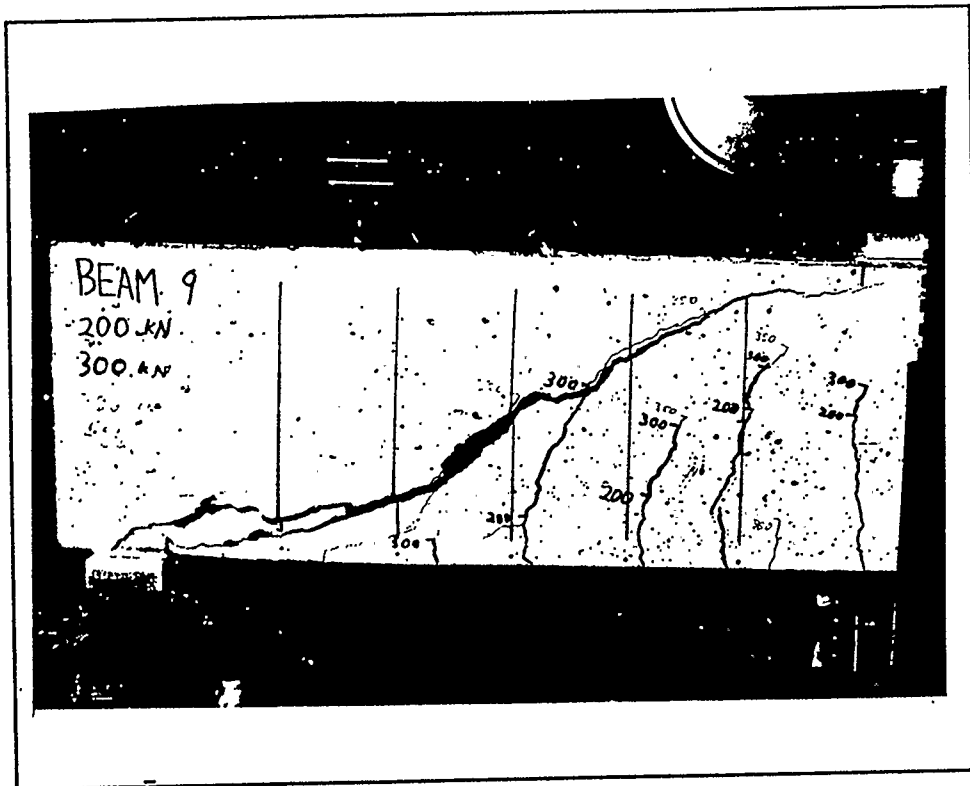


Figure 5.9: Beam 9 after failure,  $a/d = 3.05$

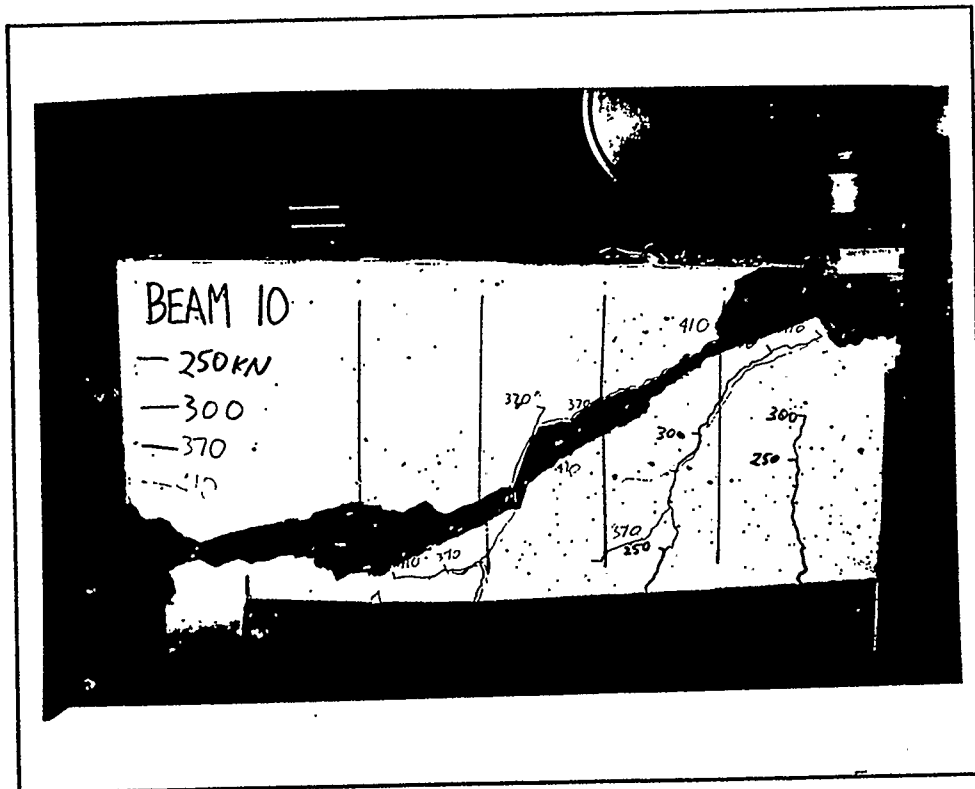


Figure 5.10: Beam 10 after failure,  $a/d = 2.61$

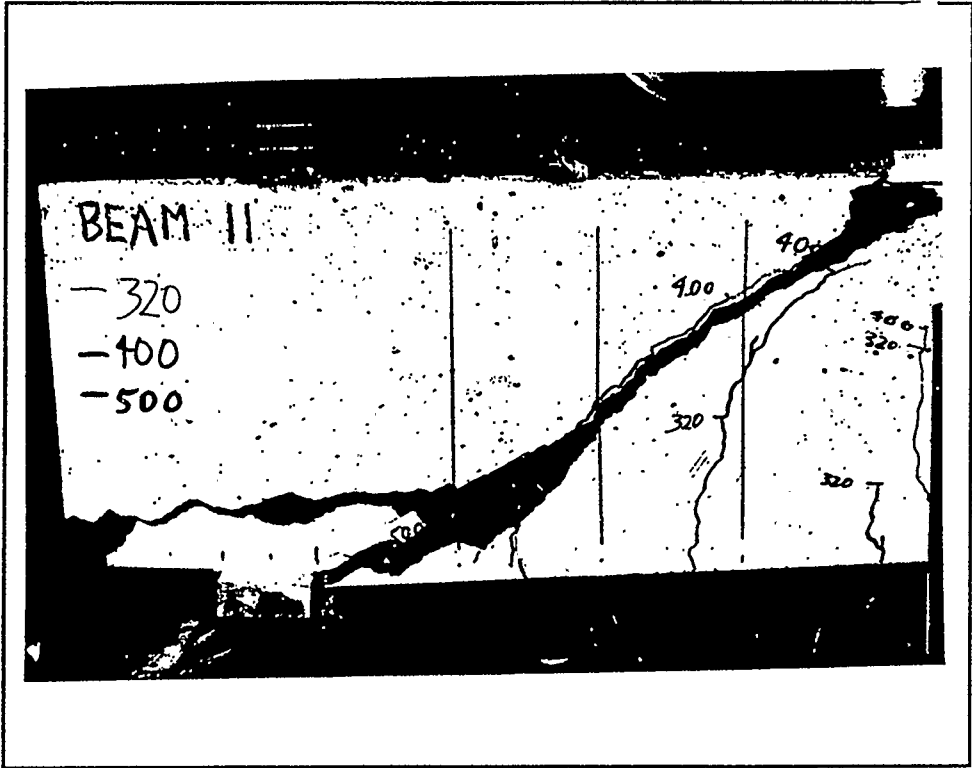


Figure 5.11: Beam 11 after failure,  $a/d = 2.17$

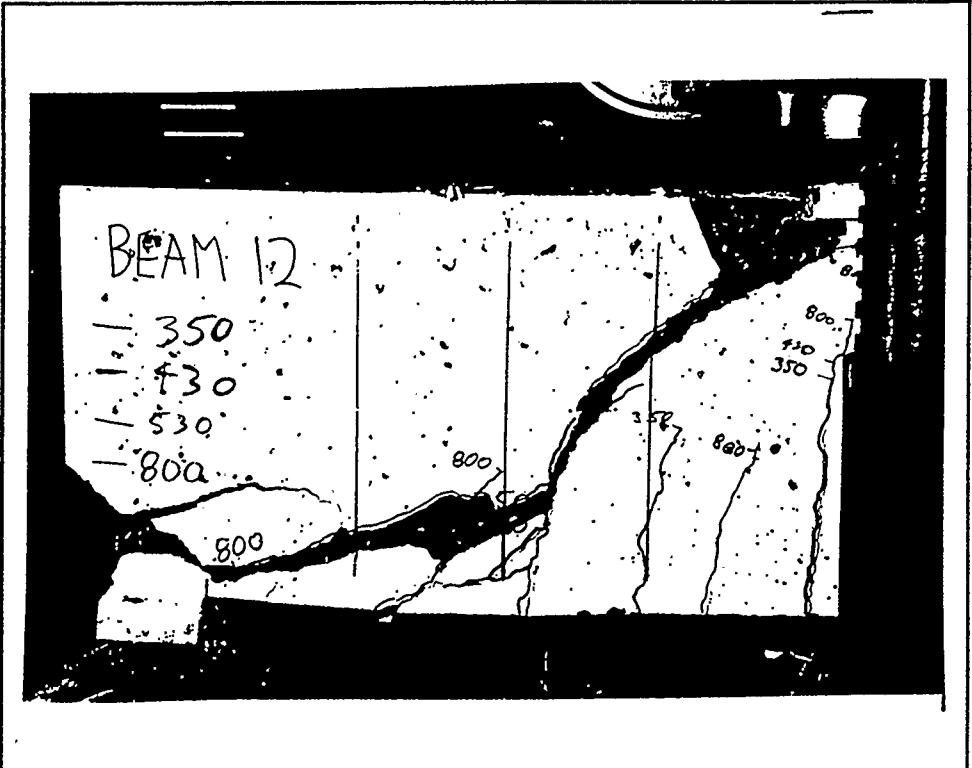
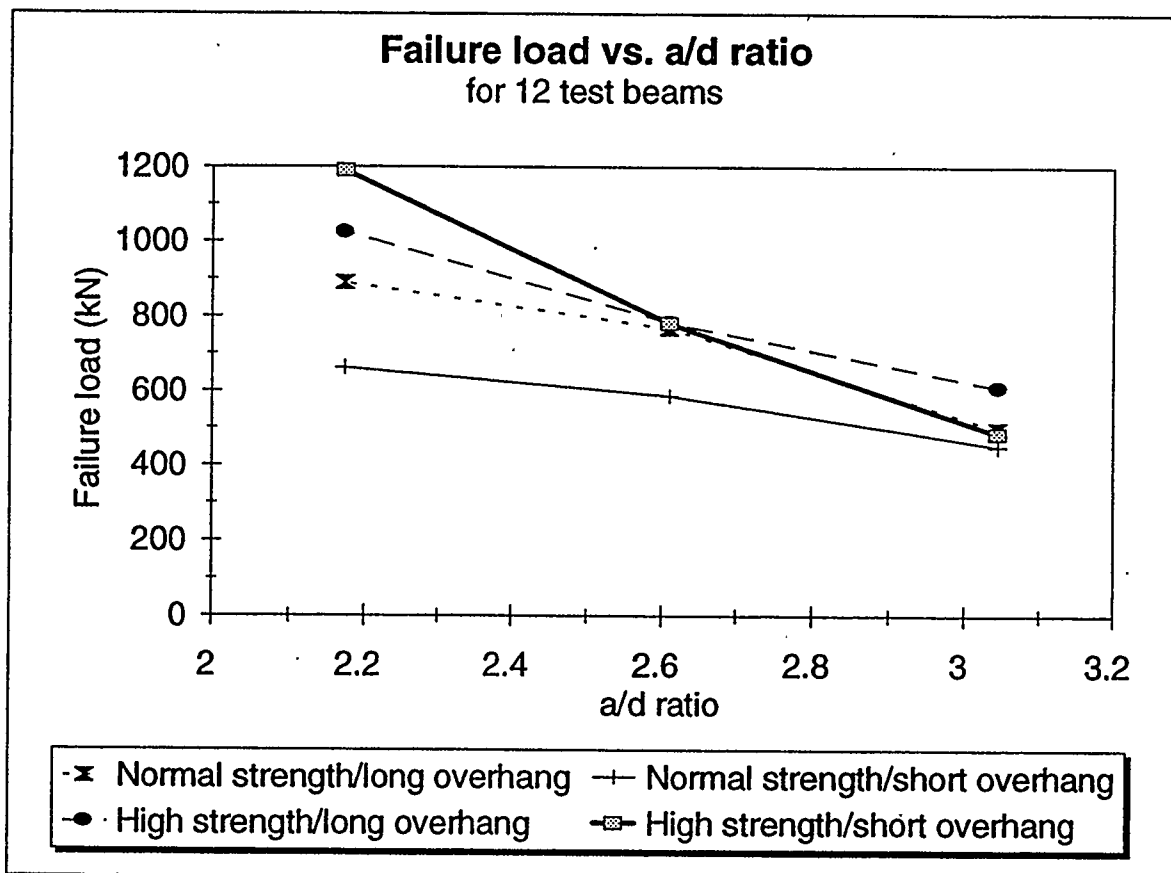


Figure 5.12: Beam 12 after failure,  $a/d = 2.17$





**Figure 5.13: Failure load versus a/d ratio**

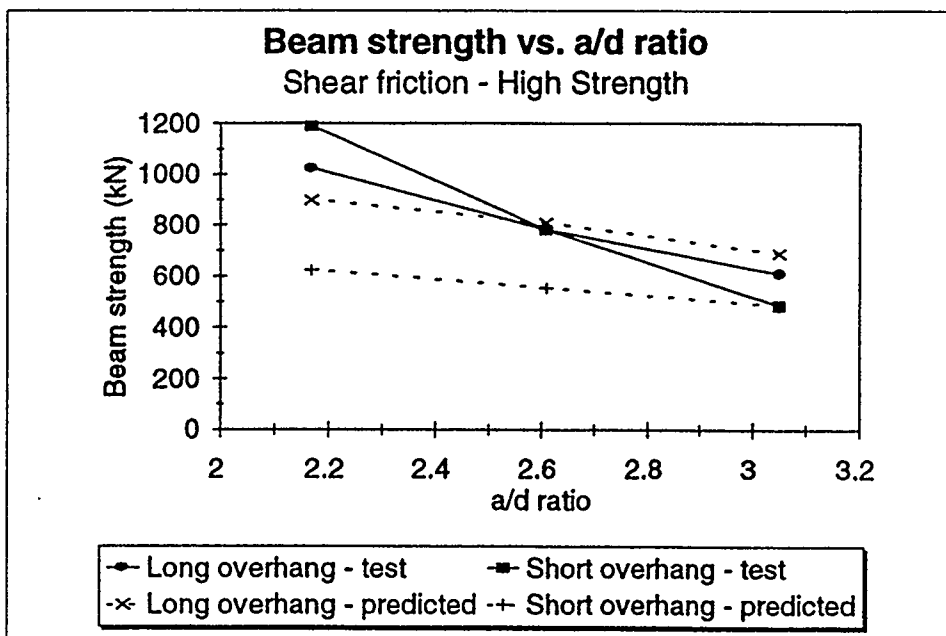
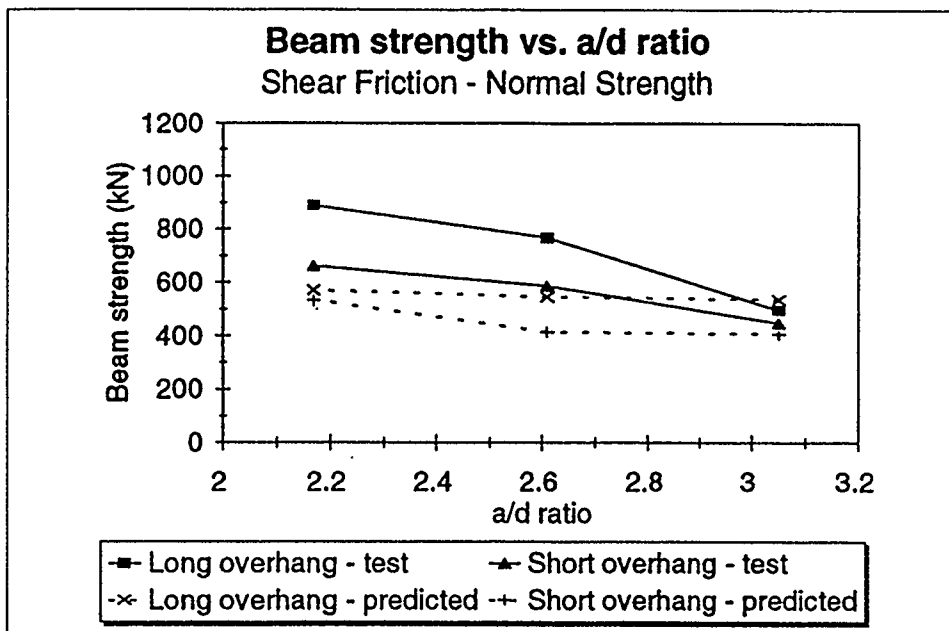
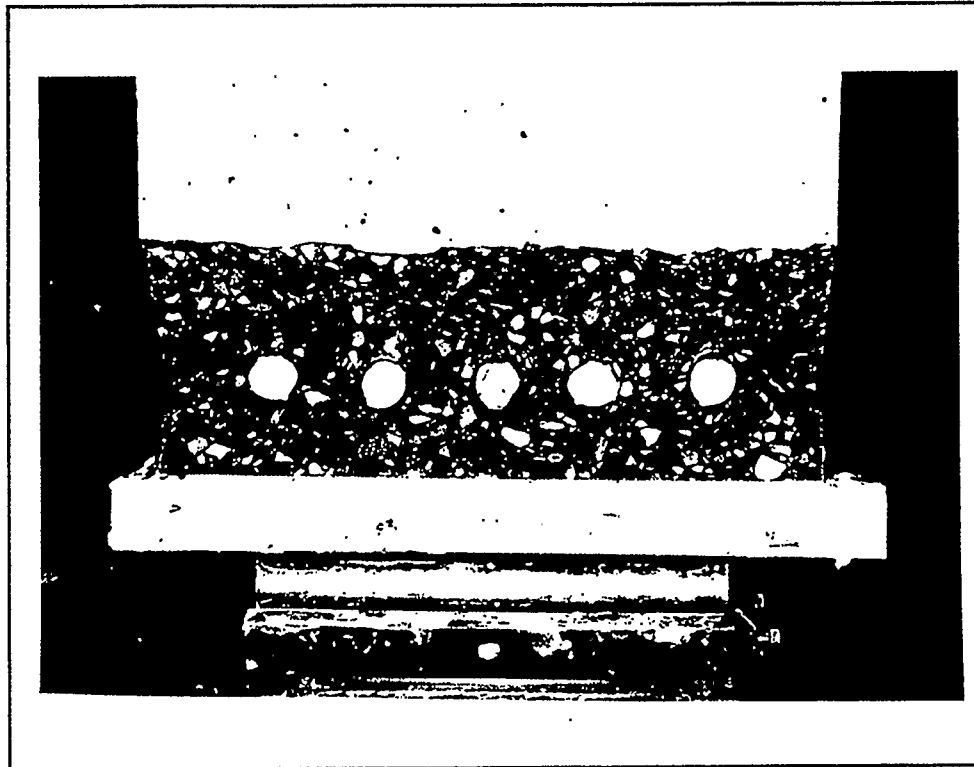
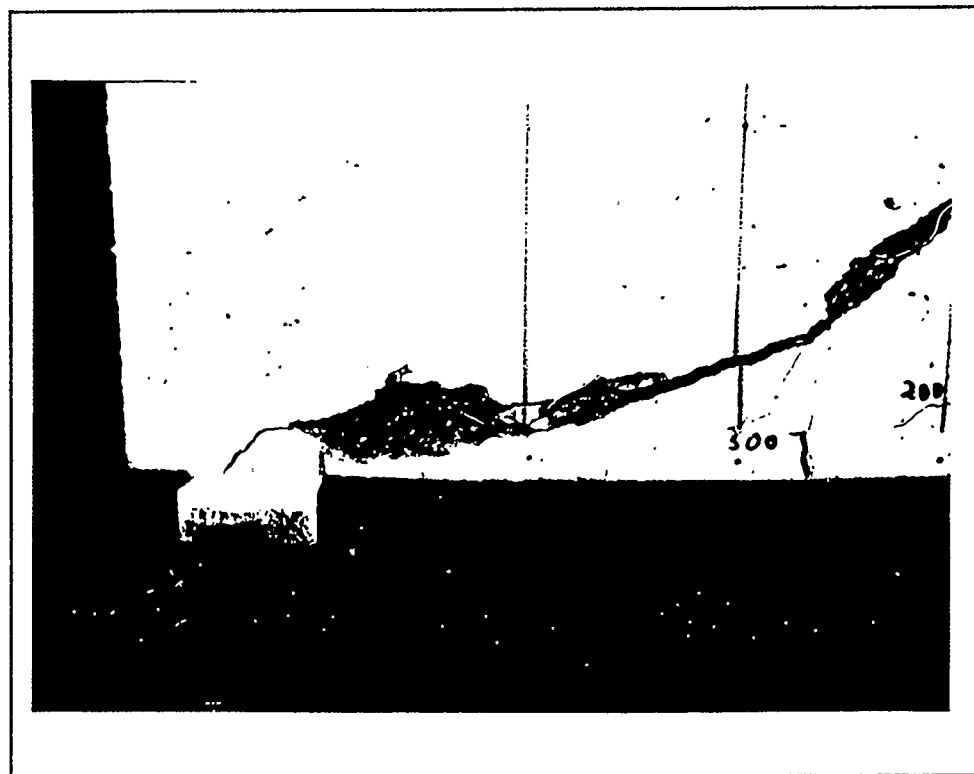


Figure 5.14: Beam strength vs. a/d ratio - shear friction



**Figure 5.15 Horizontal crack after failure (end view)**



**Figure 5.16 Horizontal crack after failure (side view)**

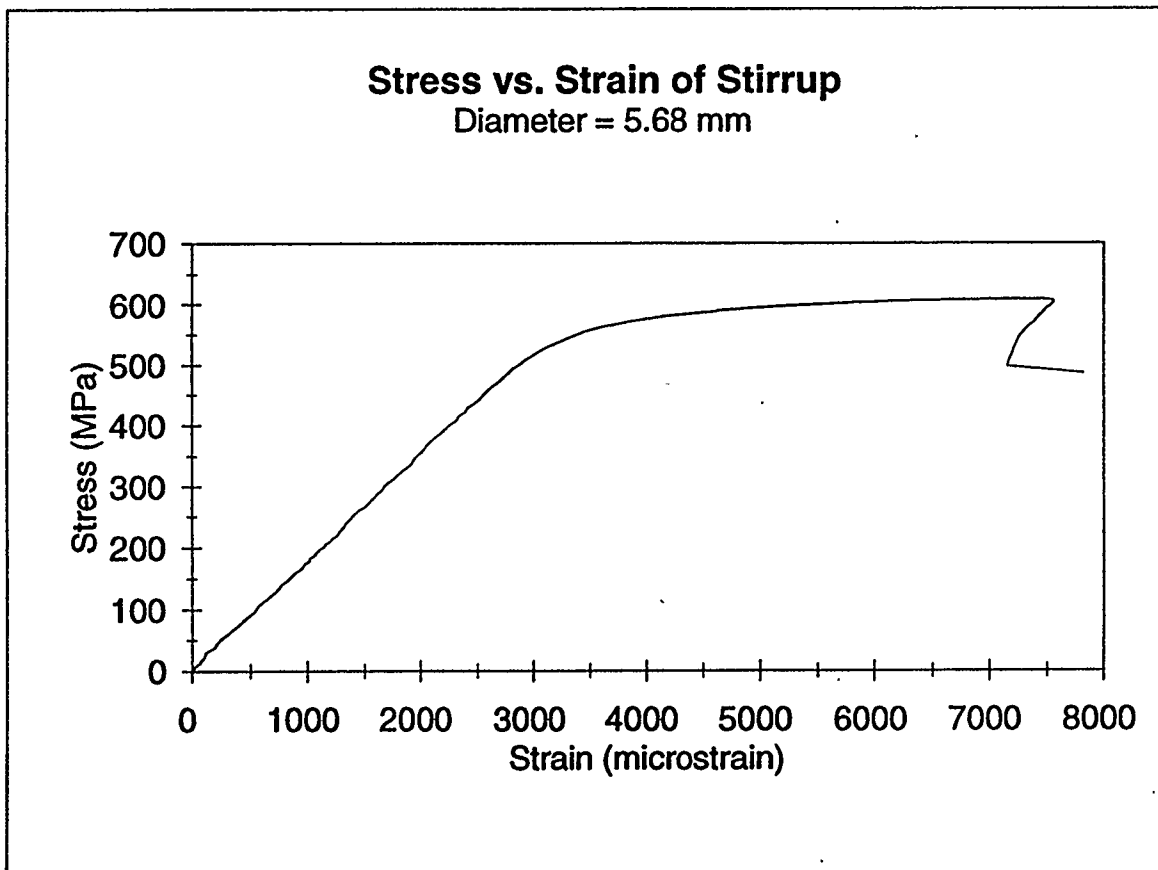


**Figure 5.17: Stress-strain curve for stirrup**

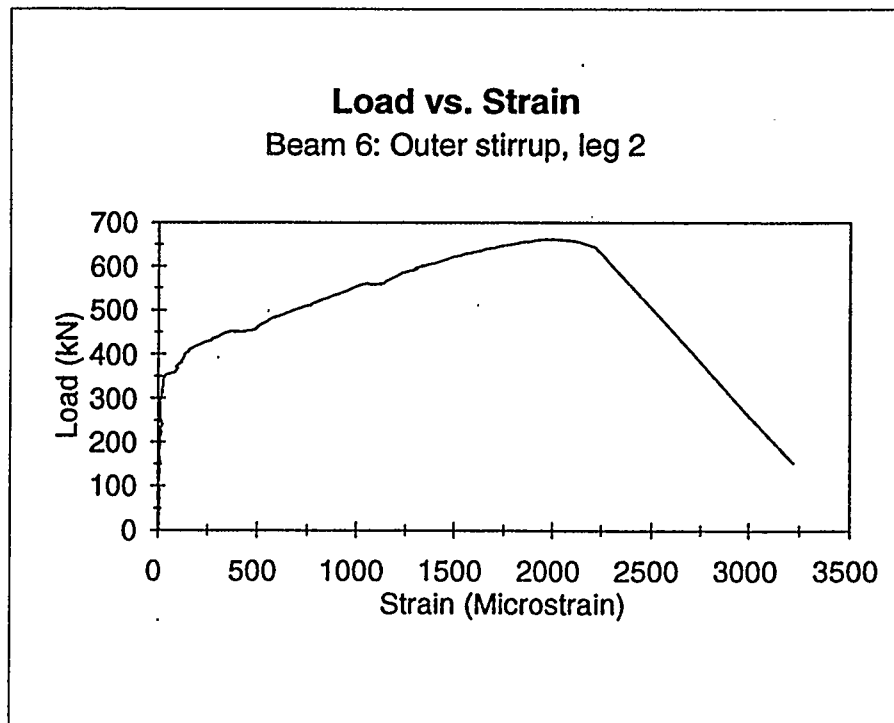
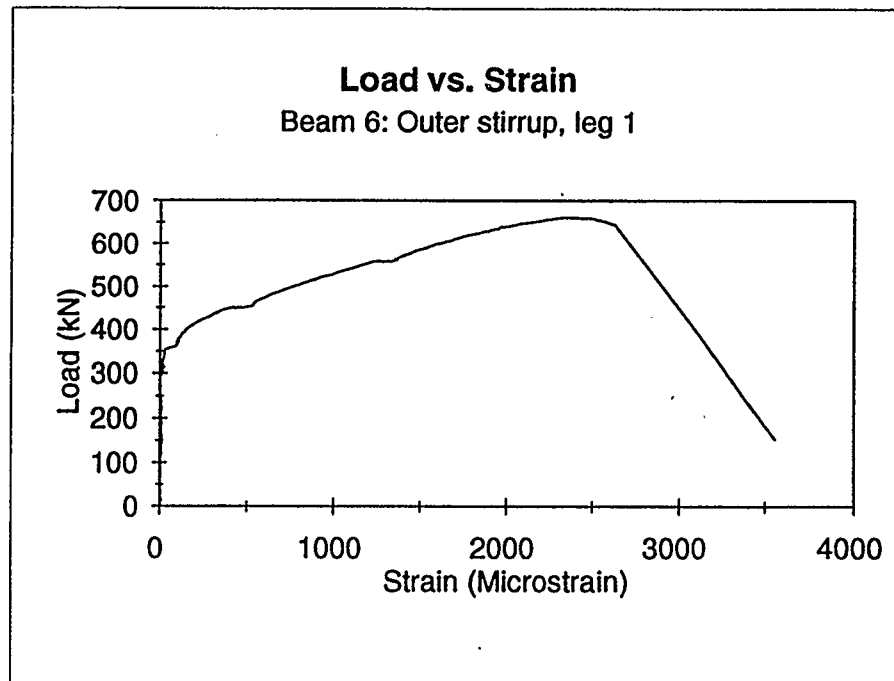


**Figure 5.18: Strains in stirrups for beam 6 (outer stirrup)**

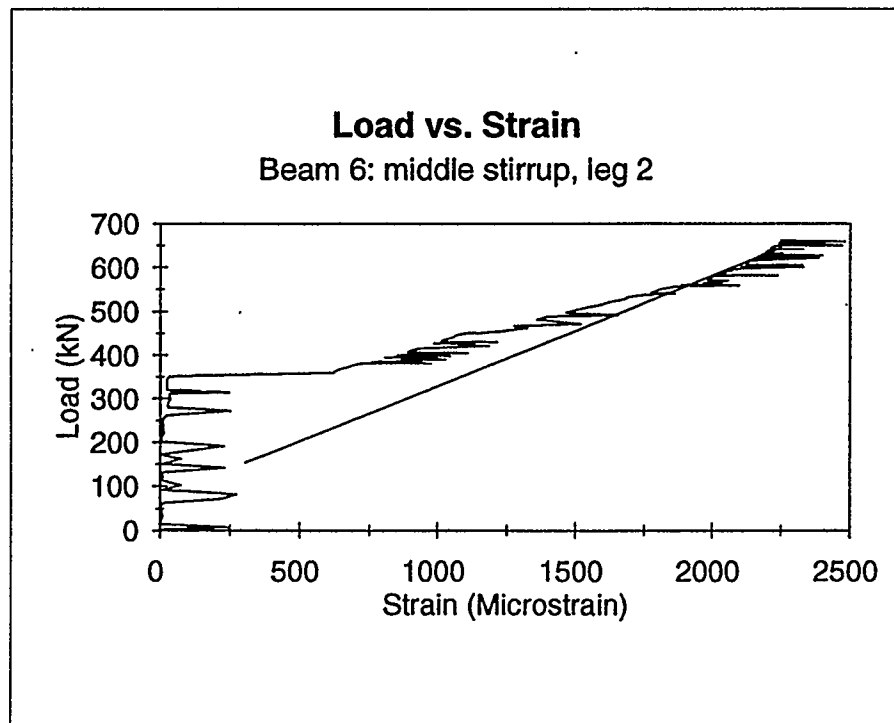
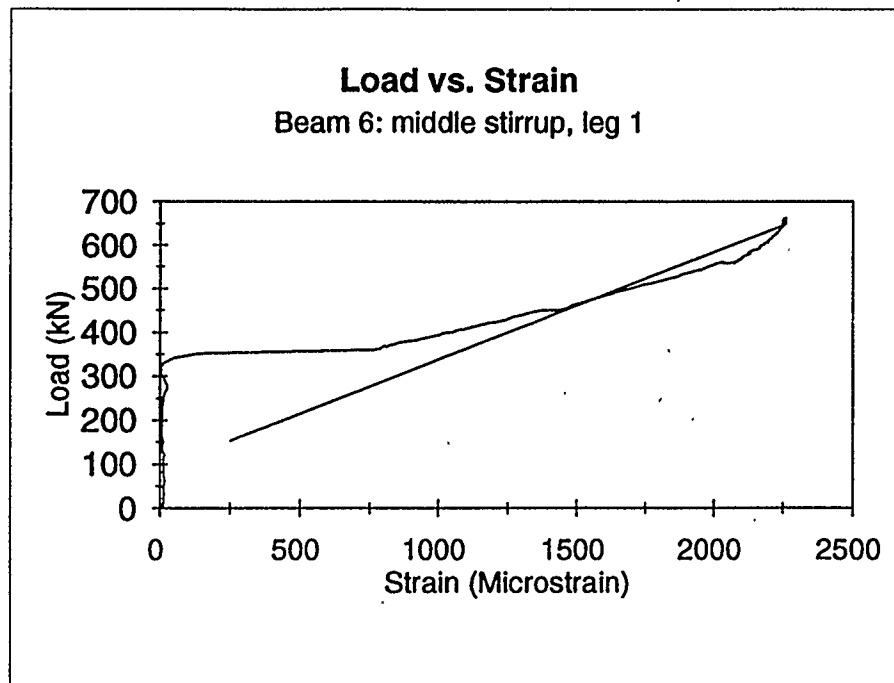


**Figure 5.19: Strains in stirrups for beam 6 (middle stirrup)**

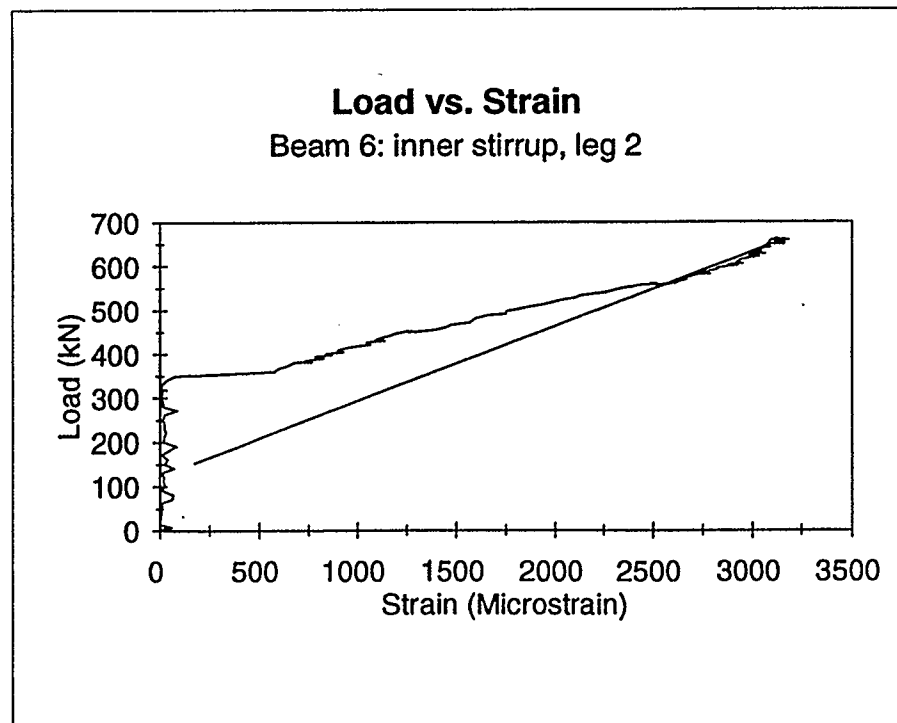
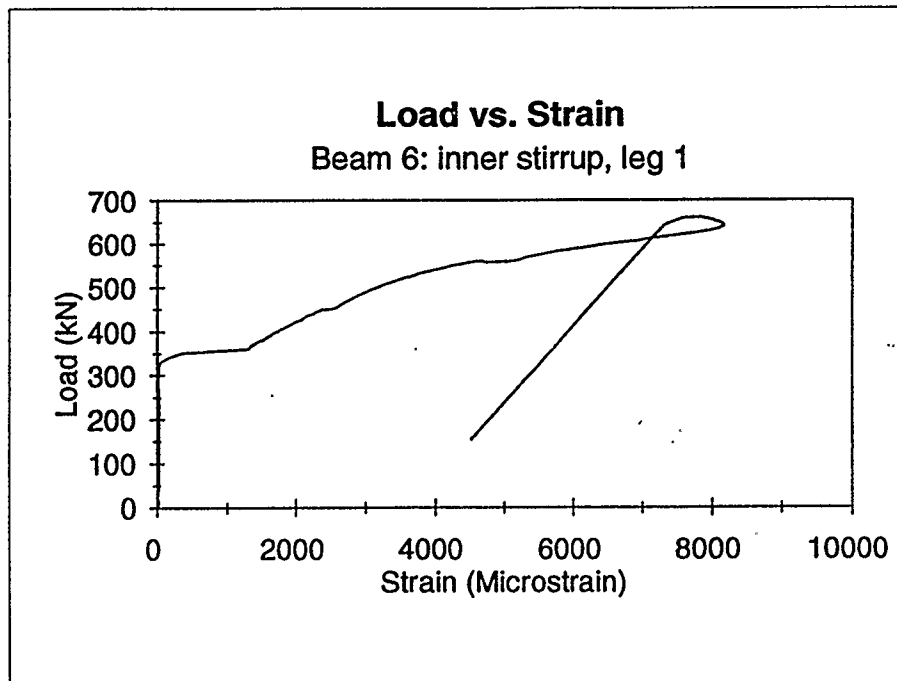


**Figure 5.20: Strains in stirrups for beam 6 (inner stirrup)**

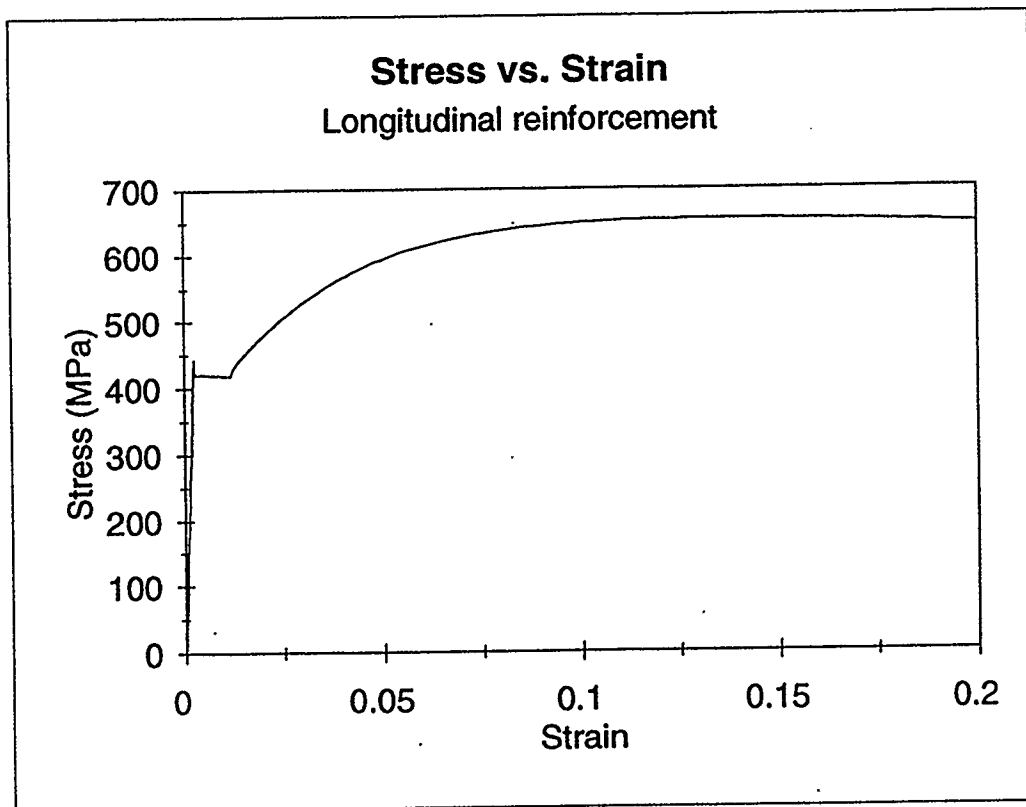


**Figure 5.21: Stress-strain curve for longitudinal reinforcement**



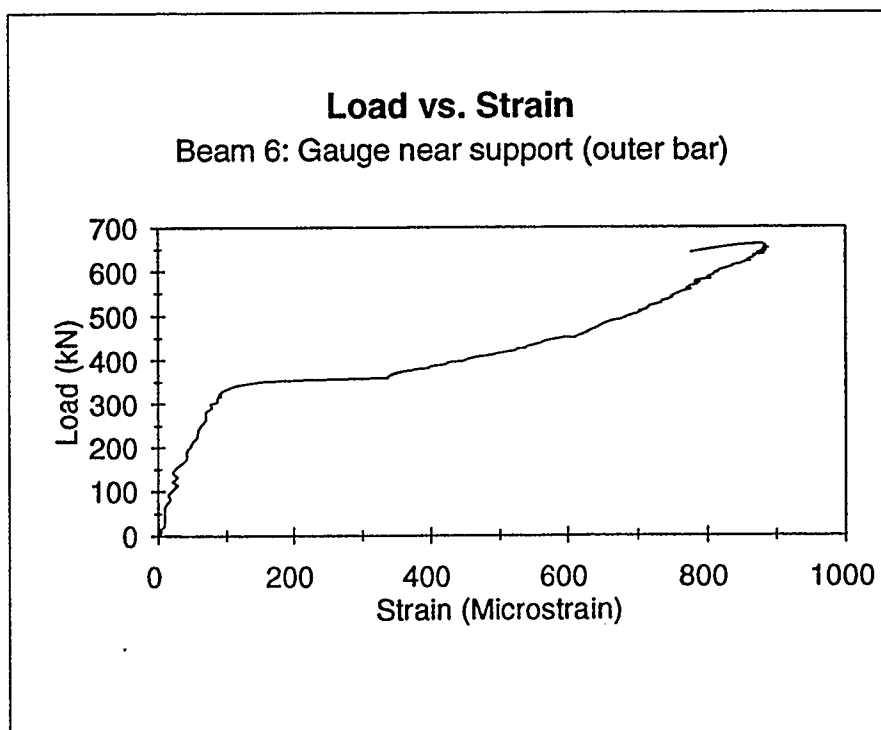
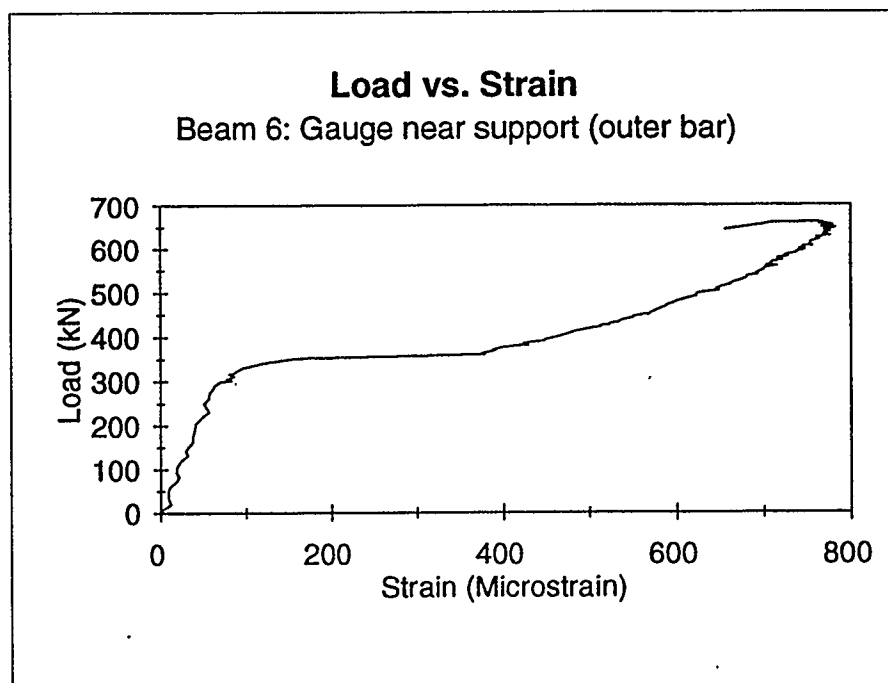


**Figure 5.22: Strains in longitudinal reinforcement for beam 6 (near support)**

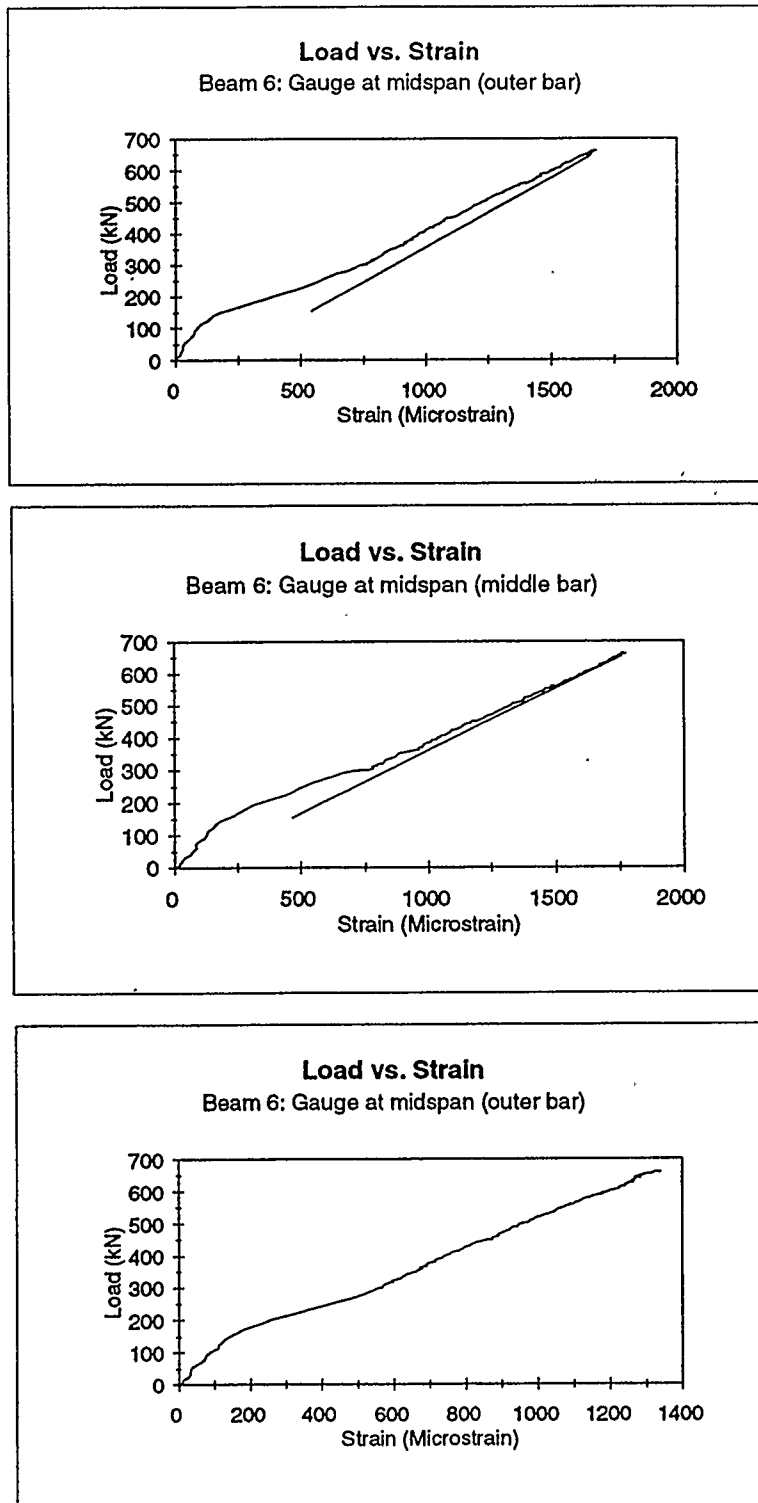


**Figure 5.23: Strains in longitudinal reinforcement for beam 6 (at midspan)**

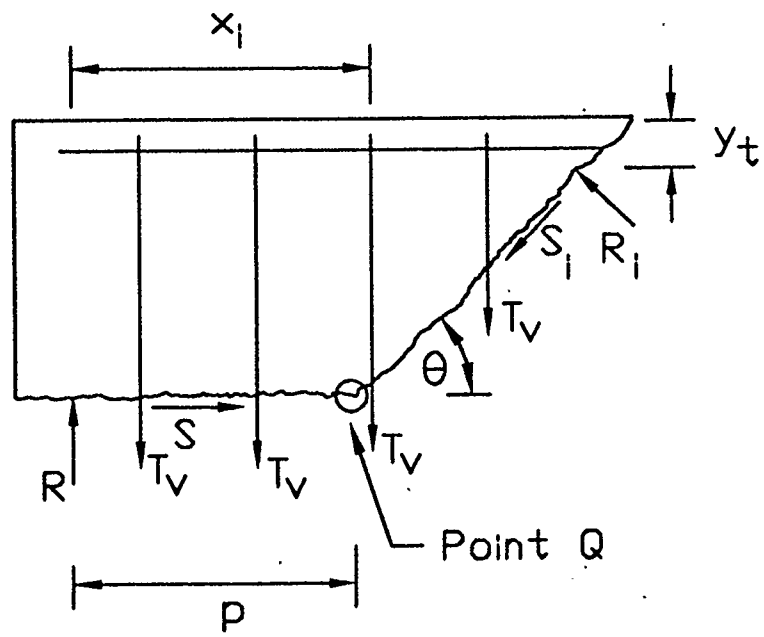


Figure 5.24: Free-body diagram of section of beam

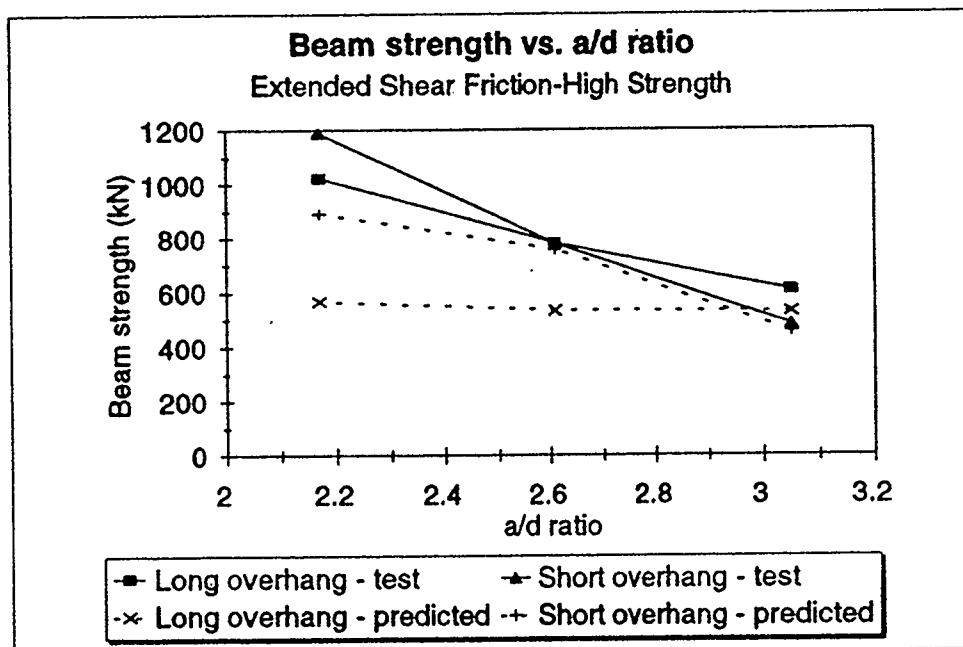
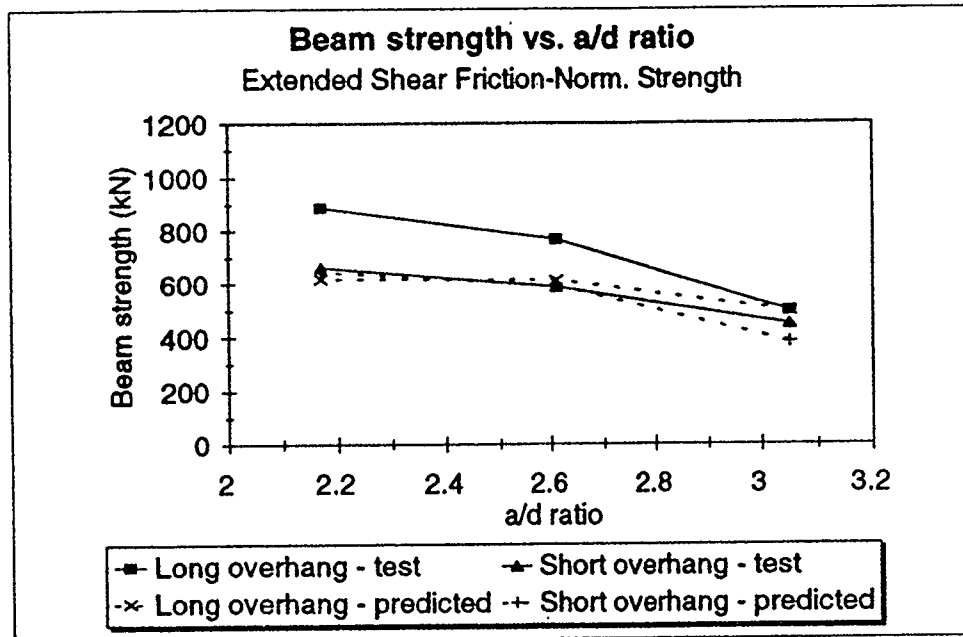


Figure 5.25: Beam strength vs. a/d ratio - extended shear friction

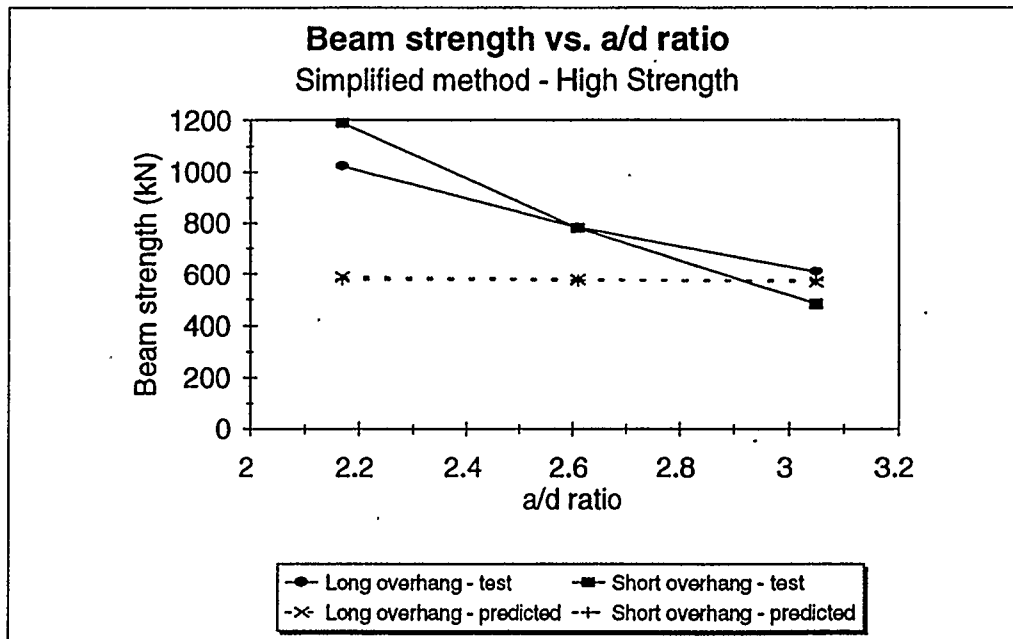
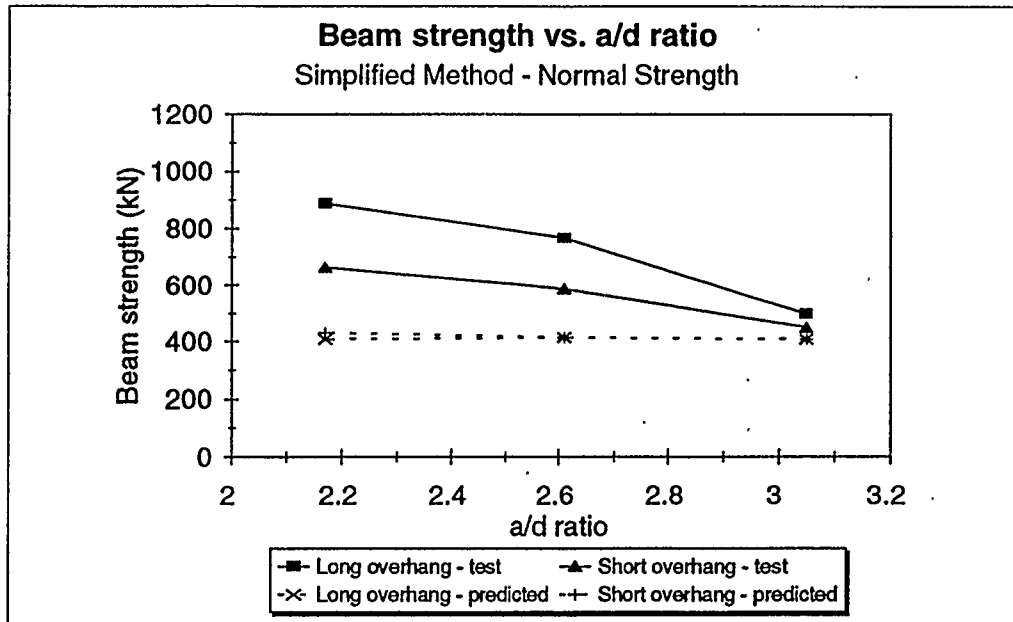
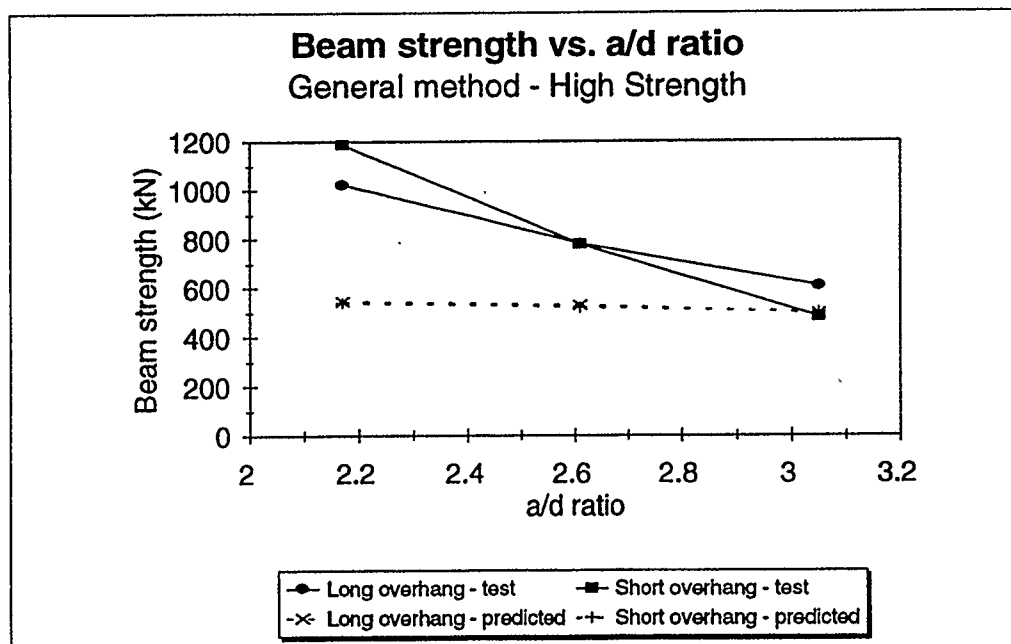
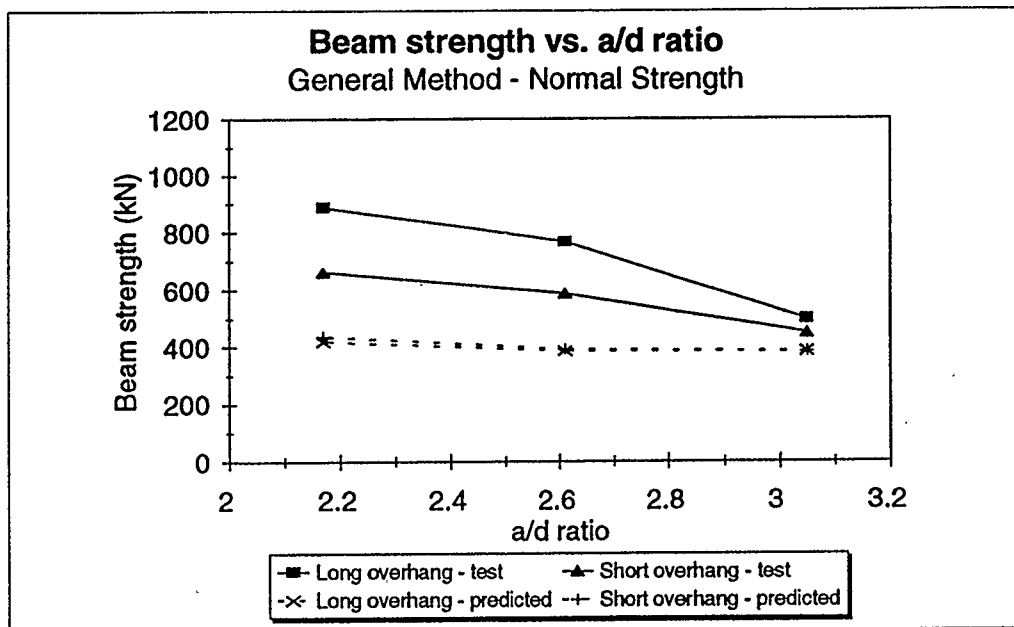
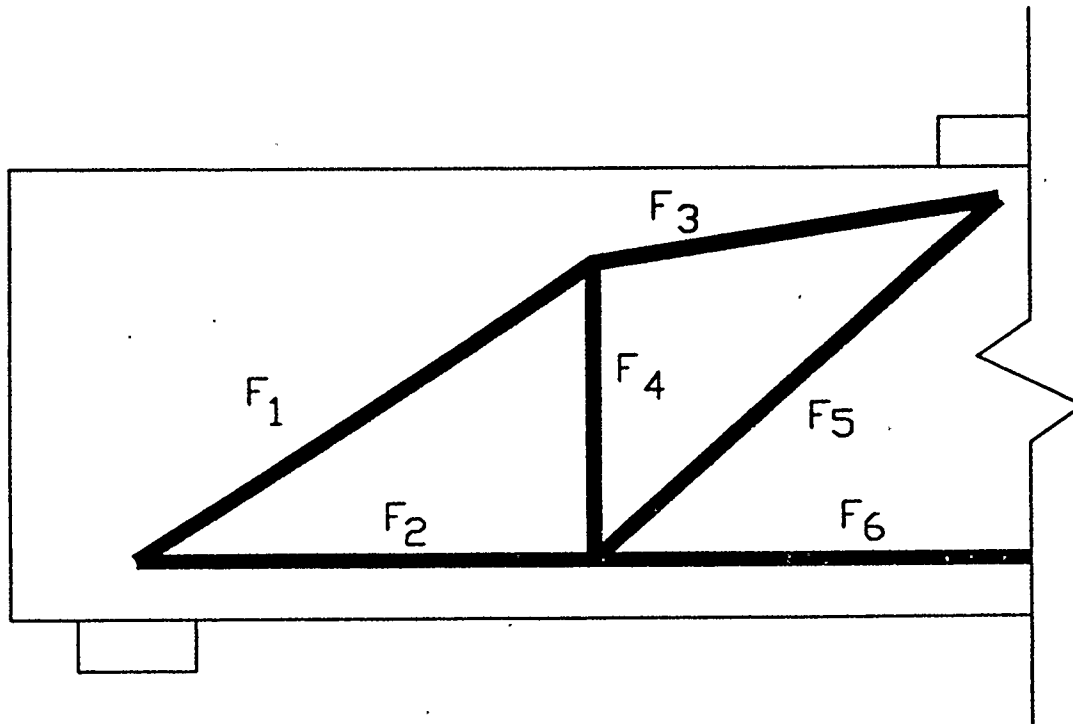


Figure 5.26: Beam strength vs. a/d ratio - CSA A23.3-94 simplified method



**Figure 5.27: Beam strength vs. a/d ratio - CSA A23.3-94 general method**



**Figure 5.28: Strut-and-tie model of test beam**

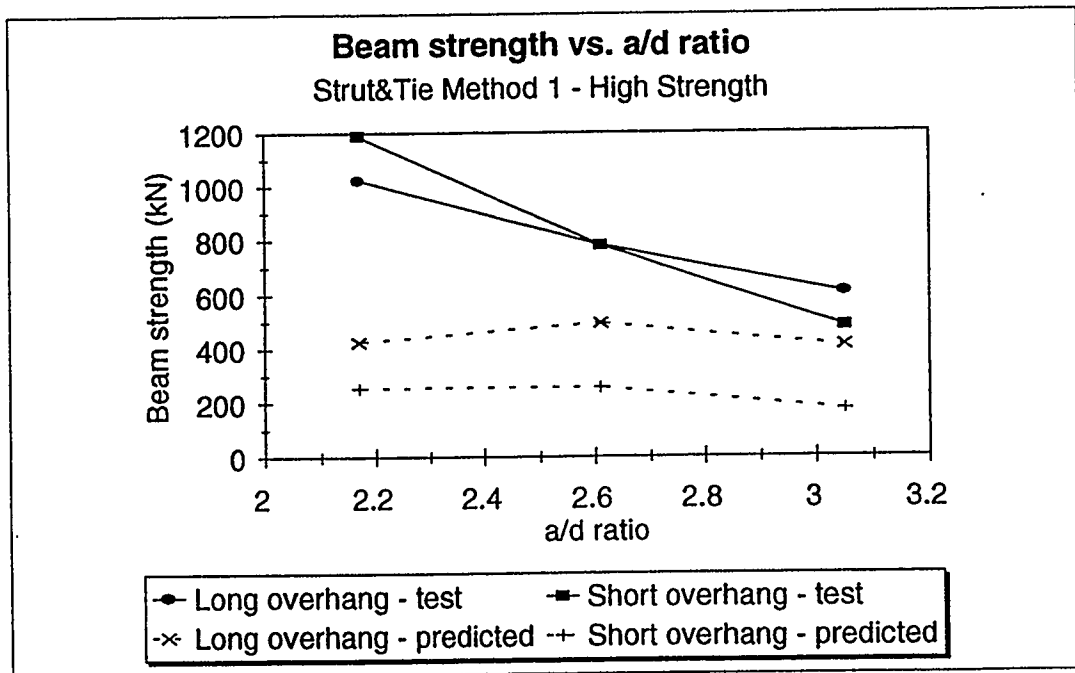
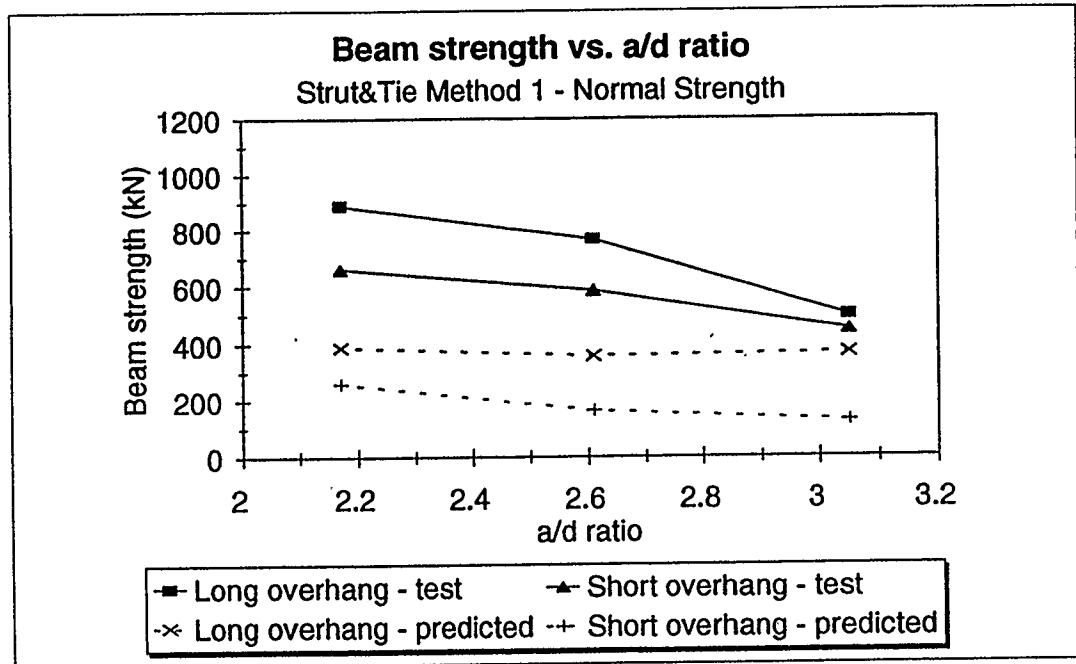


**Figure 5.29: Beam strength vs. a/d ratio - strut-and-tie using code equations**



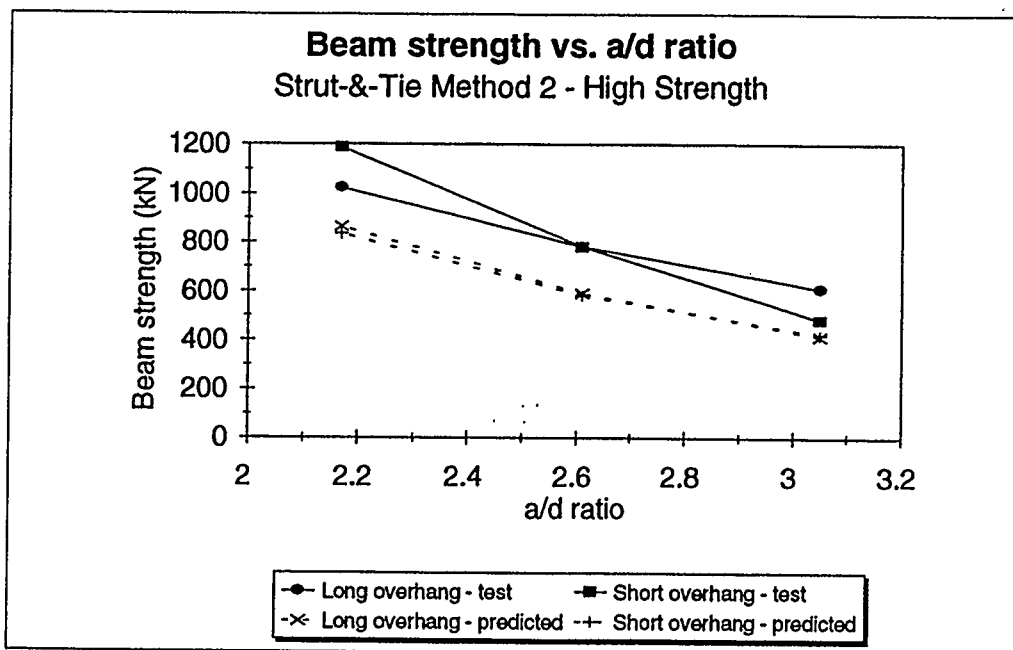
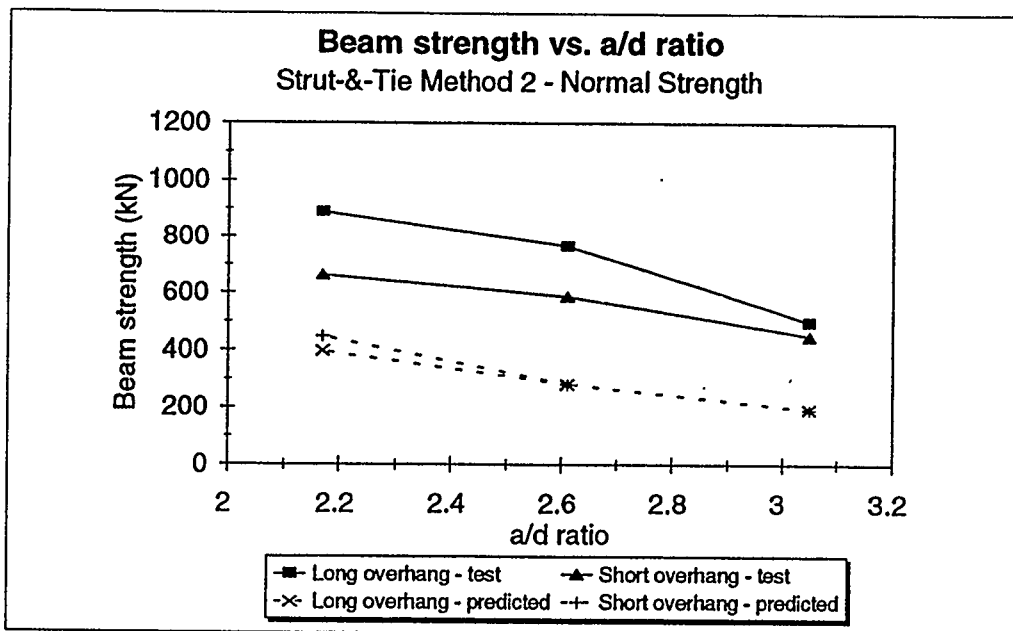


Figure 5.30: Beam strength vs. a/d ratio - strut-and-tie without development eqn.

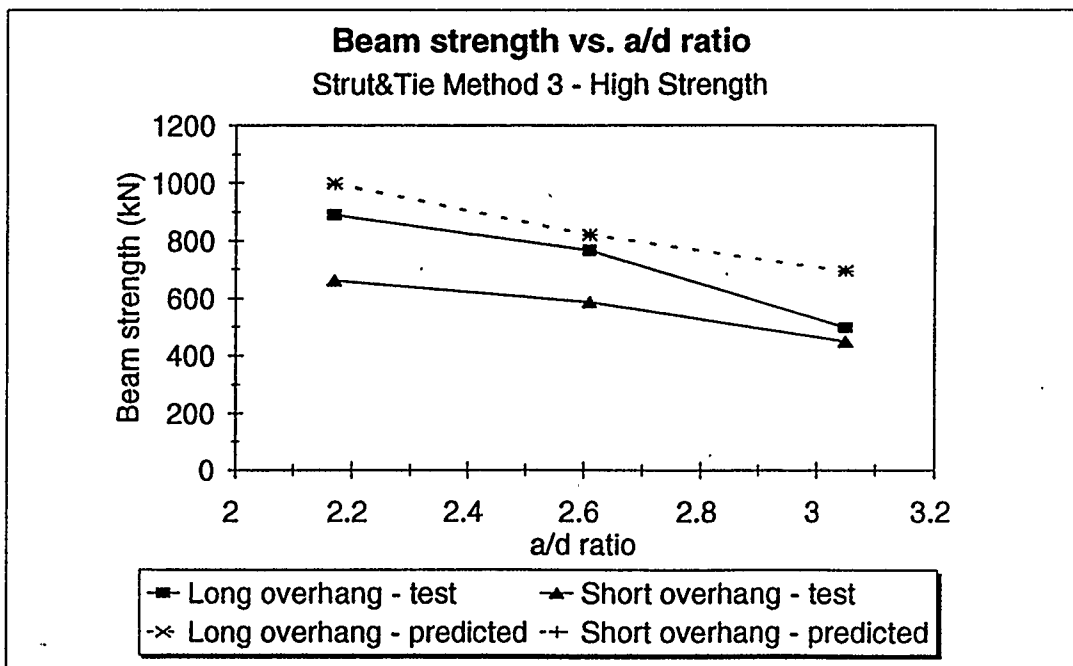
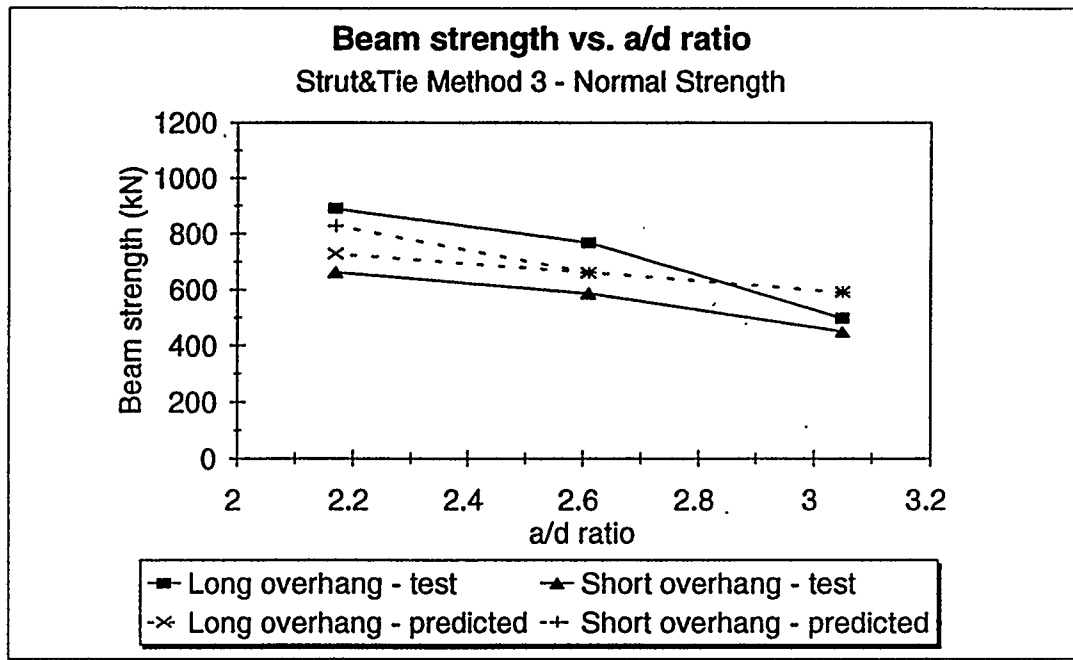
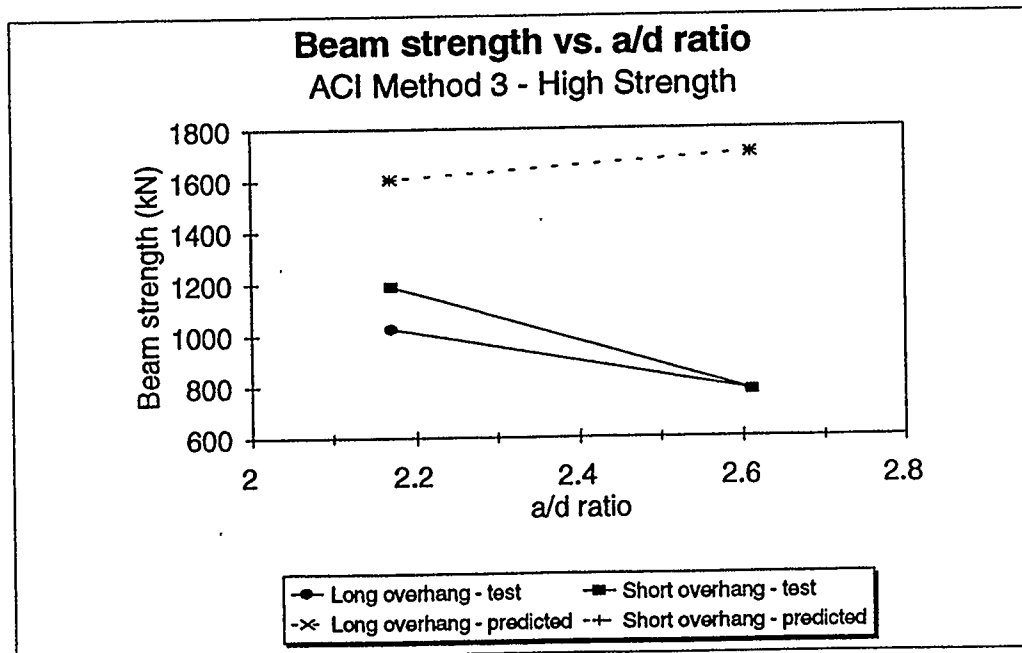
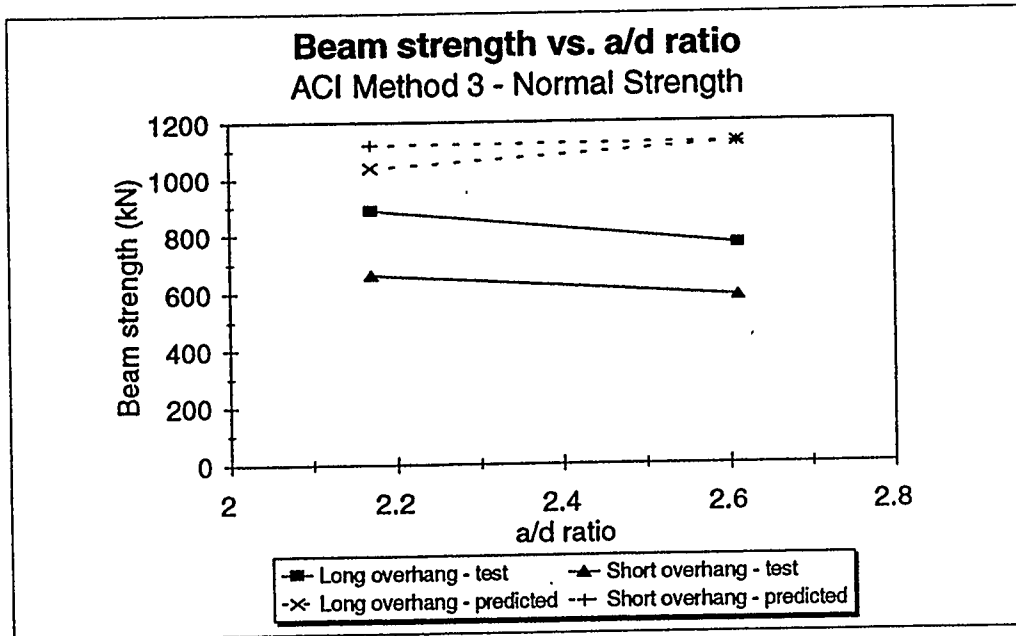


Figure 5.31: Beam strength vs. a/d ratio - strut-and-tie without  $f_{2max}$  restriction



**Figure 5.32: Beam strength vs. a/d ratio - ACI method using Eqn. 2.25**

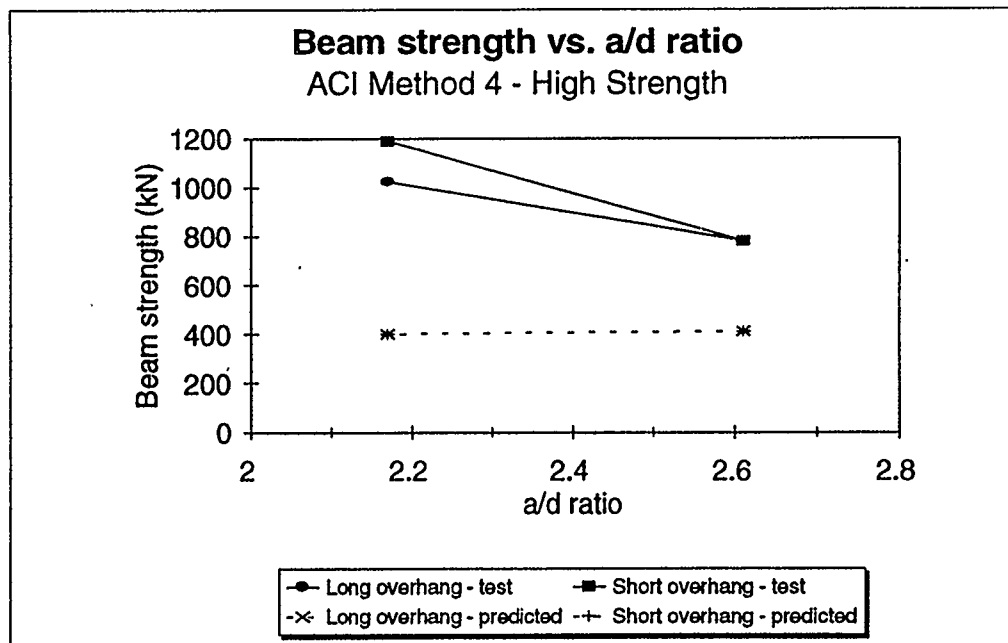
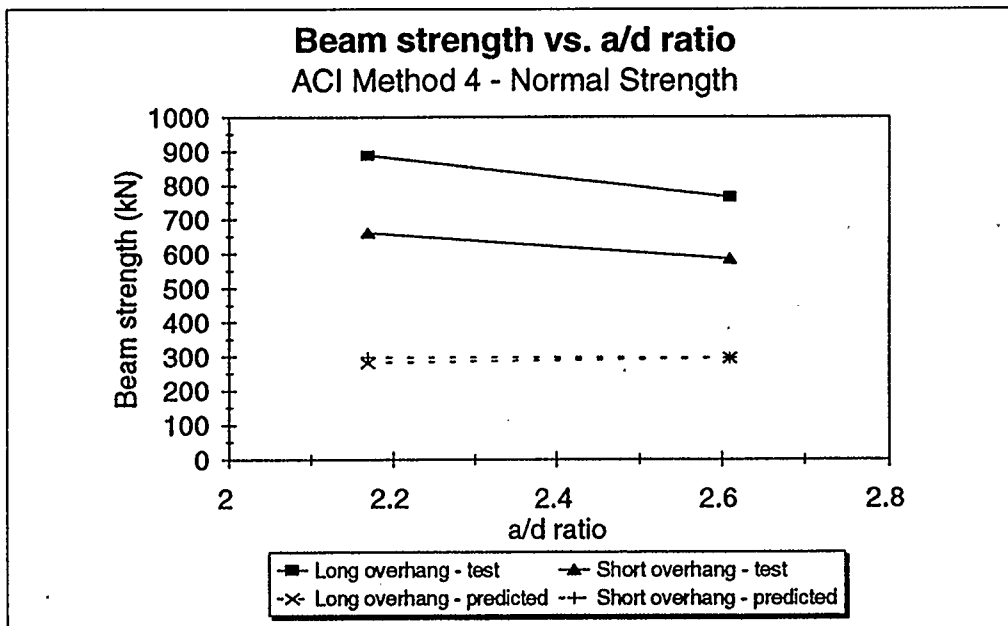
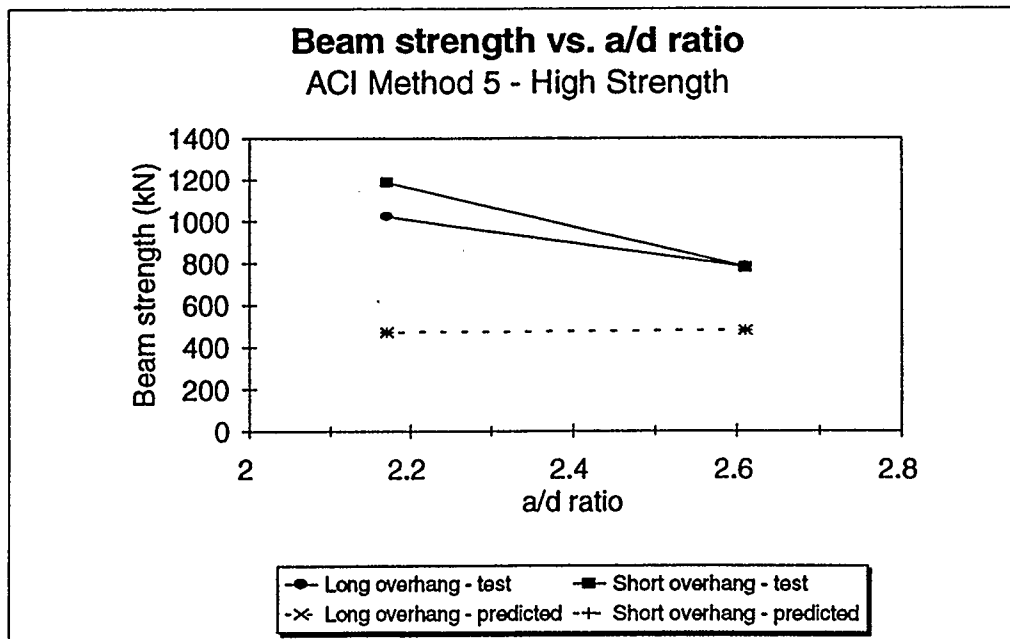
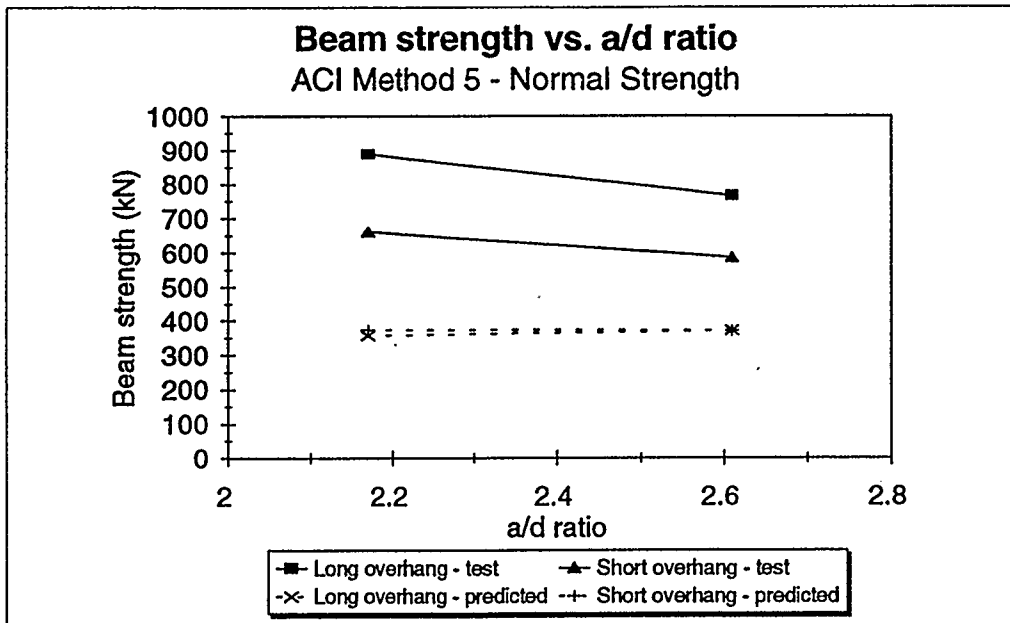


Figure 5.33: Beam strength vs. a/d ratio - ACI method using Eqn. 2.26



**Figure 5.34: Beam strength vs. a/d ratio - ACI method using Eqn. 2.27**

## 6. CONCLUSIONS

The following conclusions were made based on the analyses of test results by Kani, Clark, Sarsam and Al-Musawi as well as from the 12 beams tested.

1. Longer end anchorages, higher concrete compressive strengths, and shorter  $a/d$  ratios usually resulted in a stronger beam.
2. The stirrup diameter of 5.68 mm and spacing of 150 mm satisfied crack width limitations according to CSA A23.3-94 under service loads and assuming interior exposure, based on the crack widths at 60% of the predicted failure loads by the CSA A23.3-94 simplified method. The crack widths also satisfied crack width limitations based on the predicted loads given by the general and strut-and-tie methods as well as all ACI methods except for the ACI method based on equation 2.25.
3. The strut-and-tie model contains very restrictive equations for  $f_{2max}$  and  $\epsilon_1$ , but potentially is a good model since it can take  $f'_c$ ,  $a/d$  ratio and anchorage length into account which appear to be important factors in determining shear strength.
4. The CSA A23.3-94 standard contains restrictive development length equations. The rate of force development in the longitudinal reinforcement of the test beams was higher than that based on the equations in the CSA A23.3-94 standard.
5. The shear friction model accounts for  $a/d$  ratio, end anchorage, concrete compressive strength, reinforcement ratio, stirrup size and spacing when calculating the shear strength of the test beams.
6. Based on the coefficient of variation for the predictions using the various models,

the shear friction, simplified and general method all gave similar predictions. The predictions using the strut-and-tie were not as good as these other methods based on the coefficient of variation and on the average P-test/P-predicted. The shear friction method had the lowest average of P-test/P-predicted equal to 1.24.

7. Based on the coefficient of variation for test beams 1, 3, 7 and 9 ( $a/d = 3.05$ ), the shear friction model gave slightly better predictions with a C.O.V. of 0.10 than the corresponding ACI methods. For the remaining beams, the shear friction model gave similar predictions to those based on the corresponding ACI methods.

## 7. RECOMMENDATIONS

### 7.1 Current Codes

It is recommended that the  $f_{2max}$  and  $\epsilon_1$  equations used in the strut-and-tie model and general method be investigated further. The CSA development equation for longitudinal reinforcement should be investigated further as it seems to be too conservative.

### 7.2 Future Research

The following research is recommended:

1. Further investigation using the shear friction model on beams is suggested to determine its range of applicability.
2. Different types of beams should be tested including continuous, cantilever, prestressed and T-beams with point loads and distributed loads. Beams with a large range of reinforcement ratios,  $a/d$  ratios, stirrup spacings and sizes should be tested.
3. The model should be improved by determining the effects of compression zone reinforcement.
4. More investigation is needed into the distribution of normal and shear stresses along the inclined plane, the length of contact providing shear friction, and the development of forces in the longitudinal reinforcement and stirrups.
5. Beams with concrete strengths greater than 80 MPa should be tested with different aggregate sizes and shapes.



## REFERENCES

American Concrete Institute (1992), "ACI Manual of Concrete Practice Part 3-1992", Detroit, pp. 1-353.

Birkeland, P.W. and Birkeland, H.W. (1966), "Connections in Precast Concrete Construction", Journal of the American Concrete Institute, March, Vol. 63, No. 3, pp. 345 - 368.

Canadian Portland Cement Association (1995), "Concrete Design Handbook", Ottawa, Ontario, pp. 1-220.

Canadian Standards Association (1994), "Design of Concrete Structures A23.3-94", Rexdale, Ontario, pp. 1-199.

Clark, A.P. (1951), "Diagonal Tension in Reinforced Concrete Beams", Journal of the American Concrete Institute, October V.23, No. 2, pp. 145-155.

Kani, M.W., Huggins, M.W., and Wittkopp, Rudi R. (1979), "Kani on Shear in Reinforced Concrete", Department of Civil Engineering, University of Toronto Press, pp. 1-225.

Kumaraguru, P. (1992), "Strength of Dapped End Beams", M.Sc. Thesis, University of

Calgary, Calgary, Alberta, pp. 1-162.

Loov, R.E. (1978), "Design of Precast Connections", Paper presented at a seminar organized by Compa International Pte, Ltd., September 25-27, Singapore, 8 pp.

Loov, R.E. and Patnaik, A.K. (1994), "Horizontal Shear Strength of Composite Concrete Beams with a Rough Interface", PCI Journal, January-February, Vol. 39, No.1, pp. 48-69.

Mattock, A.H. (1974), "Shear Transfer in Concrete Having Reinforcement at an Angle to the Shear Plane", ACI Publication SP-42, Vol. 1, pp.17-42.

Pillai, S.U., and Kirk, D.W. (1988), "Reinforced Concrete Design", McGraw-Hill Ryerson Ltd., Toronto.

Sarsam, K.F. and Al-Musawi, J.M.S. (1992), "Shear Design of High and Normal Strength Concrete Beams with Web Reinforcement", ACI Structural Journal, Vol.89, No. 6, pp. 658-664.

Schlaich, J., and Schaefer, K. (1991), "Design and Detailing of Structures using Strut-and-Tie Models", The Structural Engineer Vol. 69, No. 6, pp. 113-125.